4.1. Survey of prevalent diseases of *Citrus reticulata* caused by pest and pathogens

The present study was undertaken to study the relation between prevalent diseases of mandarin orange (*Citrus reticulata*) and strategies for bio control of the same from area specific screened microorganisms. Though other diseases were also prevalent but due consideration was given to symptoms of fungal origin as related works on disease caused by fungal pathogens is comparatively negligible to the study on diseases of viral and bacterial origin. Darjeeling district is located in the northern-most part of West Bengal and is bordered by Sikkim and Bhutan in the North, districts of West Dinajpur and Purnia in the south, Nepal in the West and Bhutan, Jalpaiguri and Bangladesh in the east. Geologically, the southern portion is covered with sedimentary rocks and the northern part by metamorphic rocks. The soil is residual and derived by the withering of the underlying rocks. The entire hill region has a more or less forest-based ecosystem which include different types of citrus species. Mandarin orchards in Darjeeling hills started to show severe dieback causing huge economic loss to the farmers. In order to know the root cause of the disease, extensive survey of citrus orchards in Darjeeling District of North Bengal was conducted during fruiting (October-December) as well as non fruiting season (March- July). The nurseries and orchards screened were mostly private enterprises; hence random screening and sample collection was undertaken in various villages which include 7 in Mirik, 2 in Kurseong, 3 in Gorubathan and 5 in Kalimpong. Cultivation in these villages was almost completely abandoned due to dieback. In general, the soil was found to be poor in nutrition. There were several fungal pathogens contributing to the dieback (Plate 3, figs A-G). Repeated surveys were conducted and an inventory was outlined, keeping in view many factors ranging from disease symptomology to host pathogen interaction. Symptoms and development of some commonly occurring fungal diseases of *Citrus reticulata* have been described below in brief.

Root

Symptoms of Charcoal root rot caused by *Macrophomina phaseolina* were characterized by a gradual decay of the root tips, lateral roots and root crown. This gradual destruction of the root system causes the seedlings to become stunted and chlorotic, and finally to die. Phytopthora foot rot/Gummosis caused by *Phytophthora nicotiane* was noticed on the bark at or just above the bud union on susceptible scions. Lesions first occur as a drop of gum on the surface of the bark which appears to be brown, discolored, necrotic and slippery. In some cases, the margin of the infected area breaks away from the healthy area and may curl back. Lesions can eventually girdle the entire tree trunk leading to the death of the tree.

Plate 3 (figs. A-G): Mandarin tree in Mirik orchard [A] Survey of diseases prevalent in Mirik orchards [B]. Different diseases of mandarin plants [C - G].

Phytophthora spp. also infects the cortex of feeder roots. The root system gets a stringy appearance. This leads to yield loss and general prolonged tree decline. Cotton root rot caused by *Phymatotrichopsis omnivore,* appears on trees that are more than three years old. The fungus kills the tree so quickly that most of the dried leaves remain attached to the branches. Besides, root rot complex caused by *Fusarium solani* and *Fusarium oxysporum* were also observed in various nursery grown seedlings.

Leaf

White powdery growth of *Oidium tingitaninum* on different surfaces of the plant specially on the young actively growing twigs causing Powdery mildew were seen. Infected leaves became yellow, dried up and fell off resulting in dying back of the branches. *Mycosphaerella citri* primarily attacks leaves but can also infect fruits. Greasy spots appear first on the upper surface of the leaf as yellow colour. The corresponding surface on the undersides turn dark and appear slightly raised and greasy. The swollen tissue starts to collapse and turn brown and eventually leaves drop prematurely. The first symptom caused by *Diaporthe citri* on leaves were small, circular, dark depressions with a yellow margin. Later, the spots became raised and turned dark brown. Leaves turn yellow and may drop prematurely. Raised spots are also found on twigs and fruits. Spots on the fruits were at first small, light brown and dunken. Later they became dark and raised. Spots sometimes develop in a tear-streaked pattern resulting from infection caused by spores which wash down over the fruit surface during heavy dews of light rains.

Fruits

Alternaria alternata attacks fruit, leaves and young shoots causing *Alternaria* brown spot disease. The first symptoms appear as small, slightly depressed black spots which can cause the young fruit to fall from the tree. Fruit is usually immune to infection after reaching 3 to 4 months of age. On susceptible varieties only the young leaves and shoots can be infected. They produce brown, necrotic, blighted areas of various sizes usually surrounded by yellow halos on the plant tissue. Anthracnose or wither-tip is caused by *Glomerella cingulata.* Brown soft decay of fruit, or discolored streaks on the rind (called tear staining) are symptomatic of anthracnose. *Alternaria citri* causes Black rot. The infection starts while the fruit is still on the tree. The fruit is infected through cracks or openings on the stylar end of fruit. The fruit colours prematurely and drops (Plate 4,figs A-G). Infected tissue is often relatively firm on navels. This decay develops mostly during storage but can be identified in the field. The same

Plate 4 (figs. A-G): *Citrus reticulata* tree bearing fruits in the experimental plot of Immuno phytopathology laboratory [A-D], Fruit drop symptoms after 4 months of fruiting [E-G].

species of *Phytophthora* that causes foot rot, also infect fruits during periods of excessive rain resulting in decayed areas that are brown, firm and leathery. Later a white velvety growth is seen on the surface of the fruit accompanied by a strong fermenting odour. Fruits are also contaminated with another fungus (*Diplodia natalensis*) in the field but diseases commonly appear at the packing house or transit. Decay occurs around the stem end and advances in streaks down the side of the fruit. There is no fungal growth on the surface of the root. *Penicillium digitatum* causes a rapid breakdown of fruit punctured of bruised during harvesting and packing operations. The fungus enters the fruit only through wounds. The fruit becomes soft and shrinks in size. White mold that later turns green can be seen on the surface of the fruit. *Leptothyrium pomi* keeps citrus fruits from turning yellow in the infected spots. Small black specks are formed on the rind in areas immediately surrounding the oil glands. There is no effect on fruit or juice quality. Postbloom fruit drop caused by *Colletotrichum acutatum* appears as peach to brown colored necrotic spots on petals of flowers and produces fruit drop and the formation of persistent buttons which remain attached to stems. The pathogen survives on the surface of leaves, twigs and buttons between flowering periods.

Viral diseases include Cachexia, Citrus tatter leaf, Exocortis and Tristeza. The pathogen *Xyloporosis* causing Cachexia makes the inner bark surface bumpy. The bark projections are smooth in contrast to the sharp projections produced by the citrus tristeza virus (CTV). CTV is a virus that is limited to the phloem tissues of its host. It is transmitted by vectors that penetrate the phloem to extract sap, mostly the aphid species that colonize the crop. The brown citrus aphid is considerably more efficient at transmitting the virus than are other aphids that infest citrus. The adult tree turns yellow (Plate 5,fig.D) and wilts rapidly, and dies within a few years. Fruit typically remain smaller than normal. Leaf symptoms including yellow foliage (Plate 5,fig A&B) and sparse shoot growth are also often apparent. Tatter leaf-citrange stunt virus causes a bud union crease, while *Citrus exocortis* causes bark-shelling and stunting of trees. In the early stages of the disease, gum exudes from pustules at the base of the trunk at the base of the trunk and may extend from below the soil line to the bud union. New bark forms beneath the pustules and the outer bark sloughs off forming the characteristic bark-shelling. The tree eventually declines.

Different insects such as mealy bug, leaf miner, fruit fly, trunk borer and citrus dog were prevalent. In the nursery grown plants *Papilio demoleus* was most abundant during the rains when its larvae (caterpillars) cause damage to citrus leaves. Caterpillars body is cylindrical,

Plate 5 (figs. A-D): Yellowing of leaves indicating appearance of virus in nursery grown seedlings [A] and in the experimental field [D] in comparison with healthy plant [C].

distinctly segmented and in young larvae pigmented black and white. Older larvae are predominantly green above and whitish below. Young larvae resemble bird droppings (Plate 6, fig.C) while older larvae appear to have no shadow and blend with the citrus leaves. The newly emerged female butterfly is attracted to the nectar of flowers, to urine and faeces, rotten fruit and other food sources, while the mature mated female is attracted to citrus oils on the leaves on which she lays her eggs. The early larvae are black and white in colour and do not attempt to hide, while the mature larva with its different colouring withdraws to parts of the plant where its light under parts cancel its natural shadow and allow it to blend with the leaves. Bright light and high temperature cause the larva to leave its resting position and actively seek shade. As a defence against predators, the caterpillar expands the third thoracic segment which bears "eye-spots". At the same time, a forked, tongue-like *osmaterium*, normally withdrawn into the first thoracic segment, is extruded and vibrated. These changes give the larva a snake-like appearance and together with a pungent, aromatic secretion from the mouth, frighten off animals that might eat it. Adult butterflies can distinguish between certain colours only and are most sensitive to the red end of the spectrum (Plate 6,fig.D).

Planococcus citri, commonly known as mealy bug occurring on ventral surface of foliage (Plate 6, fig.A) cause nearly the same damage as aphids. Body oval; slightly rounded in lateral view; light orange to pink; body contents crushed are reddish brown; mealy wax covering body, not thick enough to hide pink body color; without longitudinal lines on dorsum; ovisac ventral only; with 17 lateral wax filaments, becoming progressively longer posteriorly, anterior pair about 1/4 width of body, straight, except posterior pair often curved apically, thin, posterior pair longest, varying from 3/4 to 1 time length of body. Surface of lateral filaments smooth. Like aphids, they suck plant sap and secrete honey dew, on which fungi can easily grow. This dirtiness gives ornamental plants a loss of quality. Viruses, however, are less transmitted by mealy bugs than by aphids. Apart from yellowing, defoliation, and cosmetic damage, mealy bugs also reduce the vigour of the plant.

Psocoptera indet, free-living insects were found under tree bark. They have long antennae, broad heads and 'bulging' eyes may grow up to 10mm in length, though they're usually less than 6mm, and the adults are often winged. The wings are held roof-like over their bodies look a little like aphids but their long antennae, broad heads and biting jaws show that they are not. Sometimes the colonies seem to move in coordinated fashion (Plate 6, fig. B).

Plate 6 (figs.A-D): Insects that feed on citrus plants. *Planococcus citri* on ventral surface of mandarin leaf [A] *Psocoptera indet* accumulated on the stem of mandarin plant [B] Young larvae [C] and adult stage of *Papilio demoleus*[D].

4.2 Root rot disease of *Citrus reticulata*

Mandarin seedlings were collected from eight different locations, viz. Rangali Rangliot, Bijanbari, Sukhia Pokhari, Kurseong, Mirik, Kalimpong Block I, Kalimpong Block II and Gorubahan and maintained in the Glass house conditions. Charcoal root rot pathogen (*Macrophomina phaseolina*) isolated from mandarin orchards of Darjeeling hill was used for present study after completion of Koch's postulate. Mycelia – septate, branched, hyaline when young becoming brown with age. Advancing zone of mycelia mat even and appressed. Sclerotia – black, moderate size (34-78 u in diameter), round or irregular (Plate 7 fig.D) uniformly reticulate with no difference in internal structure.

Healthy seedlings of mandarin (*Citrus reticulata*) plants (1-year-old) grown in earthenware pots were inoculated with this isolated organism and incubated for a period of 4 weeks. Pathogenicity of *M. phaseolina* was tested on twenty mandarin plants each of eight different locations. The inoculated plants were examined after 4 weeks. Colour of root, root rot index and percentage loss in dry weight of roots were noted. Young seedlings showed light brown discolouration of the root at the soil line initially which gradually turned dark brown to blackish brown and finally to black. In advanced stage of disease symptoms also appeared at ground level. Lower leaves turned yellow and remained attached, sometimes showed wilting symptoms. In advanced stage defoliation of lower leaves were evident (Plate 7 figs. E-G; Plate 8 figs. F-H). When epidermis was removed, small, black bodies (sclerotia) were discerned. These propagating bodies were abundant enough to impart a grayish black colour like charcoal to the tissues.

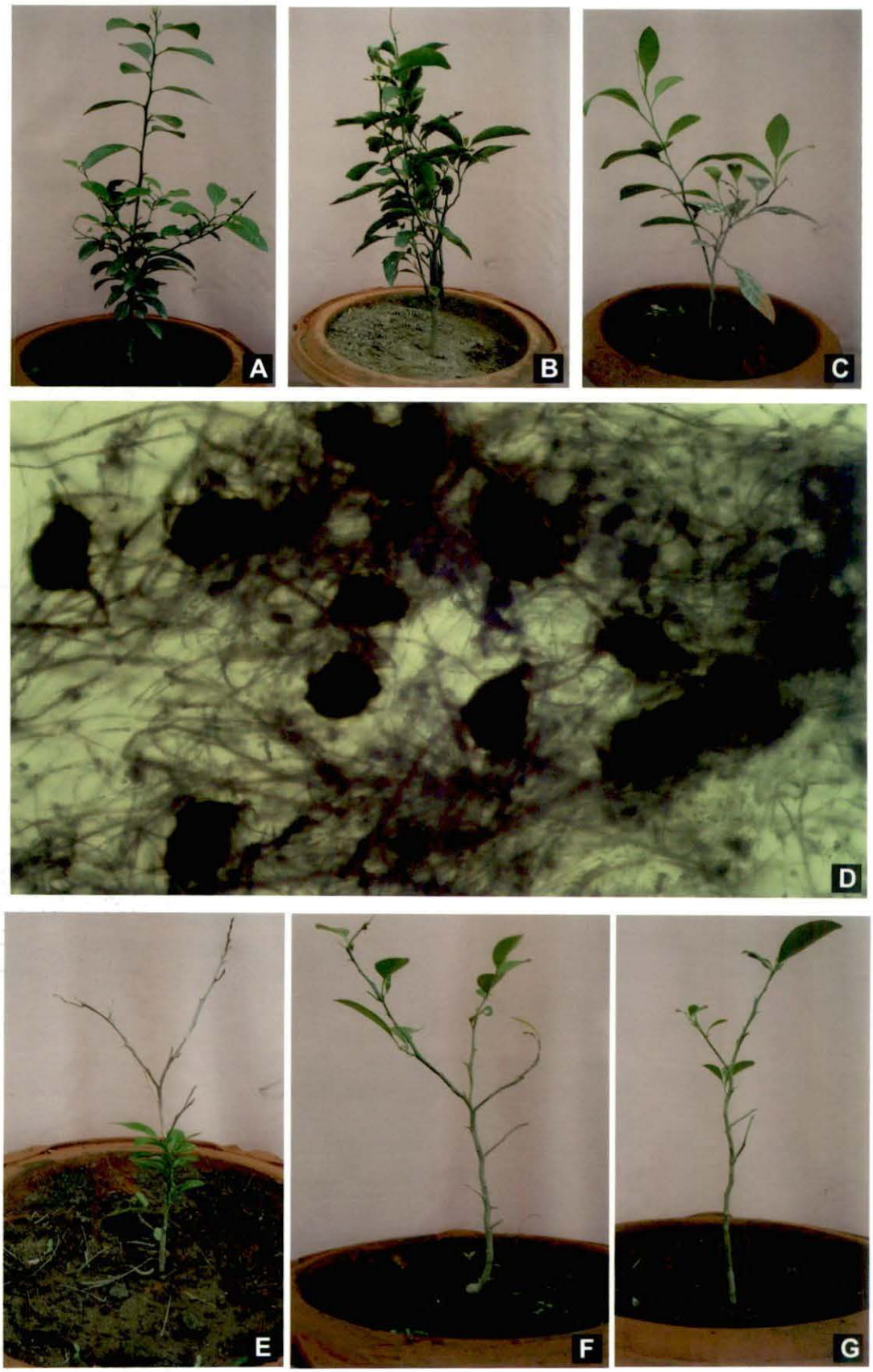

Plate 7 (figs. A-G): Healthy mandarin plants in pots [A-C], *Macrophomina phaseolina* (root rot pathogen) [D], Infected mandarin plants showing symptoms 30 days following artificial inoculation with *M. phaseolina* [E-G].

Table 1 : Pathogenicity test of *Macrophomina phaseolina* on different root samples of *Citrus reticulata*

Locality of *C. reticulata* saplings	* Root rot index	**Colour intensity
Rangli Rangliot	0.10	+
Bijanbari	0.25	++
Sukhia Pokhari	0.75	++++
Kurseong	0.25	++
Mirik	0.75	++++
Kalimpong Block I	0.75	++++
Kalimpong Block II	0.50	+++
Gorubathan	0.50	+++

* On the basis of root area affected; 0-10% (0.10); 11-25% (0.25); 26-50% (0.50); 51-75% (0.75); 76-100% (1.0).
** + Light brown, ++ Deep brown , +++ Blackish brown, ++++ Black

The root rot index as well as percentage loss in dry weight of roots were very low at the initial stage of infection which increased significantly with time in compatible interaction. Mandarin seedlings of three locations (Mirik, Kalmpong Block-I and Sukia Pokhri) were found to be highly susceptible (Table 1).

Culture filtrate of the pathogen (*M. phaseolina*) following two weeks growth in Richards' media at 28^0C, was collected and the young seedlings of mandarin (*Citrus reticulata*) of three different locations ((Mirik, Kalmpong Block-I and Sukia Pokhri) which showed susceptible reaction, were further tested in *in vitro* conditions in comparison with sterile distilled water control (Plate 8, figs A-D). It is interesting to note that seedlings showed same symptoms in this case also. Wilting followed by chlorosis and browning reaction of green leaves were evident in seedlings grown in culture filtrate of the pathogen. Wilting symptoms first appeared 7 days after treatment. However within two weeks leaves of all the seedlings turned into brown colour.

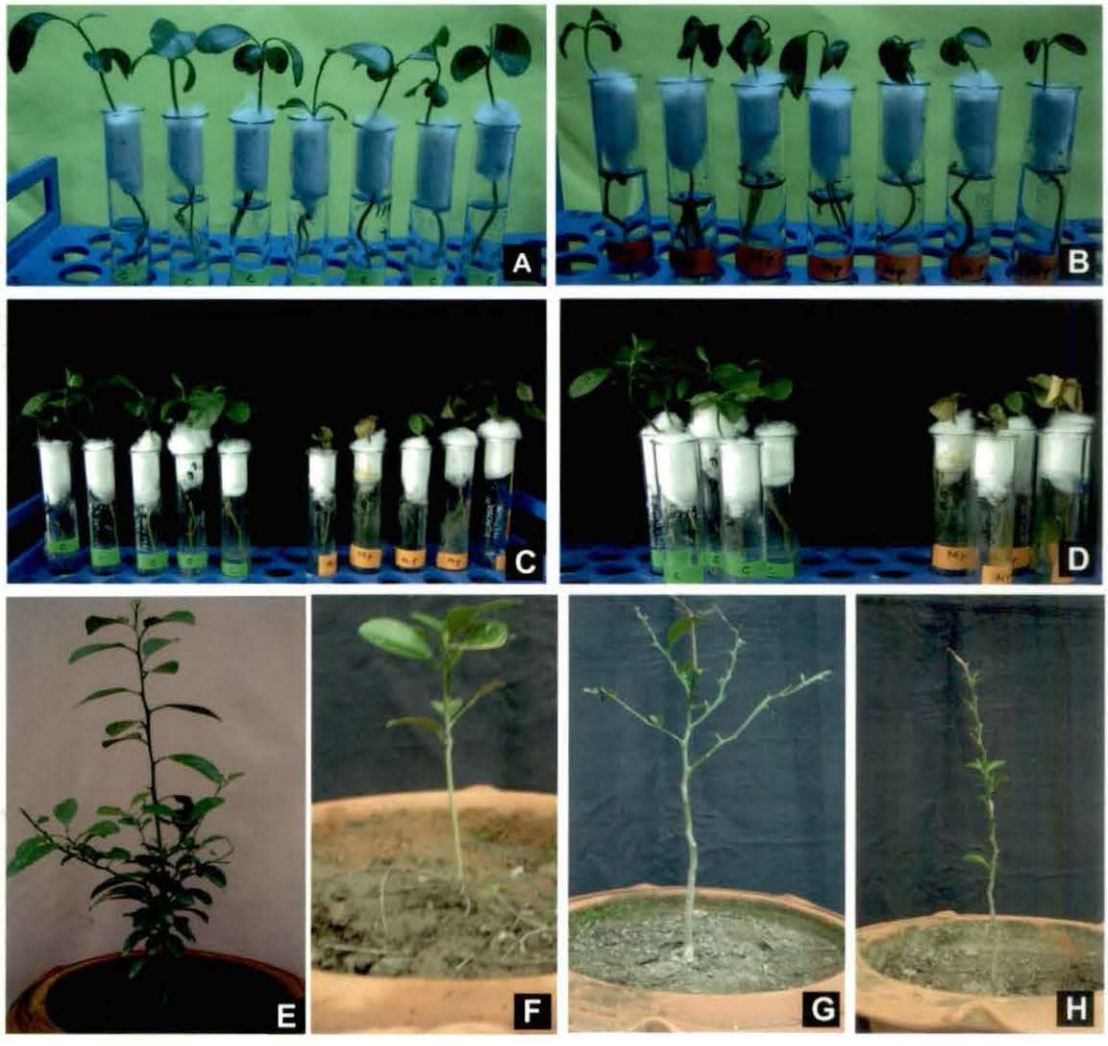

Plate 8 (figs. A-H): Mandarin seedlings grown in distilled water [A, C & D - left] and culture filtrate of *Macrophomina phaseolina* [B, C & D - right]. Healthy [E] and *M. phaseolina* infected plants [F-H].

4.3 Cultural conditions affecting growth of the pathogen (*M. phaseolina*)

Macrophomina phaseolina infect mandarin plant roots and their interactions affect the development of root rot disease. Initially it was considered worthwhile to study the effects of some major factors such as incubation time, temperature and pH of substrate on growth of the pathogen *in vitro*.

4.3.1. Effect of incubation time

The effect of incubation time on the growth of *M. phaseolina* was studied *in vitro*. *M. phaseolina* was grown in Richard's media for a period of 24 days at 28^{0}C. Mycelial growth of the fungus was recorded after 2,4,8,12,16,20, and 24 days. The results are embodied in Table 2. Maximum growth of *M. phaseolina* (755 mg) was observed after 12 days of incubation and then the rate of growth declined. Mycelial growth increased by 24% from 8 to 12 days of incubation and decreased by 5% from 12 to 16 days.

Table 2 . Effect of incubation time on growth of *M. phaseolina*

Incubation Time (days)	Average dry weight of mycelia (mg)
2	97.20 ± 2.24
4	214.35 ± 4.44
8	618.00 ± 3.72
12	755.00 ± 1.81
16	717.52 ± 1.58
20	689.32± 2.86
24	653.62± 2.43

Average of 3 replicates/treatment; Temperature 28^{0}C; pH of medium – 5.4

4.3.2. Effect of pH on growth

It is well known that the pH of the medium usually plays an important role in the growth of microorganisms. The utilization of nutrients depends partially upon the pH of the culture medium. Therefore, it was considered imperative to use a buffer system to stabilize the pH of the culture medium during incubation. In the present study, buffer solutions with pH values ranging from 4-8 (4.0, 5.0, 6.0, 7.0 and 8.0) were prepared by mixing KH_2PO_4 and K_2HPO_4 each at a concentration of M/30. The pH of the medium was adjusted using N/10 NaOH or N/10 HCl to obtain the corresponding range of pH values (4.0-8.0). Both the medium and the phosphate buffer were sterilized. Equal parts of the buffer solution and medium were mixed before use. Each flask containing 50ml of the medium was inoculated with fungus and

incubated for 12 days at 28^{0}C. The results are given in Table 3. It appears that *M. phaseolina* grew well over a range of pH (4.0-8.0) and optimum growth was recorded at pH 5.5. It is necessary to mention that mycelia growth increased up to pH 5.5 and then gradually declined.

Table 3. Effect of different pH on the growth of *M. phaseolina*

pH	Average dry weight of mycelia (mg)
4.0	310.50 ± 2.33
4.5	581.25 ± 3.40
5.0	616.00 ± 3.12
5.5	695.00 ± 2.61
6.0	437.55 ± 2.53
6.5	409.32± 3.86
7.0	325.12± 2.63
8.0	310.33± 1.95

Average of 3 replicates/treatment; Temperature 28^{0}C; Incubation time – 12 days

4.3.3. Effect of temperature on growth

Temperature is also a major factor affecting growth of a pathogen. Therefore, the effects of different temperatures (15, 20, 25, 28, 30, 35, 40^{0}C) on growth of *M. phaseolina* was studied *in vitro*. Maximum mycelial growth was noted at 30^{0}C with a decline at 40^{0}C (Table 4).

Table 4. Effect of different temperature on the growth of *M. phaseolina*

Temperature (^{0}C)	Average dry weight of mycelia (mg)
15	95.00 ± 2.43
20	181. 05 ± 2.40
25	246.00 ± 3.22
28	595.00 ± 2.82
30	737.55 ± 3.53
35	665.42± 2.85
40	125.25± 3.63

Average of 3 replicates/treatment; pH adjusted to 5.5 ; Incubation time – 12 days

4.4 Isolation of microorganisms from mandarin rhizosphere and their identification

4.4.1. Analyses of soil samples of mandarin orchards

The soil samples were collected from eight different locations- Rangli Rangliot, Bijanbari, Sukhia Pokhari, Kurseong, Mirik, Kalimpong Block I , Kalimpong Block II and Gorubathan. These samples were given for analysis in Soil Testing laboratory, Institute of Plantation Science and Management, North Bengal University before the isolation of microorganisms. Moisture content, pH, soil type, soil texture, carbon and nitrogen ratio, available K and P etc were determined for all eight soil samples. Results have been presented in Table 5.

Table 5: Analyses of soil samples collected from mandarin orchards

Sample area	Moisture %	pH	Organic carbon	nitrogen	Soil type	Soil texture			Available	
						Silt %	Clay %	Sand %	K_2O (ppm)	P_2O_5 (ppm)
Rangli Rangliot	16.67	4.38	1.05	0.11	Clay	10	51	39	120.96	38.09
Bijanbari	18.35	4.11	1.15	0.12	Sandy Clay	5	45	50	154.57	40.26
Sukhia Pokhari	15.85	3.90	1.10	0.11	Sandy Clay	2	43	55	88.70	31.56
Kurseong	26.35	4.43	1.27	0,13	Sandy Clay	4	40	50	123.65	26.12
Mirik	18.62	4.69	1.35	0.14	Sandy Clay	10	34	56	177.41	50.06
Kalimpong Block I	20.28	4.76	1.09	0.11	Sandy Clay	13	42	52	168.00	54.41
Kalimpong Block II	22.75	4.58	1.08	0.12	Sandy Clay	15	45	54	165.55	53.35
Gorubathan	21.22	3.86	1.32	0.11	Sandy Clay	12	40	55	146.22	50.75

4.4.2. Fungal isolates

The mycelial growth and sporulation behavior of fungi isolated from rhizosphere of *Citrus reticulata* were examined separately on PDA medium. Nature and rate of mycelial growth as well as sporulation time were recorded. Radial growth patterns of different fungal isolates have been presented in Plate 9 Morphological characters and microscopic observations under bright field of the isolated fungi have been presented in Table 6 . On the basis of hyphal character, nature of conidiophore and conidia these were identified. It was found that most of the fungal isolates belonged to the genera *Aspergillus, Fusarium, Penicillium, Sporotrichum, Rhizopus, Macrophomina, Emenicella* and *Trichoderma.*

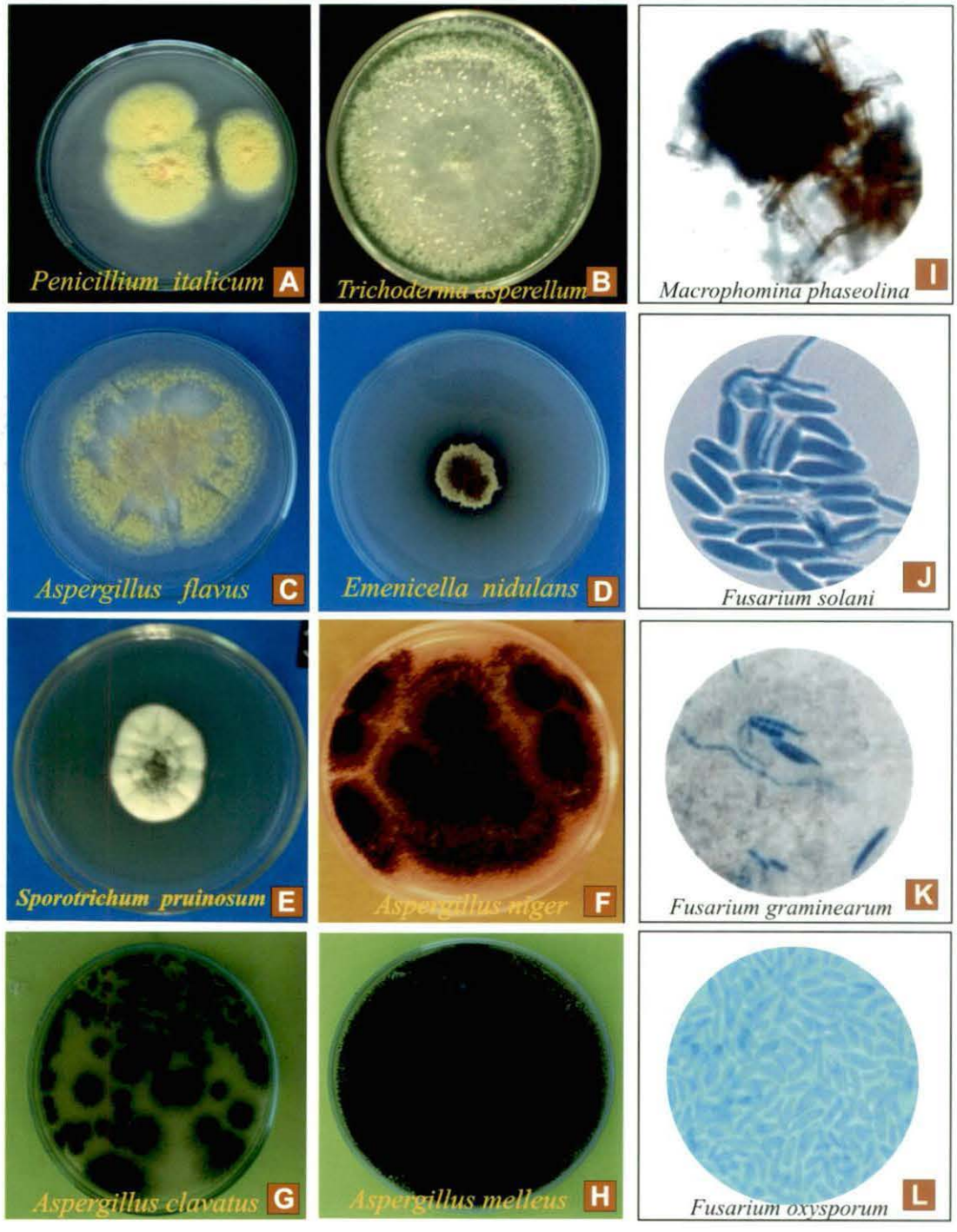

Plate 9 (figs. A-L): Radial growth [A-H] and microscopic observation [I - L] of fungi isolated from rhizosphere of mandarin plants.

Table 6 : Morphology and Microscopical Characters of fungi isolated from mandarin rhizosphere

Organisms identified	Morphology and Microscopical Character
A. niger RHS/M492	**Colonies:** Black on PDA mediam **Mycelia:** Hyaline, aseptate **Conidia:** Conidial heads radiate. Conidia brown, ornamented with warts and ridges, subspherical, 3.5-5.0 µm diam. **Conidiophore:** Consisting of a dense felt of conidiophores. Conidiophore stipes smooth-walled, hyaline. Vesicles subspherical, 50-100 µm diam
Aspergillus flavus (RHS/M495)	**Colonies:** Colonies on Czapek and PDA usually spreading, yellow green, reverse colourless to dark red brown, occasionally dominated by hard sclerotia, white at first, becoming red brown to almost black with age, 400-700 µm diam **Mycelia:** hyaline, aseptate **Conidia:** Conidial heads typically radiate, splitting into several poorly defined columns, rarely exceeding 500-600 µm diam., mostly 300-400 µm, smaller heads occasionally columnar up to 300-400 µm. Conidia typically globose to subglobose, conspicuously echinulate, variable, (3-) 3,5-4,5 (-6) µm diam., sometimes elliptical or pyriform at first and occasionally remaining so, and then 4.5-5.5 x 3.5- 4.5 µm. **Conidiophore:** Conidiophores thick-walled, hyaline, coarsely roughened, usually less than 1 µm long, 10-20 µm diam., just below the vesicle; vesicles elongated when young, becoming subglobose to globose, 25-45 µm diam.; both metulae and phialides present; metulae usually 6-10 x 5,5 µm but sometimes up to 15-16 x 8-9 µm; phialides 6,5-10 x 3-5 µm.
A. mellus RHS/M493	**Colonies:** Black on PDA mediam **Mycelia:** Hyaline, aseptate **Conidia:** Conidia globose to subglobose , smooth walled or irregularly roughened, 2.8-3.5 µm diam. **Conidiophore:** Conidiophore usually 0.5-2 µm tall, thickwalled, roughened.
A. clavatus RHS/M494	**Colonies:** Colonies on Czapek and malt agar usually spreading, occasionally floccose, blue-green, mycelium white, inconspicuous. **Mycelia:** Hyaline, aseptate **Conidia:** Conidial heads clavate, usually splitting into several divergent columns. Conidia smooth-walled, ellipsoidal, 3-4,5 x 2,5-3,5 µm diam. **Conidiophore:** Conidiophores very long, 500-900 µm long, smooth-walled, hyaline to slightly brown near vesicle. Vesicle clavate, 15-75 µm diam. Phialide 7-10 x 2-3,5 µm; metulae absent.
A. fumigatus RHS/M498	**Colonies:** Colonies (CzA) dark blue-green, consisting of a dense felt of conidiophores, intermingled with aerial hyphae. **Mycelia:** hyaline, aseptate **Conidia:** Conidia verrucose, (sub)spherical, 2.5-3.0 µm diam Conidial heads columnar; conidiogenous cells uniseriate. **Conidiophore:** Conidiophore stipes smooth-walled, often green in the upper part. Vesicles subclavate, 20-30 µm wide.

Organisms identified	Morphology and Microscopical Character
Aspergillus oryzae RHS/M499	**Colonies:**. Colonies on potato dextrose agar at 25°C are white to yellow to drab gray to brown, but never green **Mycelia:** Hyphae septate and hyaline **Conidia:**. Conidial heads are radiate to loosely columnar and biseriate Conidia are globose, 3-4.5 µm, with very rough walls **Conidiophore:** Conidiophores 30-350 µm, smooth-walled, and brown. Vesicles are globose to subglobose, 7-16 µm in diameter. Metulae and phialides cover the upper portion of the vesicle.
Fusarium graminearum RHS/S566	**Colonies:**. Raddish white **Mycelia:** Hyaline, aseptate **Conidia:** Conidia often formed sparsely, falcate, sickle-shaped or markedly dorsi-ventral, 3-7-septate, 25-50 x 3-4 µm, with a well developed, often pedicellate foot cell. Microconidia absent. Macroconidia produced from doliiform phialides 10-14 x 3,5-4,5 µm, formed laterally or on short multibranched conidiophores; sporodochia may form in older cultures **Conidiophore:** Chlamydospores, when present, are intercalary, single, in chains or clumps, globose, thick-walled, hyaline to pale brown with a smooth or slightly roughened outer wall, 10-12 diam. Many strains fail to develop chlamydospores on standard media
Fusarium solani RHS/M532	**Colonies:**. Colonies growing rapidly, with white to cream-coloured aerial mycelium, usually green to bluish-brown **Mycelia:** hyaline, aseptate **Conidia:** Microconidia usually abundant, produced on elongate, sometimes verticillate conidiophores, 8-16 × 2.0-4.5 µm. Chlamydospores frequent, singly or in pairs, terminal or intercalary, smooth- or rough-walled, 6-10 µm diam **Conidiophore:** Conidiophores arising laterally from aerial hyphae. Monophialides mostly with a rather distinct collarette. Macroconidia produced on shorter, branched conidiophores which soon form sporodochia, usually moderately curved, with short, blunt apical and indistinctly pedicellate basal cells, mostly 3-septate, 28-42 × 4-6 µm, occasionally 5-septate
Fusarium oxysporum RHS/M535	**Colonies:**. Colonies growing rapidly, with white mycelium **Mycelia:** hyaline, aseptate **Conidia:** Microconidia usually abundant, produced on elongate. **Conidiophore:** conidiophores, 8-16 × 2.0-4.5 µm. **Chlamydospores:** frequent, singly or in pairs, terminal or intercalary, smooth- or rough-walled, 6-10 µm diam
Sporotrichum pruinosum RHS/M496	**Colonies:**. Distinct greyish or pinkish hue; **Mycelia:** hyaline, aseptate **Conidia:** Blastoconidia from unbranched conidiophores ellipsoidal to ovoid pyriform or nearly cylindrical, 5.8 x 3.5 µm. Chlamydospores terminal or intercalary, hyaline, (sub)globose to broadly ellipsoidal or more rarely pyriform, 11- 60 µm diam or 11 x 7.5 µm, with granular contents and thick walls (up to 4.5 µm). **Conidiophore:** Conidiophores simple or typically branched. Branching racemose, each branch forming a terminal blastoconidium.

Organisms identified	Morphology and Microscopical Character
Macrophomina phaseolina RHS/S565	**Colonies:**. Pycnidia dark brown, solitary or gregarious on leaves and stems, immersed, becoming erumpent, 100-200 µm diam **Mycelia:** hyaline, aseptate **Conidia:**. Conidia hyaline, ellipsoid to obovoid, 14-30 x 5-10 µm **Conidiophore:** Conidiophores (phialides) hyaline, short obpyriform to cylindrical, 5-13 x 4-6 µm.
Trichoderma asperellum RHS/M517	**Colonies:**. Dark green **Conidia:**. subglobose to ovoidal, 3.5 to 4.0 µm long, smooth, green **Conidiophores**: Typically with paired branches forming over 150 µm of the length of terminal branches. Cells supporting the phialides equivalent in width to, or at most only slightly wider than, the base of phialides arising from them. **Phialides:** 6.5-6.7 µm long, 2.5-3.5µm wide at the widest point 1.6-2.5 µm at the base; supporting cell 2.4-3.6 µm; Terminal phialides in a whorl or solitary, typically cylindrical or at least not conspicuously swollen in the middle and longer than the subterminal phialides.
Penicillium italicum RHS/M510	**Colonies:**. Velutinous to fasciculate, crustose **Mycelia:** hyaline, aseptate **Conidia:**. Smooth-walled, ellipsoidal to cylindrical, 3.5-5 x 2.2-3.5 µm **Conidiophore:** Terverticillate, appressed elements, born from subsurface hyphae
Emenicella nidulans RHS/M509	**Colonies:**. Colonies (PDA) growing rapidly, green, cream-buff or honey-yellow; reverse dark purplish **Mycelia:** Hyaline, aseptate **Conidia:**. Conidial heads short, columnar, up to 80 µm long **Conidiophore:** Conidiophore stipes brownish, 60-130 x 2.5-3.0 µm. Vesicles hemispherical, 8-10 µm diam. Conidiogenous cells biseriate, 5.9 x 2-3 µm. Metulae 5.6 x 2.3 µm. Conidia spherical, rugulose, subhyaline, green in mass, 3-4 µm diam
Rhizopus oryzae (RHS/M 497)	**Colonies:**. Colonies (MEA, 30°C) expanding, up to 1 cm high, whitish to greyish-brown. **Mycelia:** Hyaline, aseptate **Sporangiophore:** Singly or in tufts, brown, 1-2 mm high, 18 µm wide, mostly unbranched, sometimes with brownish swellings up to 50 µm diam. Rhizoids sparingly branched, up to 250 µm long, brownish. Sporangia spherical, 50-250 µm diam, brownish-grey to black; columella comprising 50-70% of sporangium, spherical; apophysis short, 3-12 µm high. Sporangiospores greyish-green, angular, subspherical to ellipsoidal, longitudinally striate, 6-8 x 4.5-5.0 µm **Chlamydospore:** Single or in chains, spherical to ovoidal, 10-35 µm diam, hyaline, smooth-walled. Zygospores. Zygospores red to brown, spherical or laterally flattened, 60-140 µm, with flat projections. Suspensors unequal, spherical and conical. Heterothallic

4.4.3. Bacterial isolates

A list of bacteria isolated from the rhizosphere soil of mandarin plants along with their codes have been presented in Table 7.

Isolated bacteria were studied under microscope after suitable staining and characterized based on morphological and biochemical studies following Bergey's manual of Systematic Bacteriology. Bacterial identification was performed on the basis of morphological, physiological and biochemical tests. Isolates were characterized for H_2S production, phosphate solubilization, starch hydrolysis, casein hydrolysis, chitin degrading, siderophore production, catalase production, protease production, urase production, cellulase production and indole production. Results (Table 7) revealed that out of 13 bacterial isolates, 10 bacteria showed gram positive reaction and rest were gram negative, where as 5 bacterial isolates showed phosphate solubilizing activity and 8 isolates showed cellulase activity. All isolates showed positive result in catalase activities. Overall, *Bacillus sp.*, *Bacillus cereus*, *Bacillus pumilus* and *Pseudomonas sp.*, were found to be more abundant.

Table 7 : Morphology and biochemical tests of isolated bacteria

Code	Shape	Pigment	Spore	Gram reaction	H_2S production	Phosphate solubilization	Starch hydrolysis	Casein hydrolysis	Chitin degrading	Siderophore production	Catalase production	Protease production	Urase production	Cellulase Production	Indolae Production	Identification
B/RHS/C1	Rod	W	+	+	-	+	+	+	+	+	+	+	_	+	-	*Bacillus pumilus*
B/RHS/M2	Rod	W	+	+	-	+	+	+	+	+	+	+	_	+	-	*Bacillus cereus*
B/RHS/M3	Rod	W	+	+	-	+	+	+	+	+	+	+	_	+	-	*Bacillus cereus*
B/RHS/M4	Rod	W	+	+	-	-	+	+	+	+	+	+	_	-	-	*Bacillus sp.*
B/RHS/M5	Rod	W	+	+	-	-	+	+	+	+	+	+	_	-	-	*Bacillus sp.*
B/RHS/M6	Rod	W	+	-	-	-	+	+	+	+	+	+	_	+	-	*Pseudomonas sp.*
B/RHS/M7	Rod	W	+	-	-	-	+	+	+	+	+	+	_	+	-	*Pseudomonas sp.*
B/RHS/M8	Rod	W	+	-	-	-	+	+	+	+	+	+	_	+	-	*Pseudomonas sp.*
B/RHS/M9	Rod	W	+	+	-	+	+	+	+	+	+	+	_	+	-	*Bacillus sp.*
B/RHS/M10	Rod	W	+	+	-	+	+	+	+	+	+	+	_	+	-	*Bacillus cereus*
B/RHS/M11	Rod	W	+	+	-	-	+	+	+	+	+	+	_	-	-	*Bacillus sp.*
B/RHS/M12	Rod	W	+	+	-	-	+	+	+	+	+	+	_	-	-	*Bacillus sp.*
B/RHS/M13	Rod	W	+	+	-	-	+	+	+	+	+	+	_	-	-	*Bacillus sp.*

4.5. Occurrence of Arbuscular Mycorrhizal fungi in rhizosphere of mandarin plants

Population of different species of AM fungi isolated from the rhizosphere of mandarin from different regions were determined. Sites selected were hilly regions of Kalimpong, Mirik, Bijanbari and Kurseong of Darjeeling hill. Among the AM fungi, *Glomus mosseae* could be determined as the most predominant, followed by other genera such as *Gigaspora, Acaulospora* and *Scutellospora.* Microscopic observations of selected AMF sores and root colonization in *Citrus reticulata* have been presented in Plate 10 (figs.A-O). Some of the characteristic features were considered for identification of all those isolates which were found as consistent association and maximum colonization with mandarin roots.

Acaulospora bireticulata . Spores single in the soil; develop laterally; sessile; light orange to yellowish brown; globose to subglobose; approx. 190µm diam; sometimes irregular; 130-180 x 170-250 µm. Subcellular structure of spores consists of a spore wall and two inner germination walls.Spore wall contains three layers. Layer 1, forming the spore surface, 1.1µm thick, closely attached to wall 2, continuous with the wall of a sporiferous saccule. Layer 2 laminate, ornamented, light orange yellowish brown, ornamentation consists of hyaline to yellowish white round-tipped polygonal structures.

Acaulospora spinosa. Color: cream to pale orange-brown. Shape: Globose or subglobose, size distribution: 140-220 µm, spore wall consists of two layers. Layer 1: Hyaline and1.2-1.6 µm thick. Layer 2: thickens by formation of pale yellow sub layers followed by synthesis of closely packed rounded spines. Layer 3: A single hyaline layer, 0.6-1.2 µm thick either is adherent to L2 or more often slightly separable (where it resembles a flexible inner wall).

Glomus fasciculatum. Colour: pale yellow to bright brown with globose to subglobose in shape. Spores produced directly with one or more subtending hyphae attached to it. Spore wall is continuous. Spore wall consisting of three layers (L1, L2, and L3). Spore size ranges from 70-120µm in diameter.

Glomus aggregatum . Spores globose to oval in shape. Size ranges from 40-120µm in diameter, color- pale yellow. Formed singly or in sporocarps. Spore wall consist of 1-2 layers. Sporocarps formed in loose clusters, from a single stalk, diameter ranges from 200-1800 x 200-1400 µm in size.

Glomus mosseae. Brown to orange-brown in colour, shape, globose to sub-globose with an average diameter of 200µm. Presence of three hyaline layers with subtending hyphae attached. Hyphae are double layered.

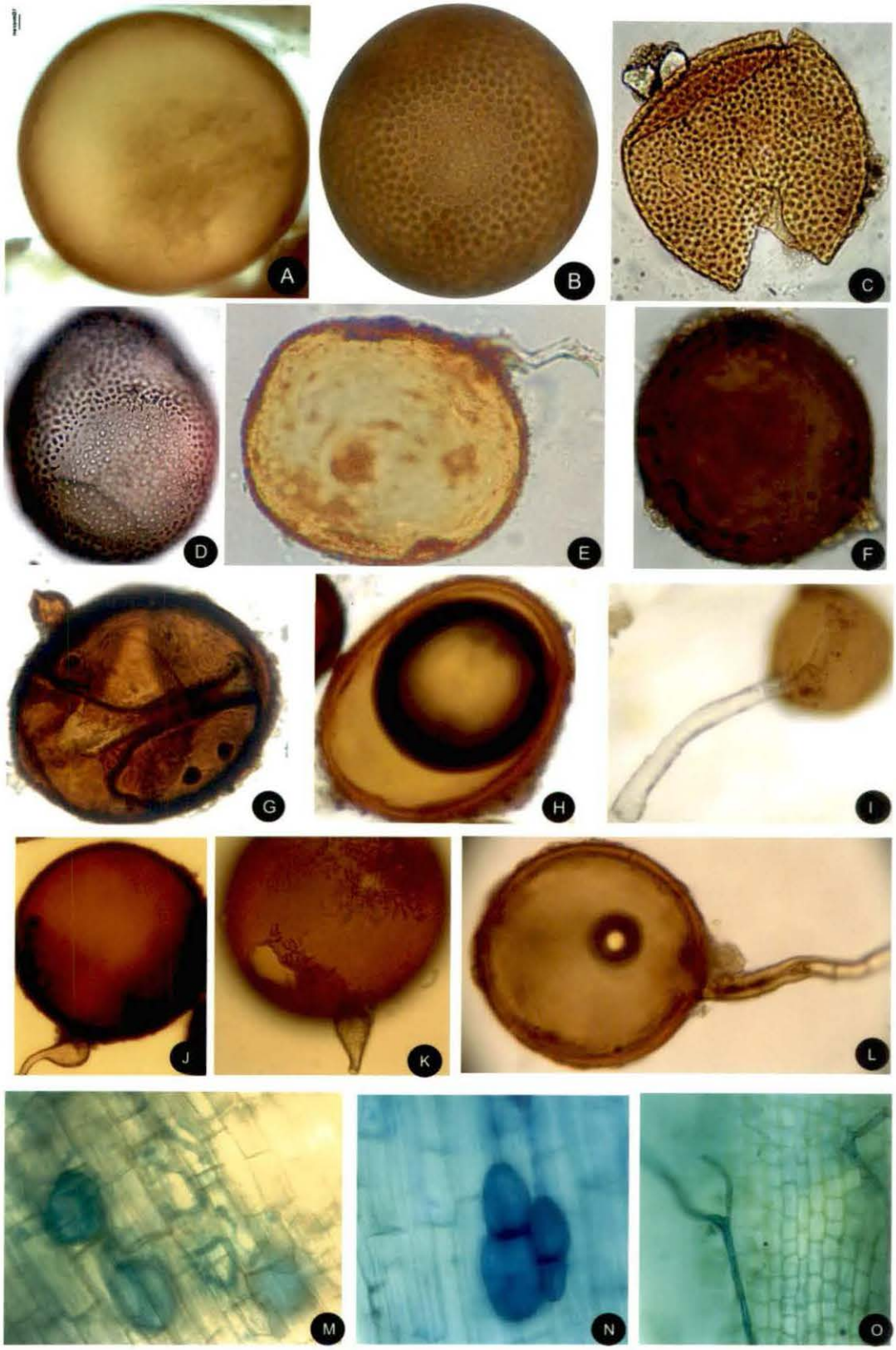

Plate 10 (figs. A-N): AMF spores and root colonization in *Citrus reticulata*. *Glomus sp.* [A], *Acaulospora bireticulata* [B & C], *Acaulospora spinosa*[D], *Glomus mosseae* [E], *Glomus constrictu*m [F], *Gigaspora gigantea*[G], *Scutellospora rubra* [H], *Glomus badium* [I], *Gigaspora margarita* [J & K] ,*Glomus fasciculatum* [L] and colonization of *Citrus reticulata* roots with AM fungi [M, N and O].

Glomus drummondii. Spores occur singly in the soil; develops from the tip of extraradical hyphae of mycorrhizal roots. Spores are golden yellow, globose to subglobose, average diameter 70µm, single subtending hypha attached with the spore. Spore wall consists of three distinct layers.

Glomus constrictum. Spores single in the soil with one subtending hypha, colour brownish orange to dark brown globose to subglobose; 160µm diam in average. Spores consists of one wall containing two layers, most juvenile spores with spore wall layer 1 only. Subtending hypha brownish orange to dark brown; straight or curved; usually markedly constricted at the spore base, sometimes cylindrical, flared to funnel-shaped; composed of two layers continuous with spore wall layers 1 and 2.

Glomus clarum . Spores single in the soil; hyaline to pale yellow, globose to subglobose; 150 µm diam; sometimes ovoid; 90-100 x 140-180 µm; with one subtending hypha. hyaline to pale yellow straight to curved; wall of subtending hypha hyaline to pale yellow ,thick at the spore base; composed of three layers

Glomus aggregatum . Spores formed singly in the soil, in aggregates, in roots, aggregates ranges from 160-1600 x 250-1900 µm, without a peridium, with two to over one hundred spores loosely distributed. Colour of spores are pastel yellow to yellowish brown; mostly globose to subglobose; rarely pyriform to irregular; usually with a single subtending hypha, rarely with two.

Glomus badium. Spores occur in dense sporocarps in the soil and on the surface of vesicular-arbuscular mycorrhizal roots. Sporocarps brownish orange to reddish brown; mainly ovoid to irregular; sometimes globose to subglobose; 250-320 µm diam; with 4-43 spores, radially originating from a hyphal plexus and separated by an interspore mycelium and occasionally by cystidium-like structures.

Gigaspora gigantean. Spores single in the soil; formed terminally or laterally on a bulbous sporogenous cell; greenish yellow (globose to subglobose; 300µm diam; sometimes ovoid; 250x 270 µm. Subcellular structure of spores consists of a spore wall with two layers and one germinal wall.

Gigaspora margarita. Spores produced singly in the soil, blastically at the tip of a bulbous sporogenous cell. Spores yellowish white to sunflower yellow; globose to subglobose; 357 µm diam; sometimes ovoid; 320 X 370 µm. Sporogenous cell orange to brownish yellow. Structure of sporogenous cell composed of two layers. Layer 1 hyaline, 1.7 µm thick approximately. Continuous with spore wall layer 1. Layer 2 orange to brownish yellow, 5.6 µm thick, continuous with spore wall layer 2.

Plate 11 (figs. A-C): Scanning Electron Micrograph of AMF spores obtained from mandarin rhizosphere. *Glomus fasciculatum* [A] Gigaspora gigantea [B] *Acaulospora bireticulata* [C].

Scutellospora pellucid. Spores single in the soil; formed terminally on a bulbous subtending hypha; hyaline to yolk yellow; globose to subglobose; 195µm diam; sometimes ovoid; 130-155 x 160-235 µm.

Scutellospora rubra. Spores color: dark orange-brown to red-brown at maturity, immature spores are white to cream with a rose tint under a dissecting microscope. Shape: globose to subglobose. Size 180 µm in average.

Scanning electron microscopic observation was made of three genera (*Glomus, Gigaspora* and *Acaulospora*) and presented in Plate 11(figs. A-C). Surface of *Glomus fasciculatum* showed adhered hyphae and few pores in the outer surface. The outer hyaline surface was sloughed and eroded (Plate 11,fig.A). SEM image of *Gigaspora gigantea* showing the outer hyaline layer and the conspicuous curved hyphal attachment is evident in Plate 11 fig.B. *Acaulospora bireticulata* with ornamentation consists of hyaline to round-tipped polygonal structures and the attached sporiferous sacule (Plate 11, fig.C).

Percentage of AM population in mandarin rhizosphere obtained from four different locations have been presented in Figure 1. Survey of Mycorrhizal fungi from the rhizosphere soil of mandarin plants grown at different places in Darjeeling hills (Mirik, Kalimpong, Biajanbari and Gorubathan) indicated the genus *Glomus* comprising of six different species, *Gigaspora* and *Acaulospor*a comprising four different species each and *Scutellospora* comprising two different species were found to be predominant AMF.

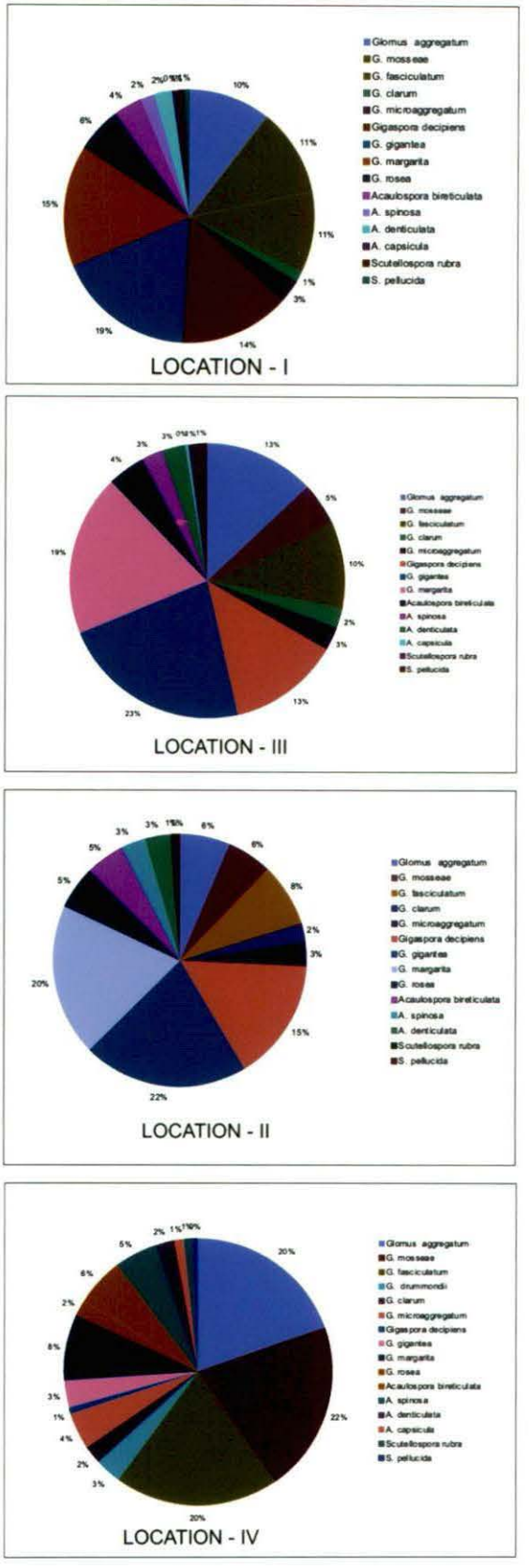

Figure 1: Percentage of AMF population in mandarin rhizosphere of four different locations of mandarin orchard

4.6. *In vitro* screening of fungal and bacterial isolates of mandarin rhizosphere for phosphate solubilizing activities

Phosphorus solubilizers produce clearing zones around the microbial colonies in solid medium. Insoluble mineral phosphates such as tricalcium phosphate or hydroxyapatite are contained in the media. The principal mechanism for mineral phosphate solubilization is the production of organic acids and acid phosphatases play a major role in the mineralization of organic phosphorus in soil. It is generally accepted that the major mechanism of mineral phosphate solubilization is the action of organic acids synthesized by soil microorganisms. Production of organic acids results in acidification of the microbial cell and its surroundings.

4.6.1. Screening in PVK medium

The fungal and bacterial isolates were screened for phosphate solubilizing activity in Pikovskaya (PVK) medium supplemented with tricalcium phosphate (TCP). The pH of the media was adjusted to 7.0 before autoclaving. Sterilized PVK medium was poured into sterilized Petri plates; after solidification of the medium, a pinpoint inoculation of fungal and bacterial isolates was made onto the plates under aseptic conditions. They were incubated at 28±2°C for 7 days with continuous observation for colony diameter. Formation of halo zones around the colony indicated positive results . Solubilization index was evaluated according to the ratio of the total diameter (colony + halo zone) and the colony diameter.

Phosphate solubilizing activities of both fungal isolates and bacterial isolates as evident in PVK medium have been presented in Plate 12, (figs.A-F). Five isolates each among fungal and bacterial isolates showed phosphate solubilizing activities. In case of *Aspergillus niger* (RHS/M492) activity reached to a maximum on the day fourth then remained constant till the end of the week whereas in *Aspergillus mellus* (RHS/M493) solubilization started within 24 h, reached maximum value on day three and remained constant throughout the week (Table 8).

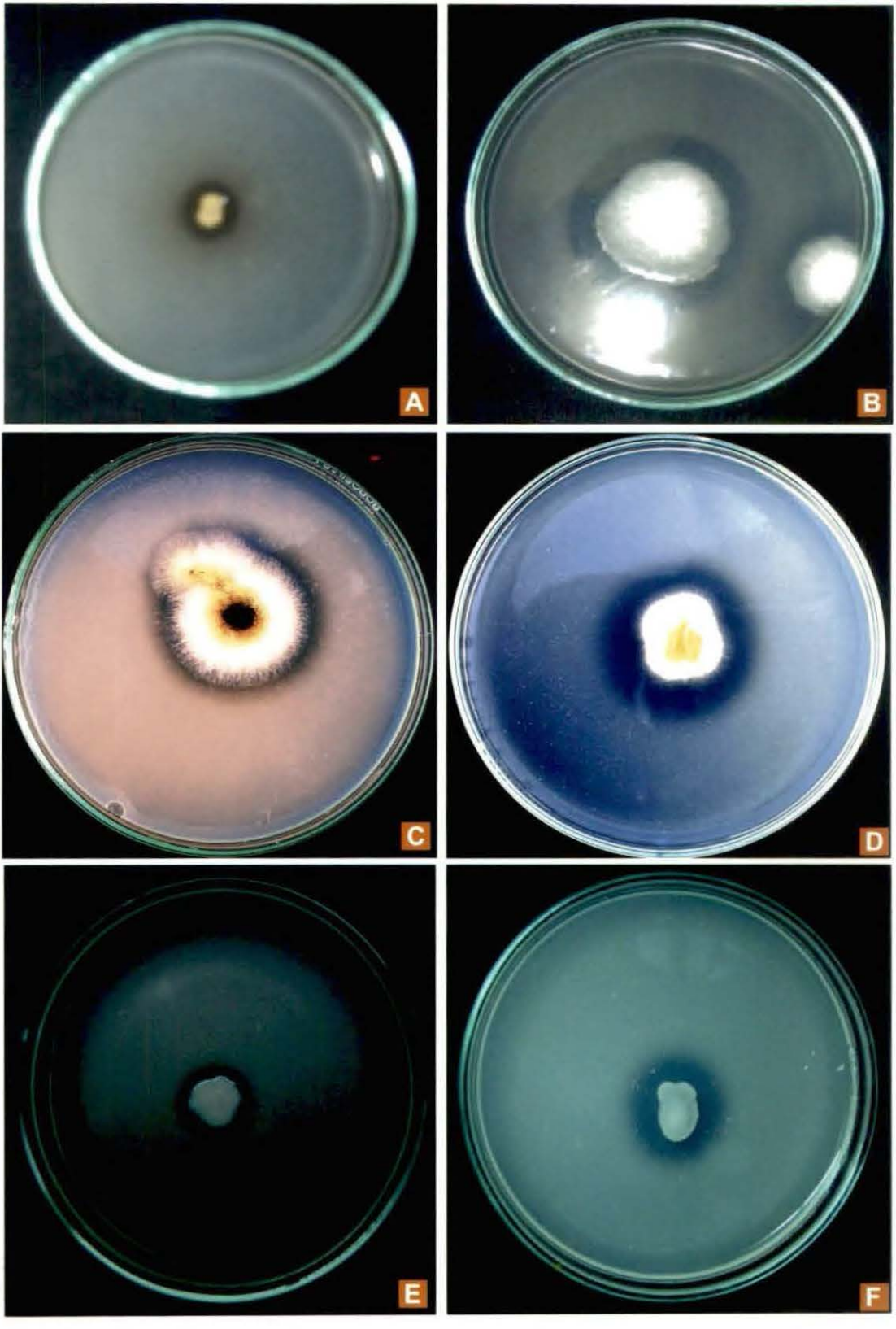

Plate 12 (figs. A-F): *In vitro* characterization of microorganisms for phosphate solubilization in PVK medium. *Aspergillus fumigatus* [A] *A. clavatus* [B] *A. niger* [C] *A. melleus* [D] *Bacillus cereus* [E] and *Bacillus pumilus* [F].

Table 8 : *In vitro* screening for phosphate solubilizing activities by fungal and bacterial isolates of mandarin rhizosphere.

Fungal and Bacterial isolates	Diameter of Clear zone (cm)*					
	24 h	48 h	72 h	96h	120h	144h
Aspergillus niger (RHS/M492)	-	0.1	0.6	0.7	0.7	0.7
A. mellus (RHS/M493)	0.1	0.3	0.5	0.6	0.6	0.6
A. clavtus (RHS/M494)	-	0.2	0.3	0.3	0.5	0.5
A. fumigatus (RHS/M498)	-	0.3	0.3	0.4	0.5	0.6
A. oryzae (RHS/M499)	0.2	0.2	0.3	0.3	0.3	0.4
B. pumilus (B/RHS/C1)	-	0.2	0.4	0.4	0.5	0.6
B.cereus (B/RHS/M2)	0.2	0.4	0.5	0.5	0.5	0.6
B. cereus (B/RHS/M3)	0.1	0.2	0.3	0.4	0.5	0.5
Bacillus sp. (B/RHS/M9)	0.2	0.3	0.5	0.5	0.5	0.5
B. cereus (B/RHS/M10)	0.1	0.2	0.3	0.4	0.5	0.5

*Average of three replicates.

4.6.2. Evaluation in liquid media

Five PSF isolates *Aspergillus niger* (RHS/M492), *A. mellus* (RHS/M493), *A. clavtus* (RHS/M494), *A. fumigatus* (RHS/M498) and *A. oryzae* (RHS/M499) were further evaluated in PVK liquid media amended with tricalcium phosphate (TCP) and rock phosphate (RP) to assess their phosphorus solubilization capacity. Results have been presented in Table 9 ; .The pH of the cultural broth samples dropped significantly as compared to the control where it remained constant around pH 7.0. *Aspergillus niger* (RHS/M492) caused decrease in pH from 7, at the beginning to 3.7 which was attributed to the varying diffusion rates of different organic acids secreted by the tested organisms. *Aspergillus oryzae* (RHS/M499) showed better efficiency of TCP solubilization after seven days of incubation (Table 9)

Table 9 : Evaluation of phosphorus solubilization by fungal isolates in liquid media amended with tricalcium phosphate (TCP) and rock phosphate (RP)

PSF isolates	TCP (mg/l)	pH	RP (mg/l)	pH
A. niger (RHS/M492)	864	3.1	351	3.6
A. mellus (RHS/M493)	875	3.2	346	3.4
A. clavtus (RHS/M494)	883	3.1	355	3.2
A. fumigatus (RHS/M498)	871	4.1	345	3.5
A. oryzae (RHS/M499)	903	3.2	363	2.8

PSF = Phosphate solubilizing fungi; TCP = tricalcium phosphate (P=997mg/l); RP= rock phosphate (P=500mg/l)

The increase of P concentration in the later stages might be due to the action of the fungi on the substrate for demands of nutrients, thus releasing more P from insoluble sources. Increase in the released P during the later stages was also attributed to cell lysis and P precipitation brought about by organic metabolites. The tested isolates reached their maximum biomass level after seven days of incubation. Such result indicated the ability of the fungal strains to solubilize P and change it to available form. Culture media with no TCP produced poor growth.

4.7. *In vitro* interactions of rhizosphere microorganisms of mandarin plants with *M. phaseolina*

Fungal isolates obtained from rhizosphere of mandarin plants excluding the root pathogens as well as bacterial isolates were grown in solid and liquid media and these were tested for their antagonistic activity against root rot pathogen (*M. phaseolina*) by dual paring tests. Their interactions were categorized into three types (A): Homogenous; free intermingling between pairing microorganisms, (B): Overgrowth; pathogen overgrown by the test organisms, (C): Inhibition; a clear zone of inhibition and of growth at time of contact. Different types of reactions developed in the pairing experiments are enlisted in Table10

Table: 10 *In vitro* interactions of fungal and bacterial isolates with *M. phaseolina*

Name of isolates	Type of reactions in test against *Macrophomina phaseolina*
Aspergillus niger (RHS/M492)	Inhibition
A. mellus (RHS/M493)	Overgrowth
A. clavtus (RHS/M494)	Overgrowth
A. fumigatus (RHS/M498)	Overgrowth
A. oryzae (RHS/M499)	Overgrowth
Trichoderma asperellum (RHS/M517)	Inhibition
Emenicella nidulans (RHS/M 509)	Homogenous
Penicillum italicum (RHS/M 510)	Homogenous
Bacillus pumilus B/RHS/C1	Inhibition
Bacillus cereus B/RHS/M2	Overgrowth
Bacillus cereus B/RHS/M3	Overgrowth
Bacillus sp. B/RHS/M4	Overgrowth
Bacillus sp. B/RHS/M5	Overgrowth
Pseudomonas sp. B/RHS/M6	Inhibition
Pseudomonas sp. B/RHS/M7	Homogenous
Pseudomonas sp. B/RHS/M8	Homogenous
Bacillus sp. B/RHS/M9	Overgrowth
Bacillus cereus B/RHS/M10	Overgrowth
Bacillus sp. B/RHS/M11	Homogenous
Bacillus sp. B/RHS/M12	Homogenous
Bacillus sp B/RHS/M13	Homogenous

Plate 13 (figs. A–C): *In vitro* antagonism of *Trichoderma asperellum* against *Macrophomina phaseolina*. Homologous pairing of *M. phaseolina* [A] and *T. asperellum* [B]. Pairing of *T. asperellum* and *M. phaseolina*[C].

In pairing experiment against the root rot pathogen (*M. phaseolina*), *Trichoderma asperellum* inhibited the growth of the pathogen (Plate 13, figs A-C). Another fungal isolate, *Aspergillus niger* also inhibited growth of *M. phaseolina* in pairing experiment.

In vitro pairing experiment was further performed against isolated fungi and bacteria against three root pathogens (*Fusarium solani*, *F. graminearum* and *F. oxysporum*). Inhibition percentage has been calculated against these pathogens and presented in Table 11. *Trichoderma asperellum* was found to be most effective inhibiting growth of the pathogens.

Table 11: Effects of interactions between the fungal isolates and root pathogens

Antagonists	***Fusarium graminearum*** **dia(mm)**			***Fusarium oxysporium*** **dia(mm)**			***Fusarium solani*** **dia(mm)**		
	Antagonist	Pathogen	Inhibition (%)	Antagonist	Pathogen	Inhibition (%)	Antagonist	Pathogen	Inhibition (%)
A.niger RHS/M492	41	30	66.7	27	34	62.2	58	29	67.8
A. mellus RHS/M493	58	29	67.8	58	29	67.8	28	36	60.0
A. clavtus RHS/M494	28	36	60.0	27	36	60.0	29	36	60.0
A. fumigatus RHS/M498	29	36	60.0	58	29	67.8	42	30	66.7
A. oryzae RHS/M499	76	14	84.4	78	15	83.4	67	33	57.8
Trichoderma asperellum RHS/M517	29	36	60.0	42	38	57.8	58	29	67.8
Emenicella nidulans RHS/M 509	27	34	62.2	44	39	56.7	59	29	67.8
Penicillum italicum RHS/M 510									

In vitro pairing experiments were also performed with bacterial isolates against root pathogens. *Bacillus pumilus* inhibited the growth significantly (Plate 14, figs A-D). Maximum percentage inhibition was noted using *Bacillus pumilus*, followed by *Bacillus cereus* and *Pseudomonas* sp. (Table 12).

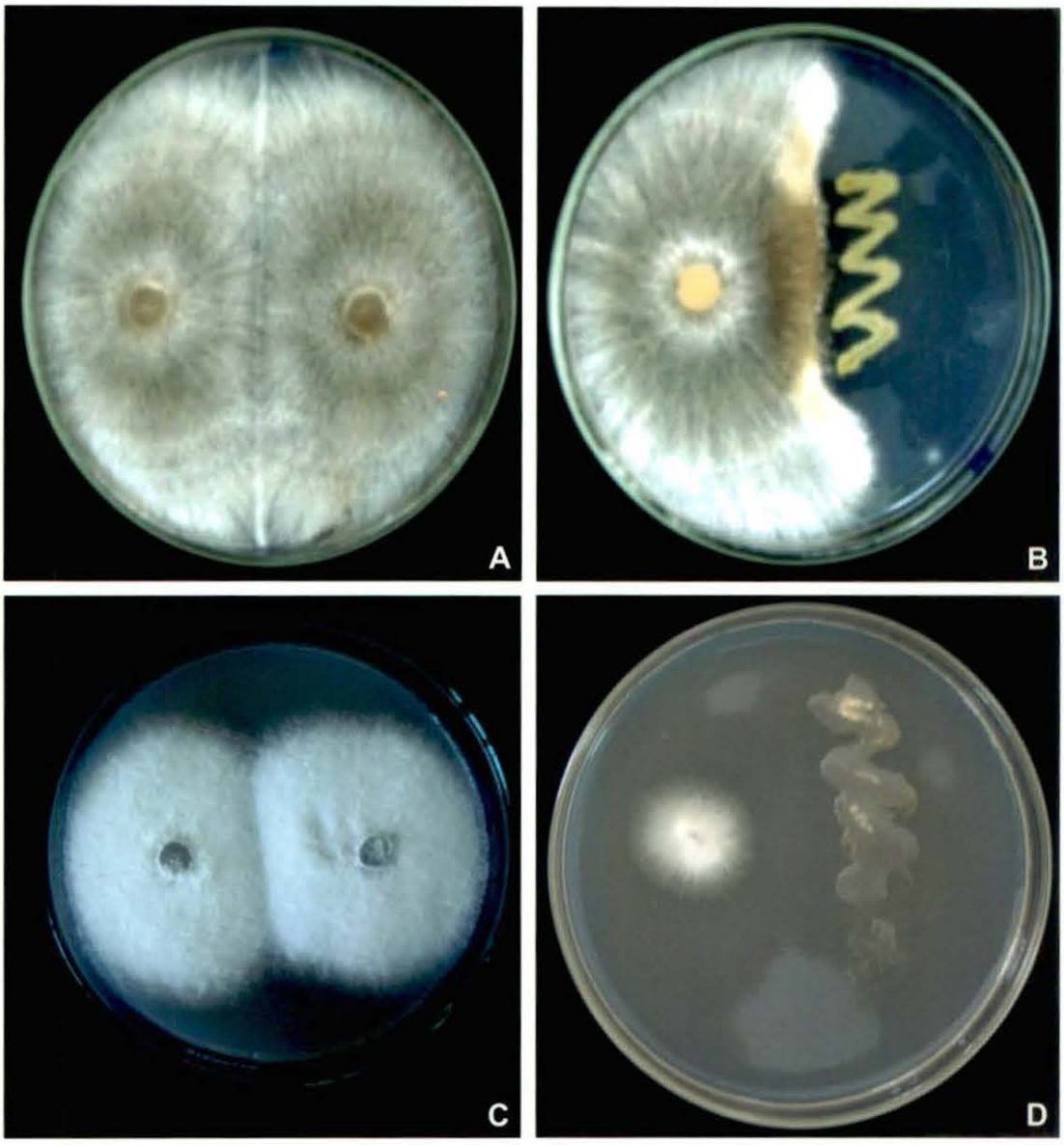

Plate 14 (figs. A–D): *In vitro* homologous pairing of *Rhizoctonia solani* [A] and *F. solani* [C]. *In vitro* antagonism of *Bacillus pumilus* with *R. solani* [B] and *F. solani* [D].

Table 12: Effects of interactions between the bacterial isolates and pathogens

Antagonists	*Rhizoctonia solani* Colony dia(mm)			*Fusarium oxysporum* Colony dia(mm)			*Fusarium solani* Colony dia(mm)		
	Antagonist	Pathogen	Inhibition (%)	Antagonist	Pathogen	Inhibition (%)	Antagonist	Pathogen	Inhibition (%)
Bacillus pumilus B/RHS/C1	77	12	86.7	76	14	84.4	79	12	86.7
Bacillus cereus B/RHS/M2	76	14	84.4	71	19	78.9	73	17	81.1
Bacillus cereus B/RHS/M3	75	13	85.6	61	23	74.4	76	14	84.4
Bacillus sp. B/RHS/M4	75	13	85.6	76	14	84.4	71	19	78.9
Bacillus sp. B/RHS/M5	71	19	78.9	79	12	86.7	73	17	81.1
Pseudomonas sp. B/RHS/M6	79	19	78.9	78	14	84.4	79	13	85.6
Pseudomonas sp. B/RHS/M7	76	14	84.4	76	14	84.4	76	14	84.4
Pseudomonas sp. B/RHS/M8	79	12	86.7	79	12	86.7	79	12	86.7
Bacillus sp. B/RHS/M9	59	29	67.8	26	31	65.6	28	36	60.0
Bacillus cereus B/RHS/M10	42	39	56.7	27	36	60.0	29	36	60.0
Bacillus sp. B/RHS/M11	42	30	66.7	58	29	67.8	27	34	62.2
Bacillus sp. B/RHS/M12	42	38	57.8	28	36	60.0	58	29	67.8
Bacillus sp B/RHS/M13	44	39	56.7	29	36	60.0	27	36	60.0

4.8. Serological and molecular detection of *M. phaseolina*

4.8.1 Soluble protein

Mycelial antigen prepared from the pathogen (*M. phaseolina*) was analysed initially by SDS PAGE. The molecular weight of protein bands visualized after staining with coomassie blue were determined from the known molecular weight marker. Mycelial protein exhibited 23 bands in SDS PAGE ranging in molecular weight (Ca. 95.4 kDa to 10.5 kDa). Bands were of varying intensities and more proteins of lower molecular were present (Plate 15,Fig C) .

4.8.2. Immunological assays

Immunological assays were performed using Polyclonal antibodies (PAb) raised against mycelial protein of *M. phaseolina* in rabbit. Effectiveness of antigen in raising antibodies were checked initially using agar gel double diffusion technique followed by dot immunobinding assay and western blot analysis. Finally Optimization of ELISA was done by considering two variables dilution of the antigen extract and dilution of the antiserum to obtain maximum sensitivity.

4.8.2.1. Immuno-diffusion

Agar gel double diffusion tests was performed using the mycelial antigens of *M. phaseolina* and homologus PAb. Strong precipitation reactions occurred in homologous reactions in immunodiffusion test which was evident by intense precipitation (Plate 15,fig. A). Cross reactive antigen shared between root antigens of manadarin (*C. reticulata*) and polyclonal antibody of two fungal pathogens (*Macrophomina phaseolina* and *Fusarium solani*) were detected using immunodiffusion tests. Antigens were prepared from root samples collected from eight different locations of Darjeeling hills as well as from root pathogens (*M. phaseolina* and *F. solani*). Cross reaction of root antigens prepared from eight different locations were performed with PAbs of *M. phaseolina* and *F. solani* . Strong precipitin reactions were noticed in root samples of four locations Mirik, Sukhia pokhri, Kalimpong Block I and Block II) when reacted with PAb of *M. phaseolina* while root samples of other four locations showed weak precipitin reaction. In the pathogenicity test also root rot index were higher in three locations. Positive reactions were also noticed in heterologous reaction of root antigens and PAb of *F. solani.* However, root antigens prepared from two locations gave no such precipitin reactions using PAb of *F. solani* (Table 13). Common antigenic relationship shared between host and pathogen was evident in such cases where susceptible reactions were noticed in pathogenicity test.

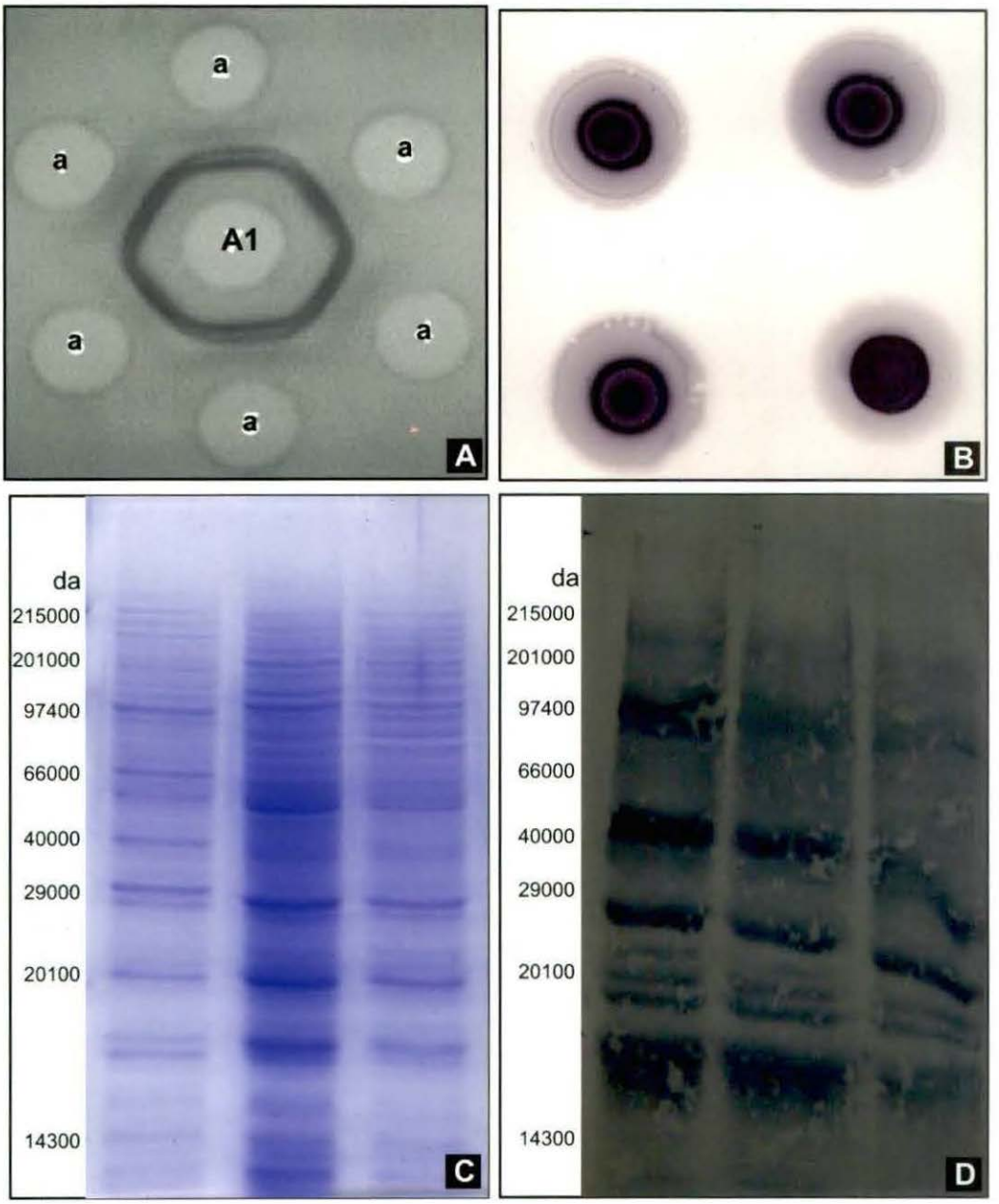

Plate 15 (figs. A-D): Immunodiffusion [A], Dot immunobinding assay [B], SDS PAGE analysis [C] and Western blot analysis[D] of *Macrophomina phaseolina* using mycelial antigen (a) and PAb of *M. phaseolina* (A1)

Table 13 : Detection of cross reactive antigens among *C. reticulata* and *F. solani* and *M. phaseolina* using agar gel double diffusion

Root antigens of *C. reticulata* and root pathogens	PAb	
	F. solani	*M. phaseolina*
Rangli Rangliot	-	±
Bijanbari	-	±
Sukhia Pokhari	+	+
Kurseong	±	±
Mirik	+	+
Kalimpong Block I	+	+
Kalimpong Block II	+	+
Gorubathan	±	±
M. phaseolina	-	+
F. solani	+	-

Common precipitin band (+) present, (-) absent, (±) weak

4.8.2.2. PTA-ELISA

Optimization of PTA- ELISA was done using purified IgGs of known concentration which was predetermined using the referred formula. Goat antirabbit IgG (whole molecule) alkaline phosphatase (Sigma) conjugate (1:10000) and p-nitrophenyl phosphate (100 mg ml^{-1}) were used for PTA-ELISA as enzyme substrate (pNPP), reaction was terminated after 60 min and the absorbance values were recorded as mean of five adjacent wells measured at 405 nm. Root antigens were prepared from healthy as well as artificially inoculated plants of *C. reticulata*. Three days and seven days following inoculation with *F. solani* and *M. phaseolina*, root antigens were prepared along with healthy root antigens and reacted with PAbs of *M. phaseolina* and *F. solani* for comparison. Absorbance values were higher in those root samples which showed susceptible reaction when tested against root pathogens. Following inoculation with the pathogens absorbance values were always higher in artificially inoculated plant roots in comparison with healthy root antigens when tested against PAbs of the respective pathogens (Table 14).

Table 14 : PTA-ELISA values showing reaction of PAbs of *M. phaseolina* and *F. solani* with antigens of healthy and inoculated roots of *C. reticulata*

Citrus saplings Locality	Antigen concentration (40 mg/L) Healthy	Inoculated	
		M.phaseolina[a]	*F. solani*[b]
Rangli Rangliot	0.812	1.264	1.182
Bijanbari	0.890	1.149	1.139
Sukhia Pokhari	1.115	1.774	1.345
Kurseong	0.972	1.880	1.265
Mirik	1.064	1.993	1.876
Kalimpong Block I	1.007	1.887	1.766
Kalimpong Block II	1.187	1.932	1.980
Gorubathan	0.938	1.872	1.765

PAb of *M. phaseolina* and *F. solani* were used at 1:125 dilution
[a] 7 days after inoculation
[b] 3days after inoculation
absorbance at 405 nm

4.8.2.3. Dot immunobinding assay

Dot immunobinding assay using mycelia antigen and PAb of *M. phaseolina* was also standardized. For this, soluble protein obtained from seven-day-old mycelia of *M. phaseolina* were reacted on nitrocellulose paper with PAb of the pathogen (*M. phaseolina*). Results shows development of deep violet colour indicating a positive reactions suggestive of effectiveness of mycelial antigen in raising PAb against the pathogen (Plate 15, fig B).

4.8.2.4. Western blot analysis

Western blot analysis using PAb of *M. phaseolina* was also performed to develop strategies for rapid detection of the pathogen. For this total soluble protein of young mycelia was used as antigen source and SDS-PAGE was performed as described previously followed by probing of the localized antigen with alkaline phosphatase conjugate. The bands on nitrocellulose membrane was compared with corresponding protein bands on the SDS-PAGE. Bands of varying intensities was observed ranging from 14 KDa to 95 KDa (Plate 15, fig. D). Bands of lower molecular weight were more in number. Hence the result suggests that Western blot formats could be used as one of a refined tool for detection of pathogen.

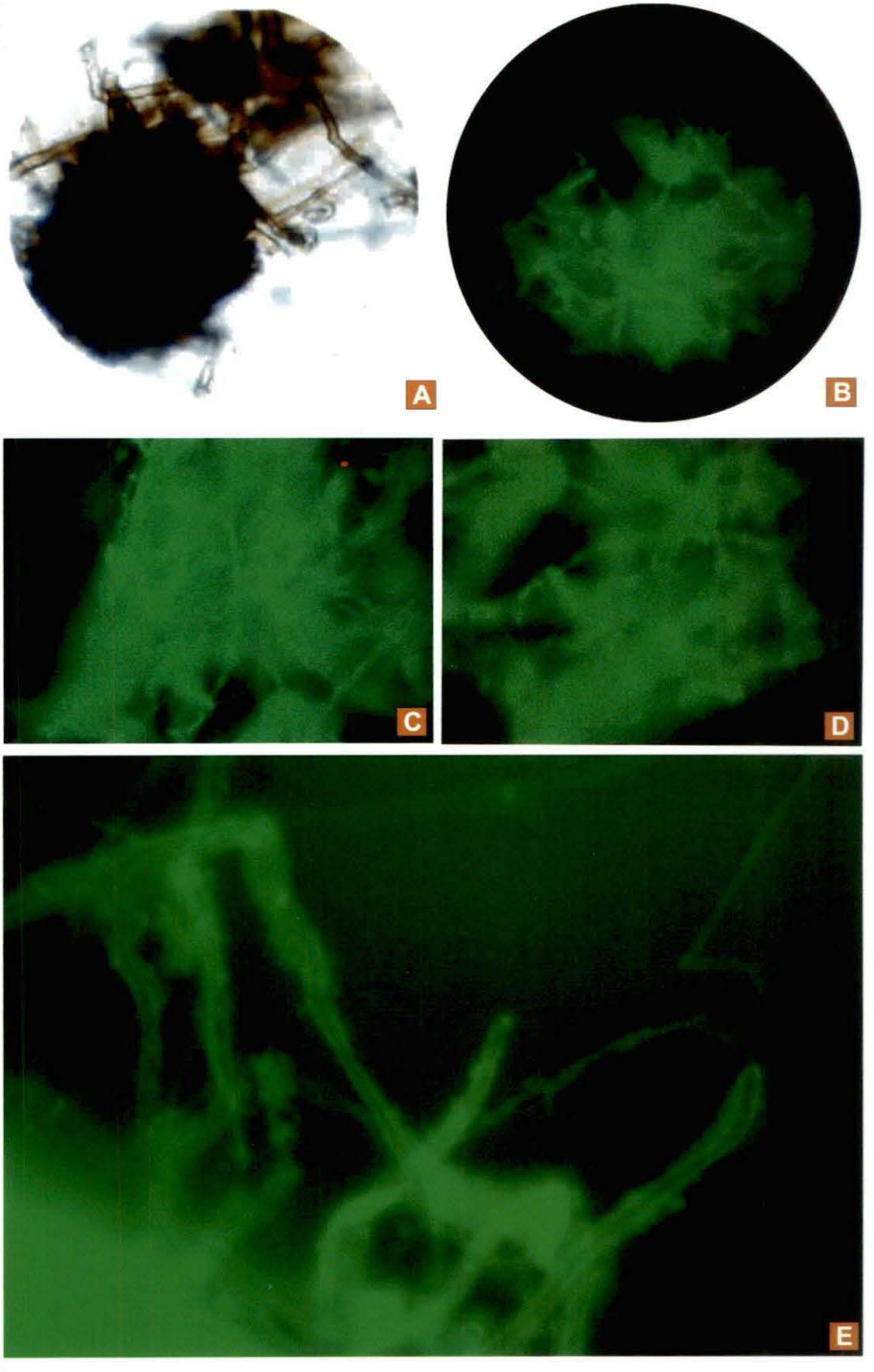

Plate 16 (figs. A-E): Microscopic observation of *Macrophomina phaseolina* under bright field [A]. Mycelia of *M. phaseolina* treated with PAb of the pathogen and labeled with FITC [B - E].

4.8.2.5. Indirect immunofluorescence

Indirect immunoflorescence of hyphae and young sclerotia of *M. phaseolina* were conducted with homologus antibody (PAb of *M. phaseolina*) and reacted with fluorescein isothiocyanate (FITC) labeled antibodies of goat specific for rabbit globulin. Strong apple green fluorescence were evident in both mycelia and scletoria which confirmed the detection of the pathogen (Plate 16, figs A-E). The presence of cross-reactive antigens (CRA) between plant host and parasite that in some instances reflect degrees of compatibility in the parasite association is well known. The unique presence of CRA in hosts and parasites continue to suggest a regulatory role of CRA in host and parasite continues to suggest a regulatory role of CRA in host parasite specificity. Antibody labeling with FITC is known to be one of the powerful techniques to determine the cell or tissue location of CRA shared by host and parasite. Cellular location of major cross reactive antigens shared by *M. phaseolina* in root tissues of *C. reticulata* was determined.

To achieve this antibodies labeled with fluorescein isothiocyanate (FITC) were used to determine location of CRA in cross sections of mandarin roots which provided positive results. Fresh cross sections of healthy roots of *C. reticulata* (Plate 17, figs A-C) were treated with PAb of *M. phaseolina* labeled with FITC conjugate and observed under UV florescent conditions. The root tissues did not exhibit any autofluorescence. On the other hand different tissues of root sections treated with PAb of the pathogen exhibited apple green florescence distributed throughout the root tissue mainly over the outer cortex and the vascular region including pith and pericycle (Plate 17, figs D-F). It appears that CRA may form a continuum between cells of host and pathogen, which favours the growth and establishment in the root tissue.

4.8.3. Molecular detection of *M. phaseolina*

4.8.3.1. ITS-PCR amplification

Genomic DNA of *Macrophomina phaseolina*, *Fusarium solani* and *Fusarium oxysporum* were amplified by mixing the template DNA, with the polymerase reaction buffer, dNTP mix, primers and Taq polymerase. Polymerase Chain Reaction was performed in a total volume of 100 µl, containing 78 µl deionized water, 10 µl 10 X Taq pol buffer, 1 µl of 1 U Taq polymerase enzyme, 6 µl 2 mM dNTPs, 1.5 µl of 100 mM reverse and forward primers and 1 µl of 50 ng template DNA. The following primer pairs were used for ITS PCR (Table 15).

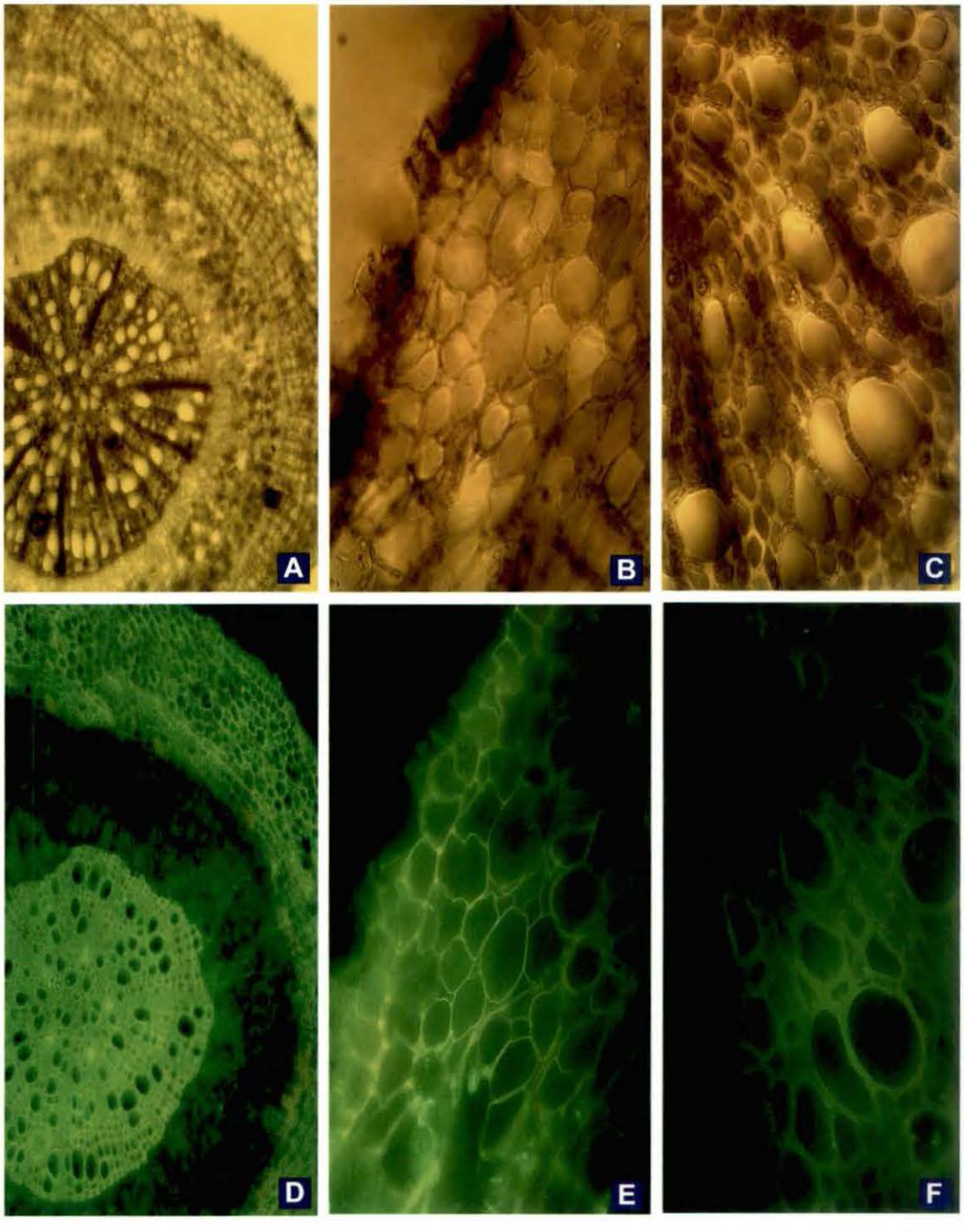

Plate 17 (figs. A-F): Cross section of mandarin root tissue under bright field [A-C]; root tissue treated with PAb of *M. phaseolina* and labeled with FITC.

Table 15 : The nucleotide sequence used for ITS PCR of root pathogens of *C. reticulata*

Seq Name	Primer Seq 5'-3'	Mer	TM	% GC	Amplicaon size (bp)
Macrophomina sp.					
ITS 1	TCCGTAGGTGAACCTGCG	18	61	56%	~620
ITS4	TCCTCCGCTTATTTGATATGC	21	63	59%	
Fusarium sp.					
Fcg17F	TCGATATACCGTGCGATTTCC	21	65	47%	~570
Fcg17R	TACAGACACCGTCAGGGGG	19	66	63%	

PCR was programmed with an initial denaturing at 94°C for 5 min followed by 30 cycles of denaturation at 94 °C for 30 sec, annealing at 59 °C for 30 sec and extension at 70°C for 2 min and the final extension at 72 °C for 7 min in a Primus 96 advanced gradient Thermocycler. PCR product (20 µl) was mixed with loading buffer (8 µl) containing 0.25% bromophenol blue, 40 % w/v sucrose in water, and then loaded in 2% Agarose gel with 0.1 % ethidium bromide for examination with horizontal electrophoresis.

In the present study, main focus was on the ITS regions of ribosomal genes for the construction of primers that can be used to identify *Macrophomina* and *Fusarium*. ITS region of rDNA was amplified using genus specific ITS-1 and ITS4 (for *Macrophomina*) and Fcg17F & Fcg17FR (for *Fusarium*) primers. Amplified products of size in the range of 550-700bp was produced by the all primers. The primer pairs Fcg17F and Fcg17R were found to be highly specific for *Fusarium* genus as reflected in Plate 18 fig.A. (Lanes 9-12), but non specific for *Macrophomina phaseolina*, as no band was detected with this primer pair (Plate 18fig.A, lanes 7&8).

4.8.3.2. DGGE analysis

In the present study *M. phaseolina, F. solani, F. graminearum* and *F. oxysporum* were used for DGGE analysis. For this, 18S rDNA (320 bp with GC clamp) of each isolates were amplified with the forward primer containing GC clamp at NS1 (5'-GTAGTCATATGCTTGTCTC-3') and GCfung (5'-CGCCCGCCGCGCCCCGCGCCC

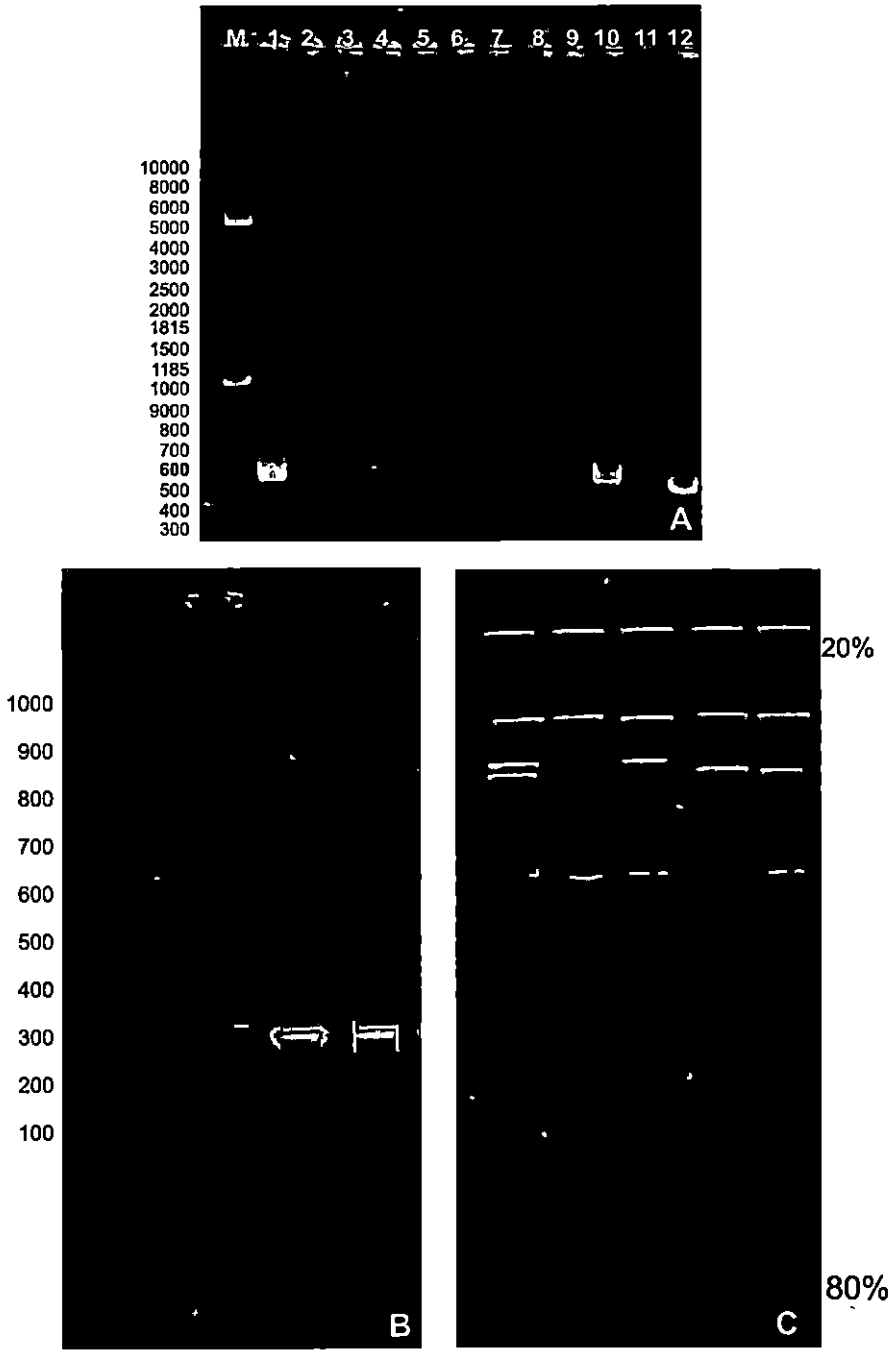

Plate 18 (figs. A-C) : ITS-PCR amplified products of root pathogens [A], Lane M-high range DNA ladder, lanes 1-2,7-8 for *M. phaseolina*, 3-4,9-10 for *F. solani*, 5-6,11-12 for *F. graminearum*. (Primer pairs- Lanes 1-6: ITS1 and ITS4 and Lanes 7-12: Fcg17F and Fcg17R respectively). ITS- PCR amplified products of root pathogens obtained with GC clamp based primer pair [B]. DGGE analysis of root pathogens. Lane 1- Mixture of *M. phaseolina*, *F. solani*, *F. graminearum*, and *F. oxysporum*, lane 2 , *M. phaseolina*, lane 3, *F. solani*, lane 4, *F. graminearum*, and lane 5, *F. oxysporum* [C].

GGCCCG CCGCCCCCGCCCCA TTCCCCGTTAC CCGTTG-3') in 25 µl of reaction mixture containing 1×PCR buffer, 2.5mM $MgCl_2$ (Bangalore Genei, India), 100 ng of the template DNA, 25.0 pmol each of the forward and reverse primers, 250 µM each of dNTPs, and 1 U of *Taq* DNA polymerase. Amplified products of ITS-PCR of root pathogens were resolved in 2% agarose gel (Plate 18, fig.B). The touchdown PCR program was performed which consisted of an initial denaturation at 95°C for 4 min, followed by 35 cycles of 95°C for 1 min, 50°C for 1 min and 10 sec, and 72°C for 2 min then followed by a last extention at 72°C for 8 min. The gels contained 10% (wt/vol) of acrylamide and a range of denaturant concentration from 0% to 100% (formamide and urea). DGGE gels were run at 110 V for 06 hours in 1X TAE buffer (pH 8.0) at 60°C and stained with ethidium bromide. DNA bands on the DGGE gels were excised under UV trans-illumination. The gel photographs were taken and analysed. In this uniform gradient gel of 0% to 100% and shorter run time, individual bands could not separate. However, suitable concentration and running time was optimized using 20 to 80% denaturant and running time 8h at 110V (Plate 18, fig.C). The profile obtained after 8 hours of run time from 20-80 % gradient showed all the bands have co migrated however the profile obtained 12 hours of run time showed a close variation in presence or absence of dominant bands. The DGGE analysis demonstrated that all the corresponding single band on DGGE gels belonged to the isolates of *Macrophomina phaseolina* and other double bands formed for isolates of *Fusarium oxysporum*, *Fusarium solani* and *Fusarium graminearum* gel due to their G+C variation in their ITS region of rDNA . A similar type of distinct band was formed for all selected isolates in the mixture lane but no separate bands were formed in this lane (Plate 18, fig.C lane 1).

4.8.3.3. Sequencing of 18SrDNA region and their phylogenetic analysis

The isolate *Macrophomina phaseolina*, obtained from mandarin root tissue collected from Mirik orchard, the causal organism of root rot of *Citrus reticulata* was finally considered for sequencing of its 18S rDNA region. PCR products produced sequences and chromatogram and 18S rDNA sequence of *M. phaseolina* (Fig 2) that could be aligned and showed satisfactory homology with ex-type strain of *Macrophomina phaseolina* sequences from the NCBI Genbank data base. The priming site of the ITS1 and ITS4 primers were determined in order to confirm that the sequences obtained corresponded to the actual ITS 1 region. ITS1 showed the highest number of nucleotide substitutions, and it was used for the phylogenetic study.

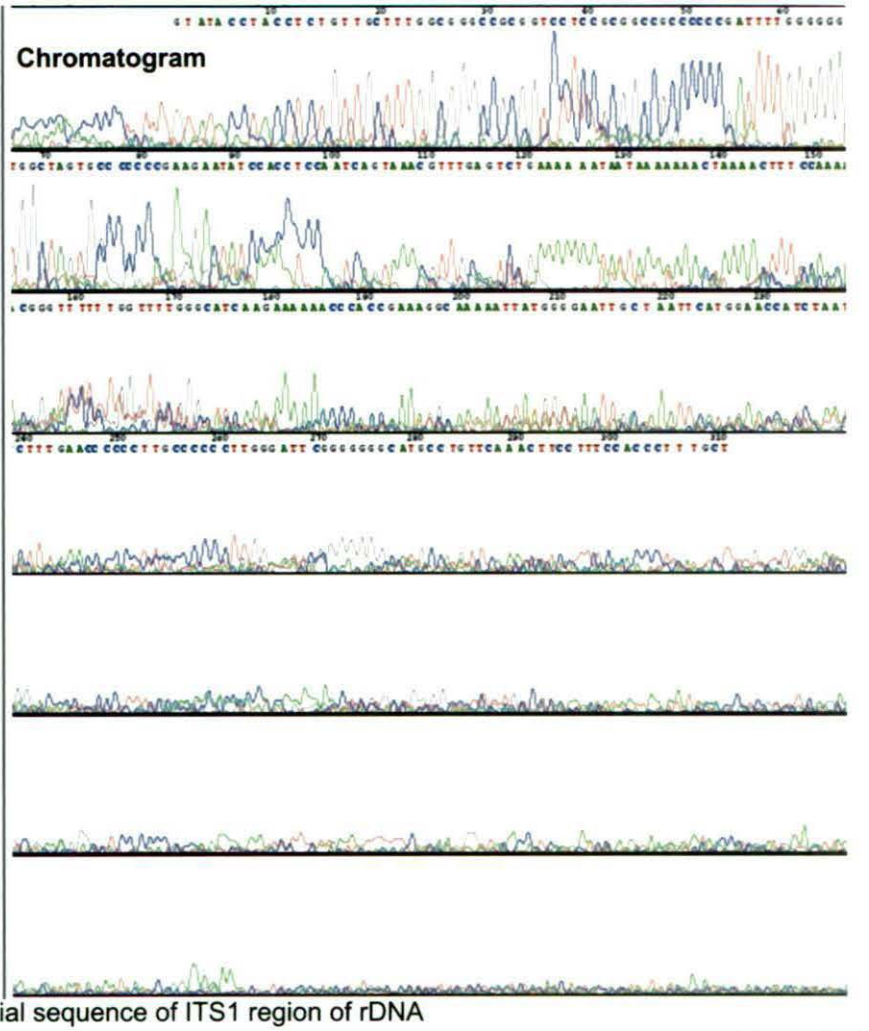

Partial sequence of ITS1 region of rDNA

CGGCGGGCGACGCCTTACGCTCCGAAGCGAGGTGTATTCTACTACGCTTGAGGCA
AGACGCCACCGCCGAGGTCTTTGAGGCGCGCCCGCAAAGGACGGTGCCCAATAC
CAAGCAGAGCTTGAGGGTTGAAATGACGCTCGAACAGGCATGCCCCCCGGAATA
CCAAGGGGCGCAATGTGCGTTCAAAGATTCGATGATTCACTGAATTCTGCAATTC
ACATTACTTATCGCATTTCGCTGCGTTCTTCATCGATGCCAGAACCAAGAGATCCG
TTGTTGAAAGTTTTAGTTTATTTAATATTTTTTTCAGACTGCAACGTTTACTGACTG
GAGTTTGATAGTCCTCTGGCGGGCACTACCCACCCCCCAAAATCGGGGGGCGG

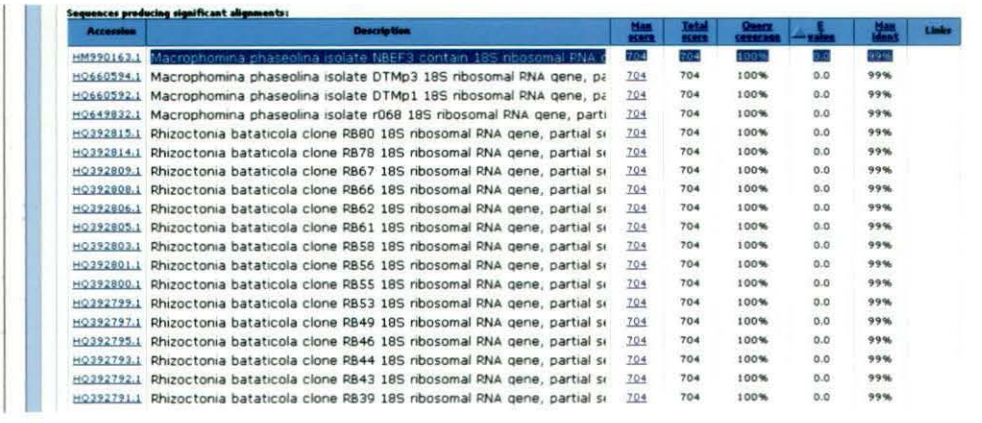

Sequences producing significant alignments:

Accession	Description	Max score	Total score	Query coverage	E value	Max Ident	Links
HM990162.1	Macrophomina phaseolina isolate NBEF3 contain 18S ribosomal RNA g	704	704	100%	0.0	99%	
HQ660594.1	Macrophomina phaseolina isolate DTMp3 18S ribosomal RNA gene, pa	704	704	100%	0.0	99%	
HQ660592.1	Macrophomina phaseolina isolate DTMp1 18S ribosomal RNA gene, pa	704	704	100%	0.0	99%	
HQ649832.1	Macrophomina phaseolina isolate r068 18S ribosomal RNA gene, parti	704	704	100%	0.0	99%	
HQ392815.1	Rhizoctonia bataticola clone RB80 18S ribosomal RNA gene, partial s	704	704	100%	0.0	99%	
HQ392814.1	Rhizoctonia bataticola clone RB78 18S ribosomal RNA gene, partial s	704	704	100%	0.0	99%	
HQ392809.1	Rhizoctonia bataticola clone RB67 18S ribosomal RNA gene, partial s	704	704	100%	0.0	99%	
HQ392808.1	Rhizoctonia bataticola clone RB66 18S ribosomal RNA gene, partial s	704	704	100%	0.0	99%	
HQ392806.1	Rhizoctonia bataticola clone RB62 18S ribosomal RNA gene, partial s	704	704	100%	0.0	99%	
HQ392805.1	Rhizoctonia bataticola clone RB61 18S ribosomal RNA gene, partial s	704	704	100%	0.0	99%	
HQ392803.1	Rhizoctonia bataticola clone RB58 18S ribosomal RNA gene, partial s	704	704	100%	0.0	99%	
HQ392801.1	Rhizoctonia bataticola clone RB56 18S ribosomal RNA gene, partial s	704	704	100%	0.0	99%	
HQ392800.1	Rhizoctonia bataticola clone RB55 18S ribosomal RNA gene, partial s	704	704	100%	0.0	99%	
HQ392799.1	Rhizoctonia bataticola clone RB53 18S ribosomal RNA gene, partial s	704	704	100%	0.0	99%	
HQ392797.1	Rhizoctonia bataticola clone RB49 18S ribosomal RNA gene, partial s	704	704	100%	0.0	99%	
HQ392795.1	Rhizoctonia bataticola clone RB46 18S ribosomal RNA gene, partial s	704	704	100%	0.0	99%	
HQ392793.1	Rhizoctonia bataticola clone RB44 18S ribosomal RNA gene, partial s	704	704	100%	0.0	99%	
HQ392792.1	Rhizoctonia bataticola clone RB43 18S ribosomal RNA gene, partial s	704	704	100%	0.0	99%	
HQ392791.1	Rhizoctonia bataticola clone RB39 18S ribosomal RNA gene, partial s	704	704	100%	0.0	99%	

Figure 2: Chromatogram and 18S rDNA sequence of *Macrophomina phaseolina* (RHS/S565) and significant alignments by BLAST analysis.

Table 16 : **Identified *Macrophoina phaseolina* and comparison with referred NCBI GenBank sequences**

Acc. No.	Source	Sequences	Country
HM990163	plant	534 bp	India
HQ660594	plant	583 bp	China
HQ660593	plant	583 bp	China
HQ660592	plant	583 bp	China
HQ660591	plant	583 bp	China
HQ660590	plant	584 bp	China
HQ660589	plant	583 bp	China
JF710587	plant	583 bp	China
HQ380051	Sunflower	685 bp	Turkey
EF446288	corneal scraping	562 bp	India
HQ713771	*Pinus sylvestris*	511 bp	Switzerland
FJ960442	plant	582 bp	China
EU250575	mulberry	582 bp	China
EF570501	plant	642 bp	Canada
DQ314733	*Glycine hispida*	527 bp	India
DQ233666	*Glycine max*	495 bp	India
DQ233664	okra	441 bp	India
DQ233663	cluster bean	519 bp	India
DQ233662	cluster bean	432 bp	India
(RHS/S565)	*Citrus reticulata*	310bp	India

Although studies involving isolates of *Macrophomina phaseolina* revealed that the 5.8S rRNA gene is as variable as ITS1 regions. The sequence information was then analysed through BLASTn program which indicated that the sequences contain the genetic information of internal transcribed spacer region of rDNA gene of *Macrophomina phaseolina* with 100% similarity . This sequence has been deposited to NCBI genebank to get accession number.

Identified *Macrophomina phaseolina* rDNA gene sequences obtained from NCBI genebank (Table 16) of various host plants were selected for comparison with the rDNA gene sequence of *M. phaseolina* (RHS/S565) isolate of mandarin plant. The sequence alignment of the isolate of *M. phaseolina* (RHS/S565) shows variation in this gene . These available sequences of *Macrophomina phaseolina* from NCBI were used in the pair wise and multiple sequence alignment using Bioedit software (Fig 3) for determining the conserved regions of rDNA gene. There were quite a number of gaps that were introduced in the multiple sequence alignment within the ITS region that were closely related and similar sequence indicated. The evolutionary history was inferred using the UPGMA method. The optimal tree with the sum of branch length = 0.56368608 is shown. The percentage of replicate trees in which the associated taxa clustered together in the bootstrap test (1000 replicates) are shown next to the branches. The tree is drawn to scale, with branch lengths in the same units as those of the evolutionary distances used to infer the phylogenetic tree. The evolutionary distances were computed using the Maximum Composite Likelihood method and are in the units of the number of base substitutions per site. Codon positions included were 1st+2nd+3rd+Noncoding. All positions containing gaps and missing data were eliminated from the dataset (Complete deletion option). There were a total of 294 positions in the final dataset. Phylogenetic analyses were conducted in MEGA4 (Fig 4).

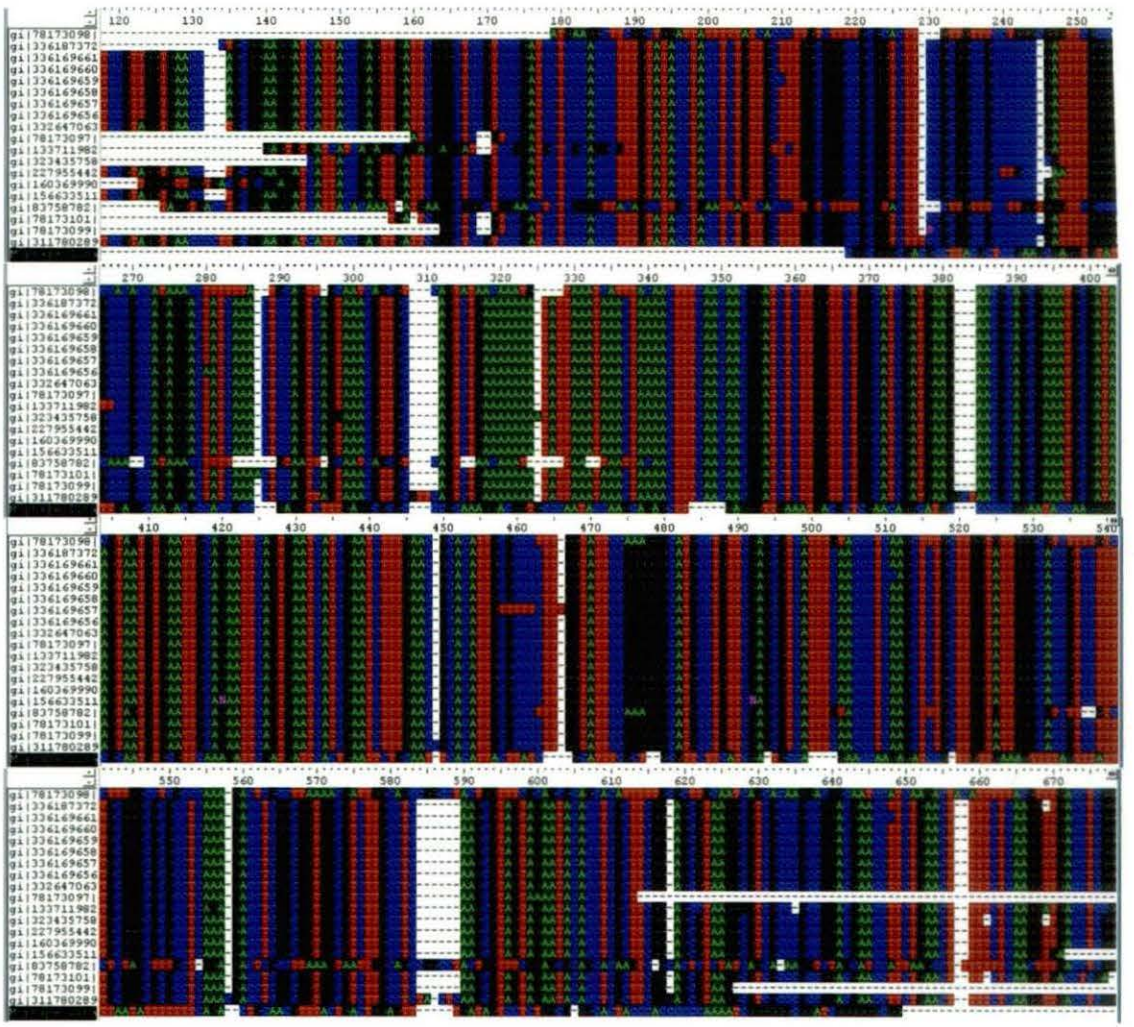

Figure 3: 18S rDNA sequence alignments of *Macrophomina phaseolina* (RHS/S565). Data for other species were gathered from NCBI. The conserved regions of the gene are demonstrated in the different colour.

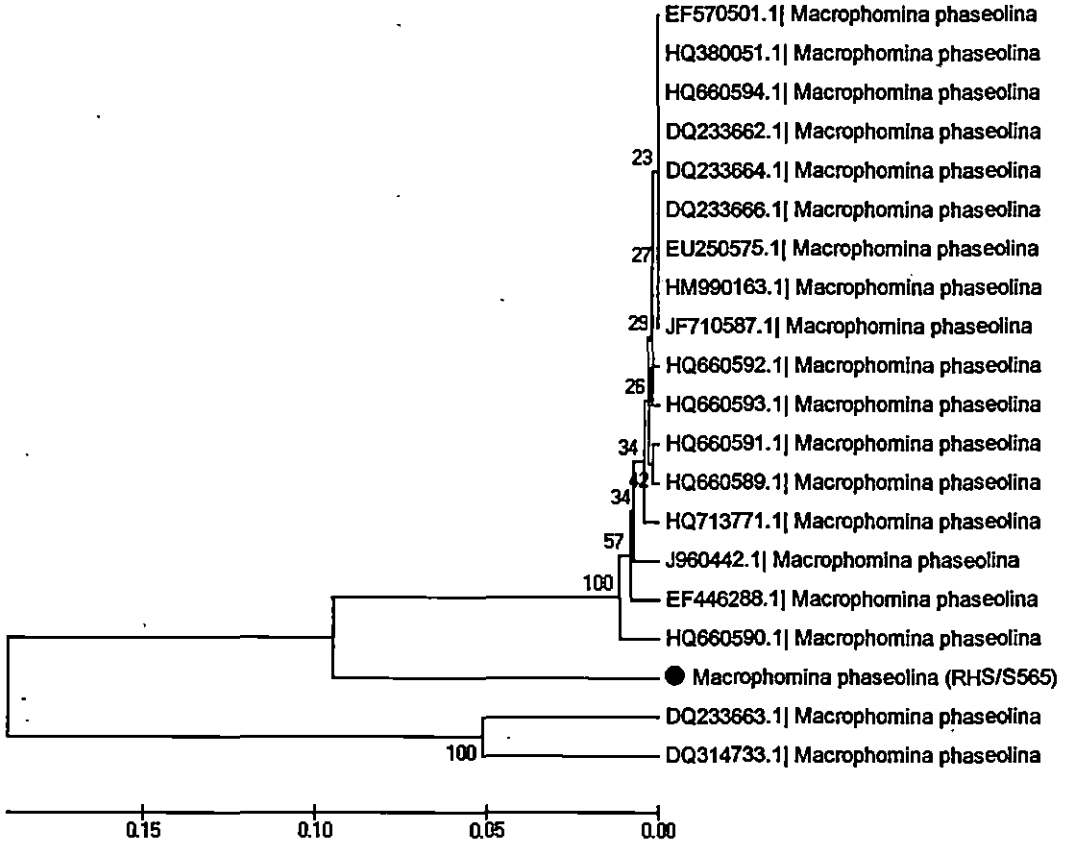

Figure 4: Phylogenetic placement of *Macrophomina phaseolina* (RHS/S565) with extype strains from NCBI genebank

4.9. RAPD-PCR and phylogenetic analysis of microorganisms of mandarin rhizosphere

PCR products of four fungal pathogens of mandarin roots, fungal and bacterial isolates of mandarin rhizosphere using RAPD primers were analysed.

4.9.1. Fungal pathogens of mandarin roots

Four fungal pathogens (*M. phaseolina*, *F. solani*, *F. oxysporum*, and *F. graminearum*) were selected for RAPD-PCR analysis using nine random primers as given in **Table 17**. PCR was programmed with an initial denaturing at 94°C for 4 min. followed by 35 cycles of denaturation at 94°C for 1 min, annealing at 36°C for 1 min and extension at 70°C for 90 s and the final extension at 72°C for 7 min in a Primus 96 advanced gradient Thermocycler. PCR product (20 µl) was mixed with loading buffer (8 µl) containing 0.25 % bromophenol blue, 40 % w/v sucrose in water, and then loaded in 2% Agarose gel with 0.1% ethidium bromide for examination by horizontal electrophoresis. RAPD-PCR products using two primers OPA4 and A-05 of the said four root pathogens resolved in agarose gel have been presented in Plate 19 (figs A&B).

Table 17 Analysis of the polymorphism obtained with RAPD markers in *Macrophomina phaseolina*, *Fusarium solani*, *Fusarium graminearum* and *Fusarium oxysporum*

Sl No.	Seq Name	Total no RAPD bands	Approximate band size (bp).		Monomorphic band	Polymorphic bands	Polymorphic (%)
			Min	Max.			
1.	OPA1	11	200	6000	0	11	100
2	OPA-4	17	200	6000	0	17	100
3.	A-05	15	100	6000	0	15	100
4.	A-11	11	100	6000	0	11	100
5.	OPD-6	03	100	6000	0	03	100
6.	AA-4	04	100	6000	0	04	100
7.	OPB-2	03	100	6000	0	03	100
8.	OPB-3	05	100	6000	0	05	100
9.	OPD-5	04	100	6000	0	04	100
	Total	**73**			**0**	**73**	**100**

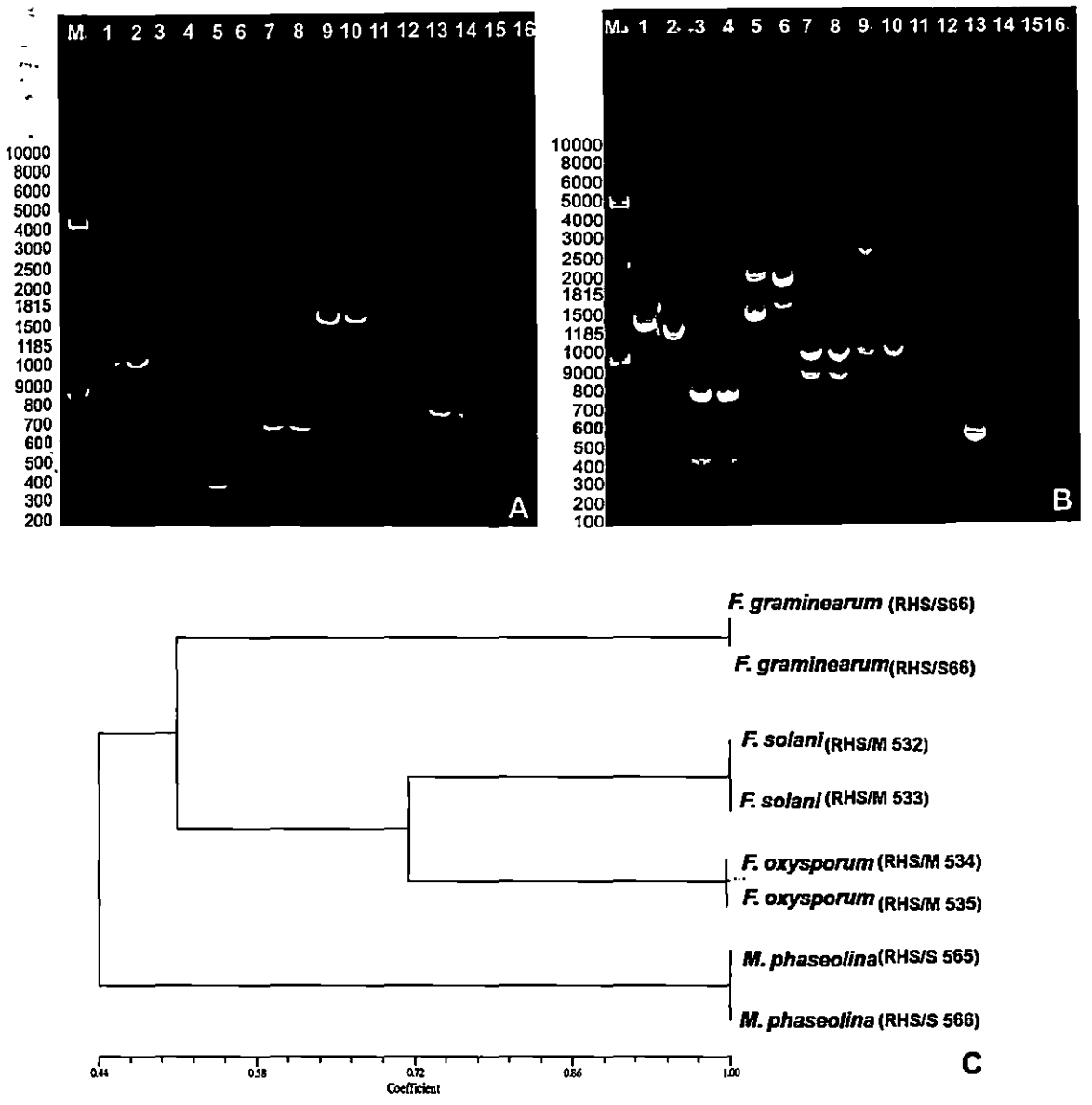

Plate 19 (figs. A-B): RAPD profiles of root pathogens. Lane M-high range DNA ladder, lane 1-2 *M. phaseolina*, 3-4 *F. solani*, 5-6 *F. graminearum*, 7-8 *F. oxysporum* analysed with primer OPA1 & lane 9-10 *M. phaseolina*, 11-12 *F. solani*, 13-14 *F. graminearum*, 15-16 *F. oxysporum* analysed with primer OPA4 [A]; Lane M-high range DNA ladder, lane 1-2 *M. phaseolina*, 3-4 *F. solani*, 5-6 *F. graminearum*, 7-8 *F. oxysporum* analysed with primer A-05 & lane 9-10 *M. phaseolina*, 11-12 *F. solani*, 13-14 *F. graminearum*, 15-16 *F. oxysporum* analysed with primer AA-11; [B] Dendrogram showing the genetic relationships among *Fusarium graminearum*, *F. solani*, *F. oxysporum*, and *Macrophomina phaseolina* based on RAPD analysis using NTSYSPc software [C].

Scoring and data analysis

The image of the gel electrophoresis was documented through Bio-Profil Bio-1D gel documentation system and analysis software. All reproducible polymorphic bands were scored and analysed following UPGMA cluster analysis protocol and computed *In Silico* into similarity matrix using NTSYSpc (Numerical Taxonomy System Biostastiscs, version 2.11W). The SIMQUAL program was used to calculate the Jaccard's coefficients. The RAPD patterns of each isolate was evaluated, assigning character state "1" to indicate the presence of band in the gel and "0" for its absence in the gel. Thus a data matrix was created which was used to calculate the Jaccard similarity coefficient for each pair wise comparison. Jaccard coefficients were clustered to generate dendograms using the SHAN clustering programme, selecting the unweighted pair-group methods with arithmetic average (UPGMA) algorithm in NTSYSpc .

The genetic relatedness among isolates of *F. solani, F. graminearum, F. oxysporum* and *M. phaseolina* were analyzed by random primers OPA-1; OPA-4; OPB2, OPB3, OPD-6; OPD5, A-5; AA-04 and AA-11 to generate reproducible polymorphisms. All amplified products with the primers had shown polymorphic and distinguishable banding patterns which indicate the genetic diversity of all isolates. A total 73 reproducible and scorable polymorphic bands ranging from approximately 200bp to 6000bp were generated in *M. phaseolina, F. solani, F. graminearum* and *F oxysporum*. In the RAPD profiles showed that primer A-5 and OPA4 scored highest bands which ranged between 200bp to 6000bp. Relationships among the isolates was evaluated by cluster analysis of the data based on the similarity matrix. The Dendogram was generated by unweighted pair-group methods with arithmetic mean (UPGMA) using NTSYSpc software (Plate 19, fig.C).

4.9.2. Fungal isolates of mandarin rhizosphere

Fifteen fungal isolates obtained from mandarin rhizosphere were further selected for RAPD-PCR analysis using following nine random primers (Table 18). PCR was programmed with an initial denaturing at 94°C for 4 min. followed by 35 cycles of denaturation at 94°C for 1 min, annealing at 36°C for 1 min and extension at 70°C for 90 s and the final extension at 72°C for 7 min in a Primus 96 advanced gradient Thermocycler. PCR product (20 µl) was mixed with loading buffer (8 µl) containing 0.25 % bromophenol blue, 40 % w/v sucrose in water, and then loaded in 2% Agarose gel with 0.1% ethidium bromide for examination by

horizontal electrophoresis. RAPD-PCR products using one primer OPA4 of the said fifteen fungal isolates of mandarin rhizosphere resolved in agarose gel have been presented in Plate 20 fig.A.

Table 18 : Analysis of the polymorphism obtained with RAPD markers in fungal isolates of mandarin rhizosphere.

Sl No.	Seq Name	Total no RAPD bands	Approximate band size (bp).		Monomorphic band	Polymorphic bands	Polymorphic (%)
			Min	Max.			
1.	OPA1	04	200	6000	0	04	100
2	OPA-4	06	200	6000	0	06	100
3.	A-5	03	100	6000	0	03	100
4.	A-11	05	100	6000	0	05	100
5.	OPD-6	03	100	6000	0	03	100
6.	AA-4	07	100	6000	0	07	100
7.	OPB-2	05	100	6000	0	05	100
8.	OPB-3	04	100	6000	0	04	100
9.	OPD-5	03	100	6000	0	03	100
	Total	**40**			**0**	**40**	**100**

Scoring and data analysis

The image of the gel electrophoresis was documented through Kodac gel documentation system and analysis software. All reproducible polymorphic bands were scored and analysed following UPGMA cluster analysis protocol and computed *In Silico* into similarity matrix using NTSYSpc (Numerical Taxonomy System Biostastiscs, version 2.11W). The SIMQUAL program was used to calculate the Jaccard's coefficients. The RAPD patterns of each isolate was evaluated, assigning character state "1" to indicate the presence of band in the gel and "0" for its absence in the gel. Thus a data matrix was created which was used to calculate the Jaccard similarity coefficient for each pair wise comparison. Jaccard coefficients were clustered to generate dendograms using the SHAN clustering programme,

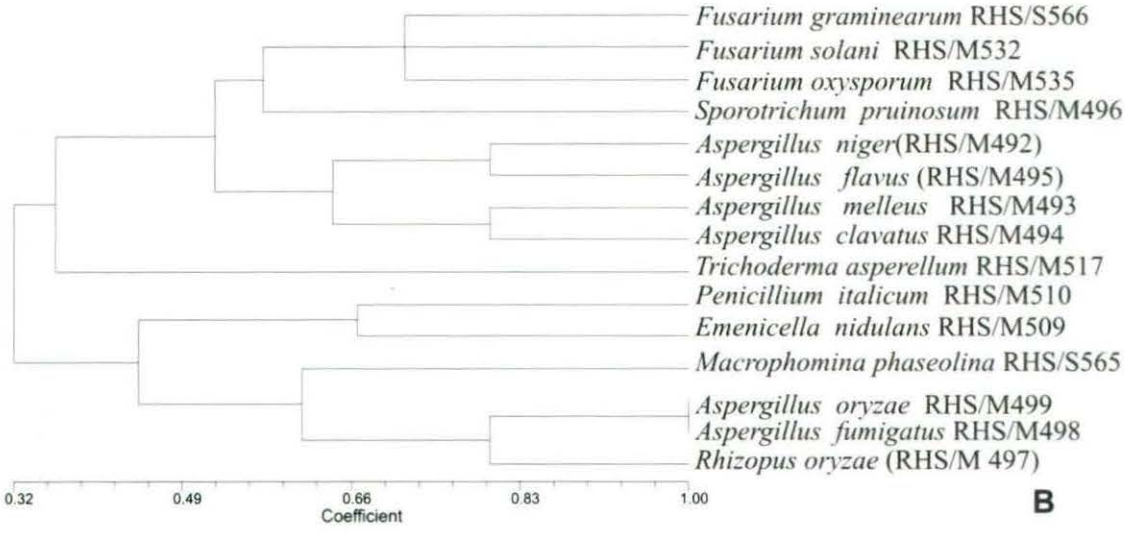

Plate 20 (figs. A-B): RAPD profiles of fungal isolates of mandarin rhizosphere obtained using primer OPA 4 [A] . Lane M-high range DNA ladder, lane 1, *A. niger* RHS/M492, lane 2, *Aspergillus flavus* (RHS/M495), lane 3, *A. mellus* RHS/M493, lane 4, *A. clavatus* RHS/M494, lane 5, *A. fumigatus* RHS/M498, lane 6 , *A. oryzae* RHS/M499, lane 7, *F. graminearum* RHS/S566, lane 8, *F. solani* RHS/M532, lane 9, *F. oxysporum* RHS/M535, lane 10, *Sporotrichum pruinosum* RHS/M496, lane 11, *Macrophomina phaseolina*, RHS/S565, lane 12, *Trichoderma asperellu*m RHS/M517, lane 13, *Penicillium italicum* RHS/M510, lane 14, *Emericella nidulans* RHS/M509, lane 15, *Rhizopus oryzae* (RHS/M 497). Dendogram showing phylogenetic relationship between different fungal isolates based on RAPD banding pattern [B].

selecting the unweighted pair-group methods with arithmetic average (UPGMA) algorithm in NTSYSpc .

The genetic relatedness among isolates of rhizopshere of mandarin were analyzed by random primers to generate reproducible polymorphisms. All amplified products with the primers had shown polymorphic and distinguishable banding patterns which indicate the genetic diversity of all isolates. A total 40 reproducible and scorable polymorphic bands ranging from approximately 200bp to 2000bp were generated. In the RAPD profiles showed that primer AA-4 and OPA4 scored highest bands which ranged between 200bp to 6000bp. Relationships among the isolates was evaluated by cluster analysis of the data based on the similarity matrix. The Dendogram was generated by unweighted pair-group methods with arithmetic mean (UPGMA) using NTSYSpc software (Plate 20,fig.B).

4.9.3. Bacterial isolates of mandarin rhizosphere

The broth cultures of bacterial isolates (*B. pumilus* . B/RHS/C1, *B. cereus* B/RHS/M2, *B. cereus* B/RHS/M3, *Bacillus sp.* , *Bacillus sp.* B/RHS/M4 B/RHS/M5, *Psedomonus sp.* B/RHS/M6, *Psedomonus sp.* B/RHS/M7, *Psedomonus sp.* B/RHS/M8, *Bacillus sp.* B/RHS/M9, *B. cereus* B/RHS/M10, *Bacillus sp* B/RHS/M11, *Bacillus sp.* B/RHS/M12 and *Bacillus sp.* B/RHS/M13) were centrifuged at 10,000 rpm at 28°C for 5 mins and the pellets were collected by discarding the supernatant. The pellets were washed thrice with distilled water and resuspended in 0.5ml of CTAB buffer was and incubated at 37°C for 3 hrs. Then 10 µl proteinase K solution (20mg/ml) was added and it was allowed to incubate at 65°C for 3min. The lysate was extracted with equal volume of tris water saturated phenol: chloroform: isoamylalcohol (25:24:1) and then centrifuged at 10,000 rpm for 5 min. The aqueous phase was collected in clean tube and 2 volume of chilled absolute ethanol was added to this aqueous phase. The mixture was centrifuged at 10,000 rpm for 5 mins at 4°C, the pellet was air dried and finally dissolved in 40µl TE buffer and stored at 4°C. Genomic DNA was re suspended in 100 µl 1 X TE buffer and incubated at 37°C for 30 min with RNAse . After incubation the sample was re-extracted with PSI (Phenol: Chloroform: Isoamylalcohol) solution and RNA free DNA was precipitated with chilled ethanol. The yield of DNA was determined spectrophotometrically as 24 µg/g of mycelial mat. The purity of DNA genome samples as indicated by A_{260}/A_{280} ratio (Table 19) and DNA quantity was evaluated by 0.8% agarose gel electrophoresis.The quantity and quality of the genomic DNA, isolated from thirty different isolates was checked on 0.8% agarose gel electrophoresis. The DNA from all isolates produced clear sharp bands, indicating good quality of DNA.

polymerase enzyme, 6µl 2mM dNTPs, 1.5µl of 100mM RAPD primers and 1µl of template

Table 19 : Spectrophotometrical A_{260}/A_{280} ratio of isolated genomic DNA

Organisms	A_{260}	A_{280}	A_{260}/A_{280}	Organisms	A_{260}	A_{280}	A_{260}/A_{280}
B. pumilus. B/RHS/C1	0.276	0.148	1.86	*Psedomonus sp.* B/RHS/M8,	0.379	0.183	2.07
B. cereus B/RHS/M2	0.379	0.183	2.07	*Bacillus sp.* B/RHS/M9,	0.276	0.148	1.86
B. cereus B/RHS/M3	0.276	0.148	1.86	*B. cereus* B/RHS/M10,	0.379	0.183	2.07
Bacillus pumilus. B/RHS/M4	0.197	0.137	1.44	*Bacillus sp* B/RHS/M11,	0.276	0.148	1.86
Bacillus sp. B/RHS/M5	0.276	0.148	1.86	*Bacillus sp.* B/RHS/M12	0.197	0.137	1.44
Psedomonus sp. B/RHS/M6	0.379	0.183	2.07	*Bacillus sp.* B/RHS/M13	0.276	0.148	1.86
Psedomonus sp. B/RHS/M7	0.379	0.183	2.07				

RAPD-PCR

All thirteen bacterial isolates were taken up for RAPD-PCR amplification. Genomic DNA was amplified by mixing the template DNA, with the polymerase reaction buffer, dNTP mix, primers and Taq polymerase. Polymerase chain reaction was performed in a total volume of 100µl, containing 78µl deionized water, 10µl 10X taq polymerase buffer, 1µl of 1U Taq polymerase enzyme, 6µl 2mM dNTPs, 1.5µl of 100mM RAPD primers and 1µl of template DNA. Two random decamers (OPA1 and OPA4) were used to prepare the RAPD profiles of the isolates (Table 20). PCR was programmed with an initial denaturing at 94°C for 5 min, followed by 30 cycles of denaturation at 94°C for 30sec, annealing at 59°C for 30 sec and extension at 70°C for 2 min and the final extension at 72°C for 7 min in a Primus 96 advanced gradient Thermocycler. After RAPD-PCR amplifications, all amplified DNA products were resolved by electrophoresis on agarose gel(2%) in TAE(1X) buffer, stained with ethidium bromide and photographed. RAPD-PCR products using two primers OPA4 and OPA1 of the said thirteen bacterial isolates of mandarin rhizosphere resolved in agarose gel have been presented in Plate 21 figs.A&B (Table 21).

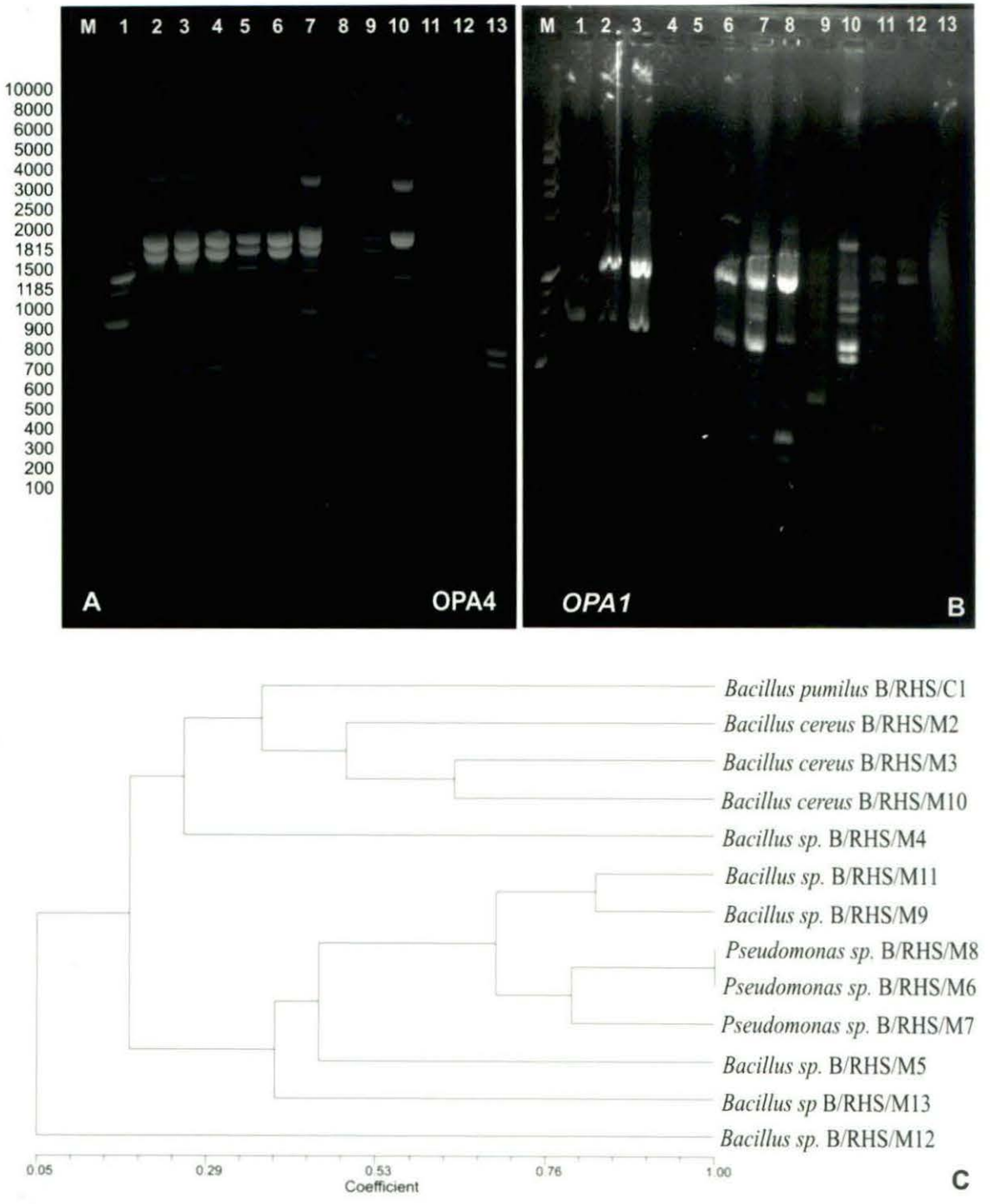

Plate 21 (figs. A-B): RAPD profiles of bacterial isolates obtained using primers OPA 4 [A] and OPA 1[B]. Lane M-high range DNA ladder, lane1, *Bacillus pumilus* B/RHS/C1, lane 2, *Bacillus cereus* B/RHS/M2, lane 3, *Bacillus cereus* B/RHS/M3, lane 4, *Bacillus* sp. B/RHS/M4, lane 5, *Bacillus* sp. B/RHS/M5, lane 6, *Pseudomonas* sp. B/RHS/M6, lane 7, *Pseudomonas* sp. B/RHS/M7 lane 8, *Pseudomonas* sp. B/RHS/M8, lane 9, *Bacillus* sp. B/RHS/M9 lane 10, *Bacillus cereus* B/RHS/M10, lane 11, *Bacillus* sp. B/RHS/M11, lane 12, *Bacillus* sp. B/RHS/M12, lane 13, *Bacillus* sp B/RHS/M13. Dendogram showing phylogenetic relationship between different bacterial isolates based on RAPD banding pattern [C].

Table 20 : The nucleotide sequence used for RAPD PCR

Seq Name	Primer Seq 5'-3'	Mer	TM	% GC
OPA1	CAGGCCCTTC	10	38.2	70%
OPA-4	AATCGGGCTG	10	39.3	60%

Table 21 Analysis of the polymorphism obtained with RAPD markers

Sl No.	Seq Name	Total no RAPD bands	Approximate band size (bp).		Monomorphic band	Polymorphic bands	Polymorphic (%)
			Min	Max.			
1.	OPA1	04	100	2000	0	3	100
2	OPA-4	05	100	1000	0	4	100

Phylogenetic analysis

The genetic relatedness among isolated thirty phosphate solubilizer bacterial isolates were analysed by two random primers (OPA1 and OPA4) to generate reproducible polymorphisms. All amplified products with the primers had shown polymorphic and distinguishable banding patterns which indicate the genetic diversity of isolates. RAPD profiles showed that primer OPA4 scored highest bands 7 (Table 21). Relationships among the isolates was evaluated by cluster analysis of the data based on the similarity matrix. The dendogram was generated by unweighted pair-group methods with arithmetric mean (UPGMA) using NTSYSpc software (Plate 21 fig.C). Similarity co-efficient ranged from 0.65-1.0. Based on the results obtained all nine isolates can be grouped into five main clusters grouped into *Bacillus pumilus*, *Bacillus cereus*, *Bacillus sp* and *Pseudomonas sp*.

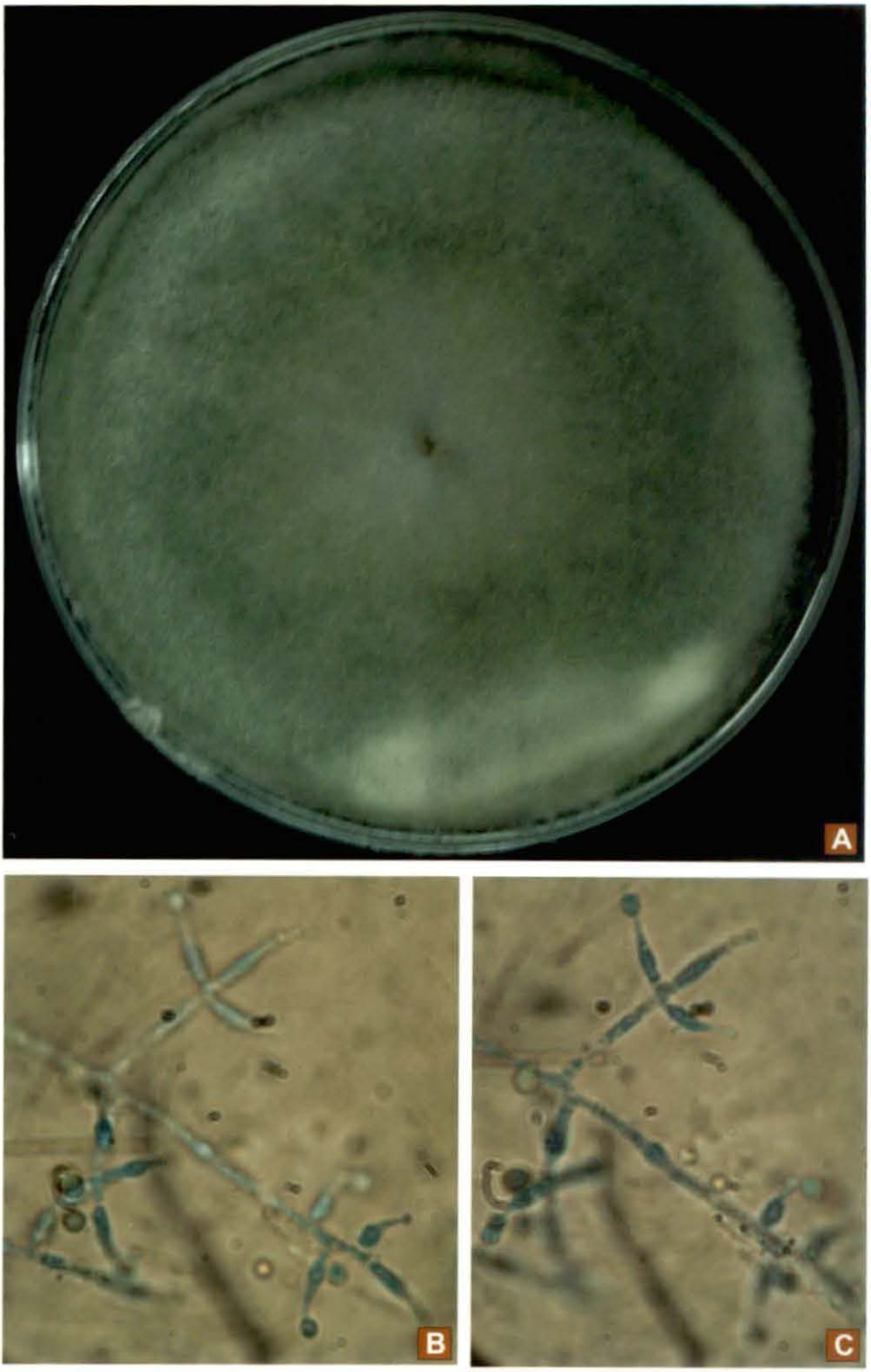

Plate 22 (figs. A-C): Radial growth of *Trichoderma asperellum* [A] and microscopic observation showing phialides and hyphae [B & C].

4.10. Morphological and molecular identification of a potential BCA isolate

4.10.1. Scanning electron microscopy

Isolate of *Trichoderma asperellum* (Plate 22 fig.A) which showed *in vitro* antagonistic activity against *Macrophomina phaseolina, Fusarium solani, Fusarium oxysporum* and *Fusarium graminearum* were selected as potential BCA isolate for SEM study. Before this, the isolate of *T. asperellum* was also taken for determining their phialide and conidia structures. Drops of spore suspension were placed on clean grease free glass- slides, mounted with lacto phenol cotton blue, covered with cover slip and sealed. The slides were then observed under the microscope following which spore characteristics were determined and size of spore measured. Microscopic observations under bright field of all these isolates have been presented in Plate 22 (figs.B&C). Detailed informations on conidiophore, conidia and phialides of these isolates have been presented in Table 20.

Table 20 Morphological characteristics of different isolates of *Trichoderma asperellum*

Morphological characteristics	*Trichoderma asperellum* (RHS/M 517)
Conidiophores Central axis (µm)	1.9 X 4.2
Conidia (µm)	2.0x 1.5
Phialide dimensions (µm)	
[width where arising from a cell]	
length	9.8
width	3.8
widest point	4.1
width at base	4.1

Scanning electron microscopic observations of the conidia of *T. asperellum* was also made. Photographic presentations of *T. asperellum* has been presented in (figs.A-C). Results revealed that isolate had smooth conidial surfaces. The conidia were an irregular pyramidal shape with a diameter within the 150 to 250 nm size range. The conidia of different isolates varied in shape from globose to sub globose and in size, with diameters ranging from 4.0 to 4.5 µm. Fragments of what appeared to be a thin layer of tissue were observed on and around the conidia in most conidial preparations.

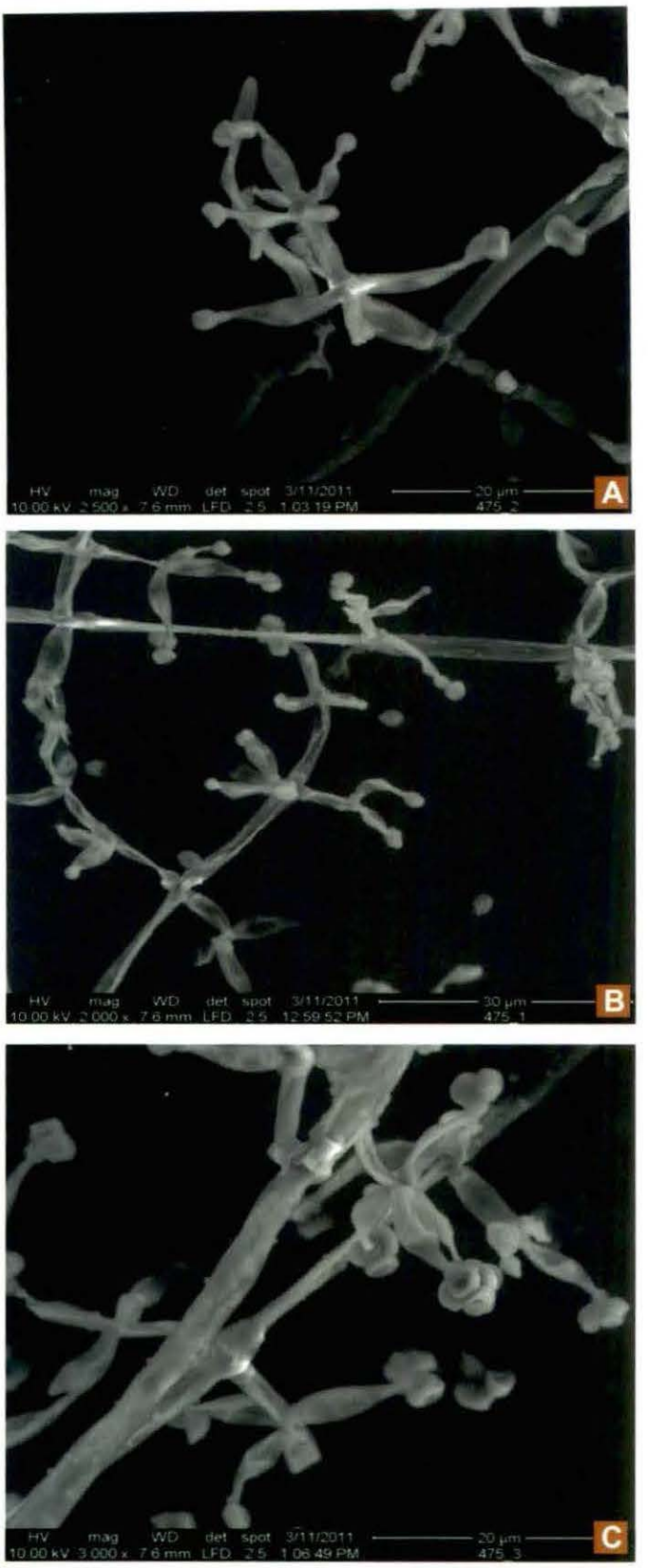

Plate 23 (figs. A-C): Scanning Electron Micrograph of *Trichoderma asperellum*.

4.10.2. 18S rDNA sequencing

Genomic DNA was prepared from *T. asperellum* isolate -RHS/M517 using lysis buffer containing 250 mM Tris-HCl (pH 8.0), 50 mM EDTA (pH8.0), 100 mM NaCl and 2% SDS,following the method as described in detail in Materials and Methods. DNA was precipitated with chilled ehanol (100%), pelleted by centrifuging at 12000 rpm for 15 min, washed in 70% ethanol by centrifugation and finally the pellets were air dried and suspended in TE buffer (pH 8.0). Genomic DNA was resuspended in 100 µl 1 X TE buffer and incubated at 37°C for 30 min with RNAse (60µg). The quality and quantity of DNA was analyzed both spectrophotometrically and in 0.8% agarose gel which produced clear sharp bands, indicating good quality of DNA. The result revealed that RNA free DNA was yielded and the size of DNA of each isolates ranging from 1.5-1.8 kb. Genomic DNA was amplified by mixing the template DNA (50 ng), with the polymerase reaction buffer, dNTP mix, primers and Taq polymerase. Polymerase Chain Reaction was performed in a total volume of 100 µl, containing 78 µl deionized water, 10 µl 10 X Taq pol buffer, 1 µl of 1 U Taq polymerase enzyme, 6 µl 2 mM dNTPs, 1.5 µl of 100 mM reverse and forward primers and 1 µl of 50 ng template DNA. For amplification of the ITS1–5.8S–ITS2 region of *T. asperellum*, the primer pair T/ITS1 TCTGTAGGTGAACCTGCGG and T/ITS4 TCCTCCGCTTATTGATATGC was used.

PCR was programmed with an initial denaturing at 94°C for 5 min. followed by 30 cycles of denaturation at 94 °C for 30 sec, annealing at 59 °C for 30 sec and extension at 70 °C for 2 min and the final extension at 72 °C for 7 min in a Primus 96 advanced gradient Thermocycler. PCR product (20 µl) was mixed with loading buffer (8 µ1) containing 0.25% bromophenol blue, 40 % w/v sucrose in water, and then loaded in 2% Agarose gel with 0.1 % ethidium bromide for examining by with horizontal electrophoresis. ITS region of rDNA was amplified using genus specific ITS-1 and ITS4 primers. Amplified products of size in the range of 600bp was produced by the primers. A single distinct DNA bands was

observered on the gel for each isolates. Midium range of DNA rular (Genei, Bangalore) was used in the marker lane. The purified PCR products of *T. asperellum* were sequenced bidirectionally in Applied Biosystems by Bangalore Genei. Partial sequence of ITS region of rDNA of *T. asperellum* have been presented in Figure 5.

4.10.3. Analyses of rDNA gene sequences

After direct sequencing of the PCR product of *T. asperellum* which showed satisfactory homology with ex-type strain of *T. asperlleum* sequences from the NCBI Genbank data base, sequence was submitted to NCBI Genbank (HQ334994). The priming site of the ITS1 and ITS4 primers were determined in order to confirm that the sequences obtained corresponded to the actual ITS 4 region. A multiple sequence alignment was carried out that included the ITS 1 region, including gaps and the complete sequences align. There were quite a number of gaps that were introduced in the multiple sequence alignment within the ITS-4 region that were closely related and similar sequence indicated.

Identified *Trichoderma asperellum* rDNA gene sequences obtained from NCBI genebank (Table 21) of various locations were selected for comparison with the rDNA gene sequence of *T. asperellum* (RHS/M517) isolate of mandarin rhizosphere. The sequence alignment of the isolate of *T. asperellum* (RHS/M517) shows variation in this gene . These available sequences of *T. asperellum* from NCBI were used in the pair wise and multiple sequence alignment using Bioedit software (Fig 6) for determining the conserved regions of rDNA gene. The ITS PCR has helped to detect polymorphism at ITS region of rDNA among the *Trichoderma asperellum* isolates. The evolutionary history was inferred using the UPGMA and Neibourhood-Joining (N J)method. The optimal tree with the sum of branch length = 1.84709756 is shown. The percentage of replicate trees in which the associated taxa clustered together in the bootstrap test (1000 replicates) are shown next to the branches. The tree is drawn to scale, with branch lengths in the same units as those of the evolutionary distances

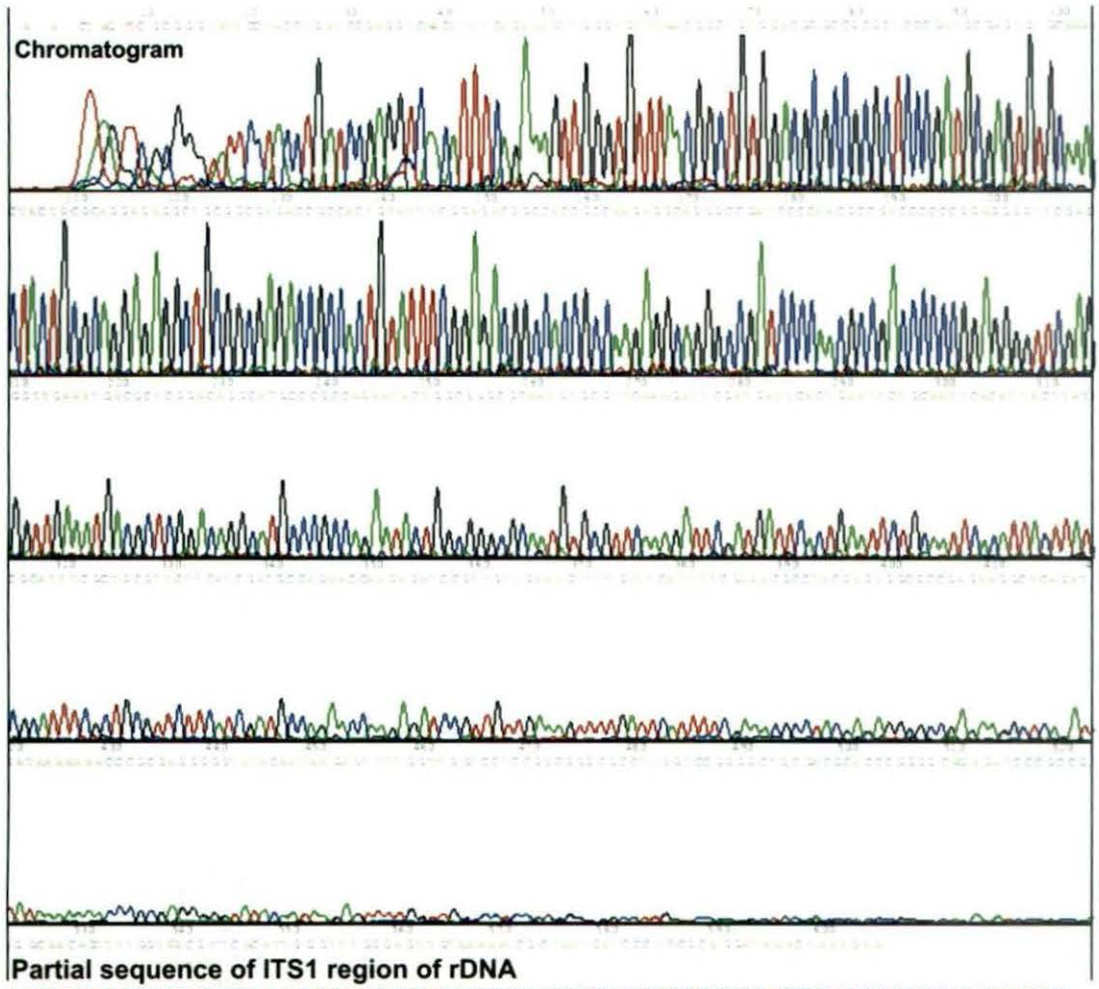

Partial sequence of ITS1 region of rDNA

ATGTGTAACGTTACCAAACTGTTGCCTCGGCGGGGTCACGCCCCGGGTGCGTCGCAGCCCCGGAAC
CAGGCGCCCGCCGGAGGAACCAACCAAACTCTTTCTGTAGTCCCCTCGCGGACGTATTTCTTACAG
CTCTGAGCAAAAATTCAAAATGAATCAAAACTTTCAACAACGGATCTCTTGGTTCTGGCATCGATG
AAGAACGCAGCGAAATGCGATAAGTAATGTGAATTGCAGAATTCAGTGAATCATCGAATCTTTGAA

Sequence Deposited: NCBI

Title : *Trichoderma asperellum* isolate RHS/M 517 18S ribosomal RNA gene, partial sequence; internal transcribed spacer 1, 5.8S

ACCESSION: HQ334994

VERSION: HQ334994.1

GI:315112485

DNA linear : 544 bp

```
  1 atgtgtaacg ttaccaaact gttgcctcgg cggggtcacg ccccgggtgc gtcgcagccc
 61 cggaaccagg cgcccgccgg aggaaccaac caaactcttt ctgtagtccc ctcgcggacg
121 tatttcttac agctctgagc aaaaattcaa aatgaatcaa aactttcaac aacggatctc
181 ttggttctgg catcgatgaa gaacgcagcg aaatgcgata agtaatgtga attgcagaat
241 tcagtgaatc atcgaatctt tgaacgcaca ttgcgcccgc cagtattctg gcgggcatgc
301 ctgtccgagc gtcatttcaa ccctcgaacc cctccgggggg atcggcgttg gggatcggga
361 cccctcacac gggtgccggc cccggaatac agtggcggtc tcgccgcagc ctctcctgcg
421 agtaggttgc acaactcgca ccgggagcgc gggcgtccac gtccgtaaac agccactttc
481 tgaaatggcg acctggatca ggtaggaata cccgcgaaat aaagctatca taggcgggga
541 gaaa
```

Figure 5: Chromatogram and 18S rDNA sequence of *Trichoderma asperellum* (RHS/M517) and significant alignments by BLAST analysis.

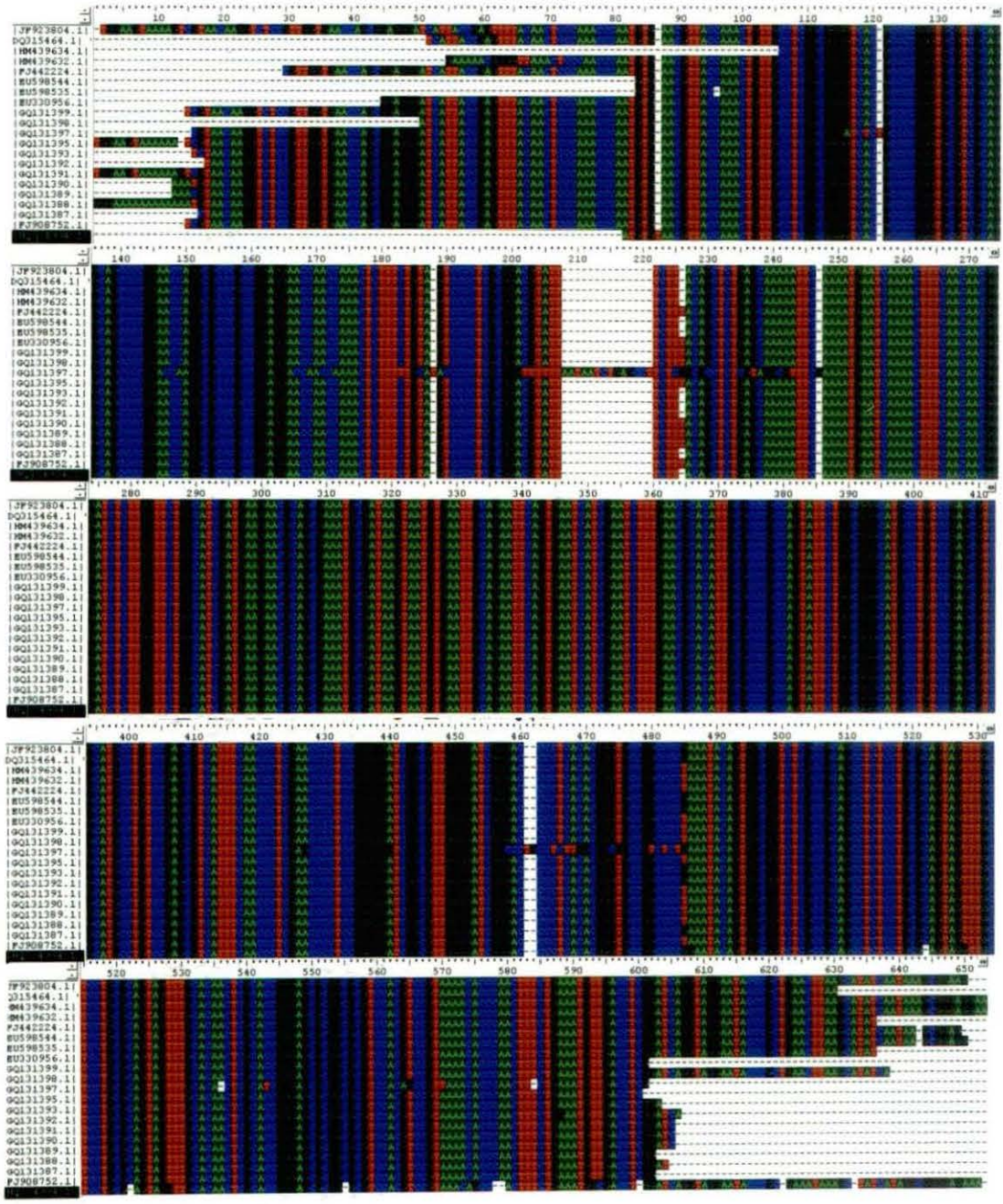

Figure 6: 18S rDNA sequence alignments of *Trichoderma asperellum* (RHS/M517). Data for other species were gathered from NCBI. The conserved regions of the gene are demonstrated in the different colour.

used to infer the phylogenetic tree (Fig 7 & 8). The evolutionary distances were computed using the Kimura 2-parameter method and are in the units of the number of base substitutions per site. Codon positions included were 1st+2nd+3rd+Noncoding. All positions containing gaps and missing data were eliminated from the dataset (Complete deletion option). There were a total of 189 positions in the final dataset. Phylogenetic analyses were conducted in MEGA4. An additional standard error test was performed with the data set using the same characters in order to evaluate the statistical confidence of the inferred phylogeny.

Table 21 : **Identified *Trichoderma harzianum* and comparison with referred NCBI GenBank**

Accession No.	Strain No	rDNA Sequence	Country	Organisms
JF923804,	NRCfBA-40	628 bp	India	*Trichoderma asperellum*
HQ334994,	**RHS/M 517**	**544 bp**	**India**	***Trichoderma asperellum***
HM439634,	IARI Mycology PP 15	528 bp	India	*Trichoderma asperellum*
HM439632,	IARI Mycology PP 13	578 bp	India	*Trichoderma asperellum*
FJ442224,	GJS 91-162	587 bp	India	*Trichoderma asperellum*
EU598544,	CNRA 361	544 bp	Africa	*Trichoderma asperellum*
EU598535,	CNRA 338	544 bp	Africa	*Trichoderma asperellum*
EU330956,	GJS 90-7	572 bp	USA	*Trichoderma asperellum*
GQ131399,	D24	567 bp	China	*Trichoderma asperellum*
GQ131398,	D21	568 bp	China	*Trichoderma asperellum*
GQ131397,	D19	583 bp	China	*Trichoderma asperellum*
GQ131395,	D3	579 bp	China	*Trichoderma asperellum*
GQ131393,	B51	567 bp	China	*Trichoderma asperellum*
GQ131392,	B10	568 bp	China	*Trichoderma asperellum*

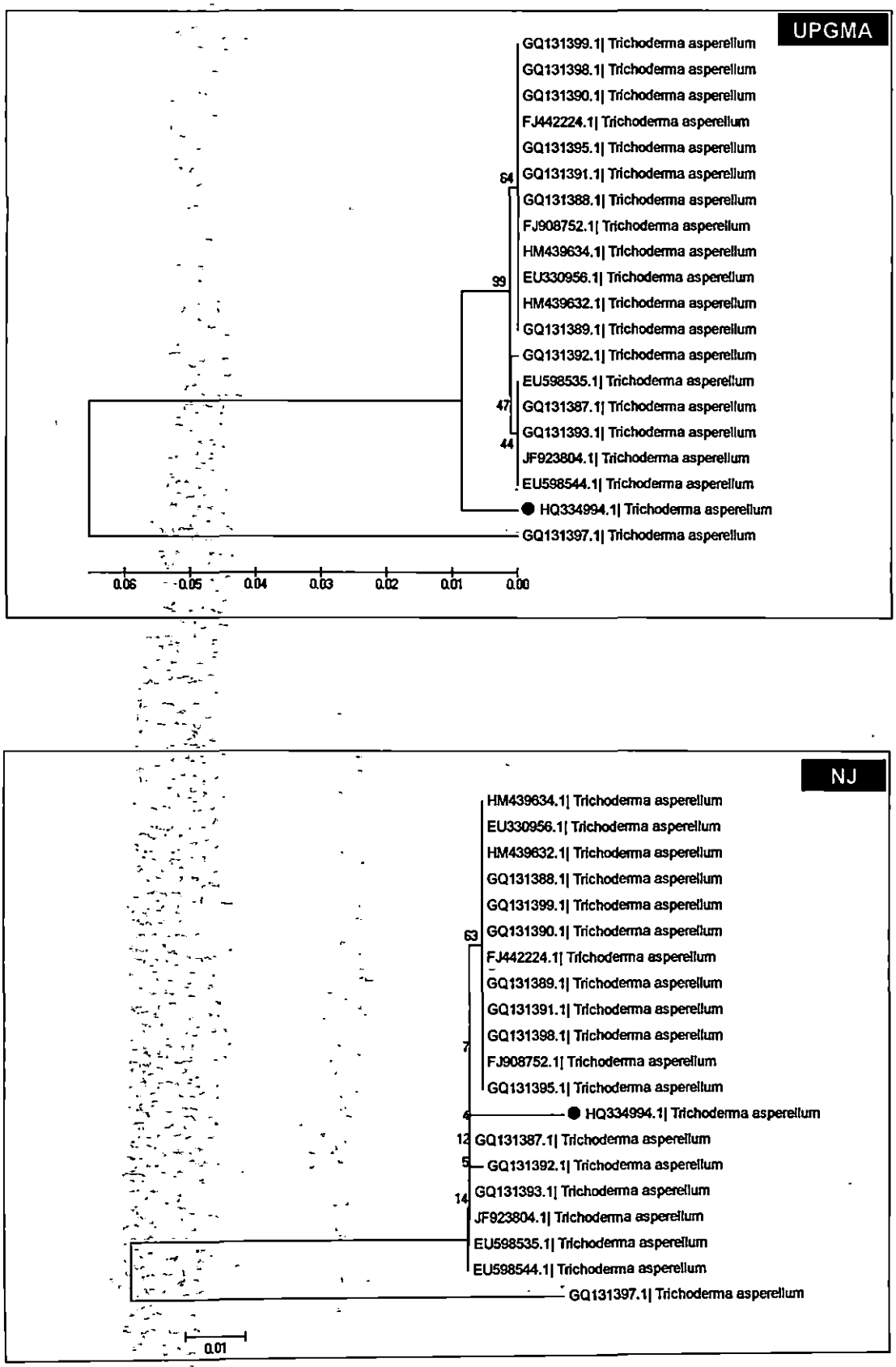

Figure 7: Phenogram of *Trichoderma asperellum* (RHS/M517) by UPGMA and NJ method

Accession No.	Strain No	rDNA Sequence	Country	Organisms
GQ131391,	A60	584 bp	China	*Trichoderma asperellum*
GQ131390,	A51	573 bp	China	*Trichoderma asperellum*
GQ131389,	A44	573 bp	China	*Trichoderma asperellum*
GQ131388,	A15	582 bp	China	*Trichoderma asperellum*
GQ131387,	A4	567 bp	China	*Trichoderma asperellum*
FJ908752	D20	568 bp	China	*Trichoderma asperellum*
HQ647325	F1002	560 bp	China	*Trichoderma harzianum*
HQ845040	T-14	582 bp	China	*Trichoderma harzianum*
JF923807	NRCfBA-46	636 bp	India	*Trichoderma harzianum*
JF923806	NRCfBA-45	643 bp	India	*Trichoderma harzianum*
JF923805	NRCfBA-44	642 bp	India	*Trichoderma harzianum*
JF923802	NRCfBA-37	642 bp	India	*Trichoderma harzianum*
JF923801	NRCfBA-31	624 bp	India	*Trichoderma harzianum*
JF923799	NRCfBA-25	637 bp	India	*Trichoderma harzianum*
JF923798	JF923798	628 bp	India	*Trichoderma harzianum*
HQ637340	JZ-179	593 bp	China	*Trichoderma harzianum*
HQ637339	JZ-77	580 bp	China	*Trichoderma harzianum*
EU718085	DMC 794b	593 bp	Germany	*Trichoderma harzianum*
GU048860	S17TH	976 bp	India	*Trichoderma viride*
|GU048859	GITXKohli-2	634 bp	India	*Trichoderma jecorina*
GU048858	GITXKohli-1	672 bp	India	*Trichoderma jecorina*
GU048857.	GITXPanog-I	898 bp	India	*Trichoderma longibrachiatum*
GU048856	GITXPanog-C	644 bp	India	*Trichoderma saturnisporum*
GU048855	S17TH	803 bp	India	*Trichoderma harzianum*
FJ442681	DIS 110A	598 bp	USA	*Trichoderma harzianum*
FJ442679	GJS 05-107	599	Italy	*Trichoderma harzianum*

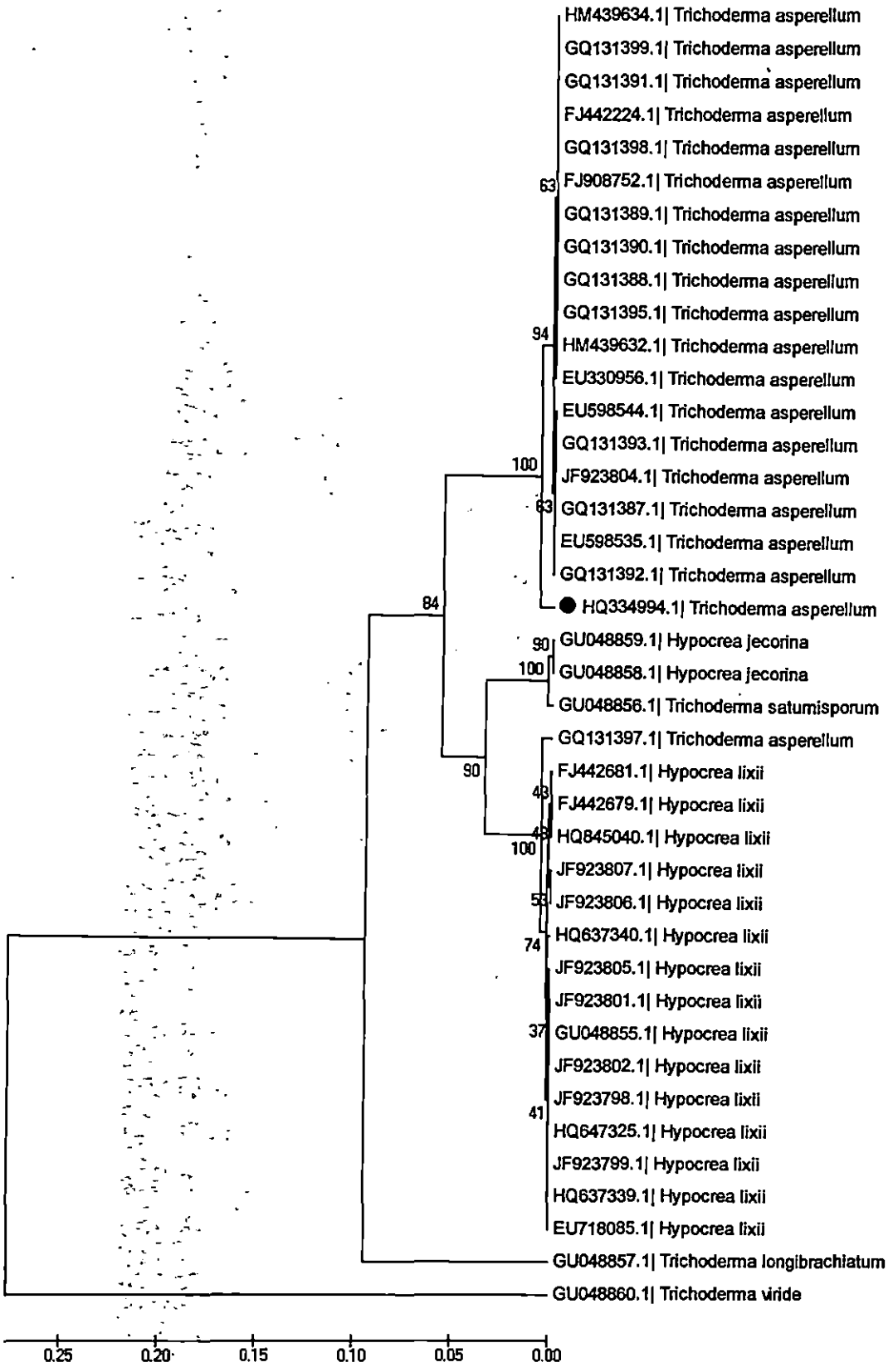

Figure 8: Phylogenetic placement of *Trichoderma asperellum* (RHS/M517) with extype strains from NCBI genebank

4. 11 Morphological and molecular identification of a potential PGPR isolate

4.11.1. Scanning electron microscopy

Isolate of *Bacillus pumilus* - B/RHS/C1(Plate24, fig.A) which showed *in vitro* antagonistic activity against *Macrophomina phaseolina, Rhizoctonia solani, Fusarium solani, Fusarium oxysporum* and *Fusarium graminearum* were selected as potential PGPR isolate for SEM study. Microscopic observation under bright field of this bacterial isolate has been presented in Plate 24 (fig.B). Scanning electron microscopic observations of *B. pumilus* isolate-B/RHS/C1 has been presented in Plate 24 (fig.C).

4.11.2. 16S rDNA sequencing

Genomic DNA was prepared from *B. pumilus* (B/RHS/C1) using lysis buffer (100mM Tris Hcl, pH 7.5, 20mM EDTA, 250mM NaCl, 2% SDS, 1mg/ml lysozyme) followed by RNase and proteinase K treatments. The lysate was extracted with equal volume of tris water saturated phenol: chloroform: isoamylalcohol (25:24:1) and then centrifuged at 10,000 rpm for 5 min. The aqueous phase was collected in clean tube, chilled with absolute ethanol, centrifuged and the pellet was air dried and finally dissolved in 40µl TE buffer and stored at 4°C. The yield of DNA was determined spectrophotometrically (A_{260}/A_{280} ratio) and the purity of DNA sample was evaluated by 0.8% agarose gel electrophoresis which produced clear sharp bands, indicating good quality of DNA. Genomic DNA of *Bacillus pumilus* (B/RHS/C1) was amplified by mixing the template DNA (50 ng), with the polymerase reaction buffer, dNTP mix, primers and Taq polymerase. Polymerase Chain Reaction was performed in a total volume of 100 µl, containing 78 µl deionized water, 10 µl 10 X Taq pol buffer, 1 µl of 1 U Taq polymerase enzyme, 6 µl 2 mM dNTPs, 1.5 µl of 100 mM reverse and forward primers and 1 µl of 50 ng template DNA. For amplification of the rDNA region of *B. pumilus* isolate B/RHS/C1) the primer pairs 5'AGAGTRTGTCMTYGCTWAC 3' and 5'CGYTAMCTTWTTWTTACGGRCT 3' were used.

PCR was programmed with an initial denaturing at 94°C for 5 min. followed by 35 cycles of denaturation at 94 °C for 30 sec, annealing at 55 °C for 30 sec and extension at 70 °C for 2 min and the final extension at 72 °C for 5 min in a Primus 96 advanced gradient Thermocycler. PCR product (20 µl) was mixed with loading buffer (8 µl) containing 0.25% bromophenol blue, 40 % w/v sucrose in water, and then loaded in 2% Agarose gel with 0.1

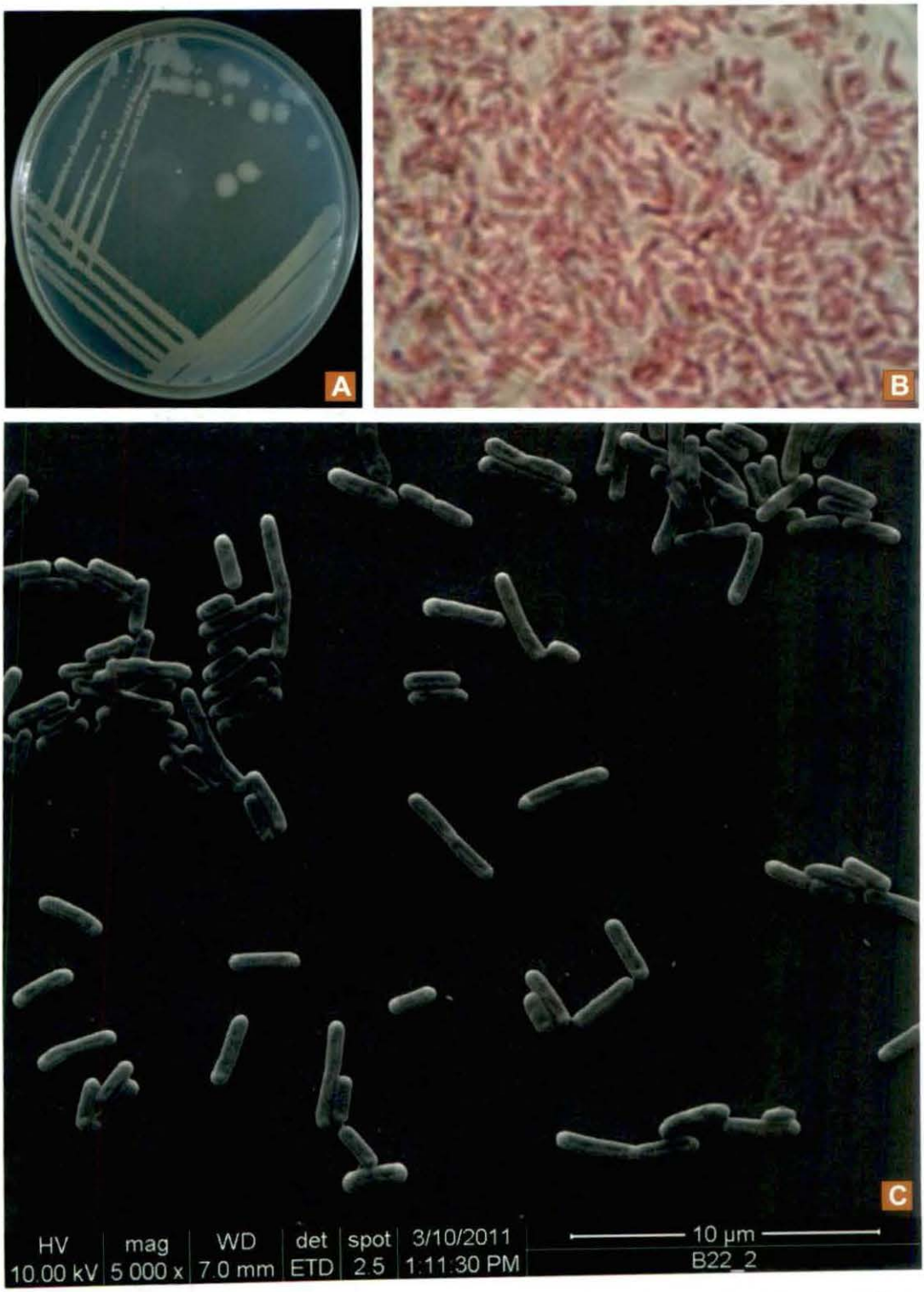

Plate 24 (figs. A-C): Phosphate solubilising bacterium *Bacillus pumilus*. Streaking NA medium [A]. Microscopic views after Gram staining [B] and Scanning Electron Microscopic view [C].

% ethidium bromide for examining by with horizontal electrophoresis. Region of rDNA was amplified using genus specific primers. Amplified products of size in the range of 1.3kbp was produced by the primers. A single distinct DNA bands was observered on the gel. The purified PCR product of *B. pumilus* (B/RHS/C1) was sequenced bidirectional primer walking method in Applied Biosystems by Chromous Biotech, Bangalore. Partial sequence of rDNA region of above mentioned bacterial isolate of *B. pumilus* has been presented in Figure 9.

4.11.3. Analyses of rDNA gene sequences

Identified *B. pumilus* rDNA gene sequences obtained from NCBI genebank (Table 22) of various host plants were selected for comparison with the rDNA gene sequence of *B. pumilus* , isolate B/RHS/C1 of mandarin plant. The sequence alignment of the isolate of *B. pumilus* (B/RHS/C1) shows variation in this gene . These available sequences of *B. pumilus* from NCBI were used in the pair wise and multiple sequence alignment using Bioedit software (Fig.10) for determining the conserved regions of rDNA gene. The evolutionary history was inferred using the UPGMA method . The optimal tree with the sum of branch length = 0.10748173 is shown. The percentage of replicate trees in which the associated taxa clustered together in the bootstrap test (1000 replicates) are shown next to the branches. The tree is drawn to scale, with branch lengths in the same units as those of the evolutionary distances used to infer the phylogenetic tree (Fig.11). The evolutionary distances were computed using the Maximum Composite Likelihood method and are in the units of the number of base substitutions per site. Codon positions included were 1st+2nd+3rd+Noncoding. All positions containing gaps and missing data were eliminated from the dataset (Complete deletion option). There were a total of 385 positions in the final dataset. Phylogenetic analyses were conducted in MEGA4. An additional standard error test was performed with the data set using the same characters in order to evaluate the statistical confidence of the inferred phylogeny.

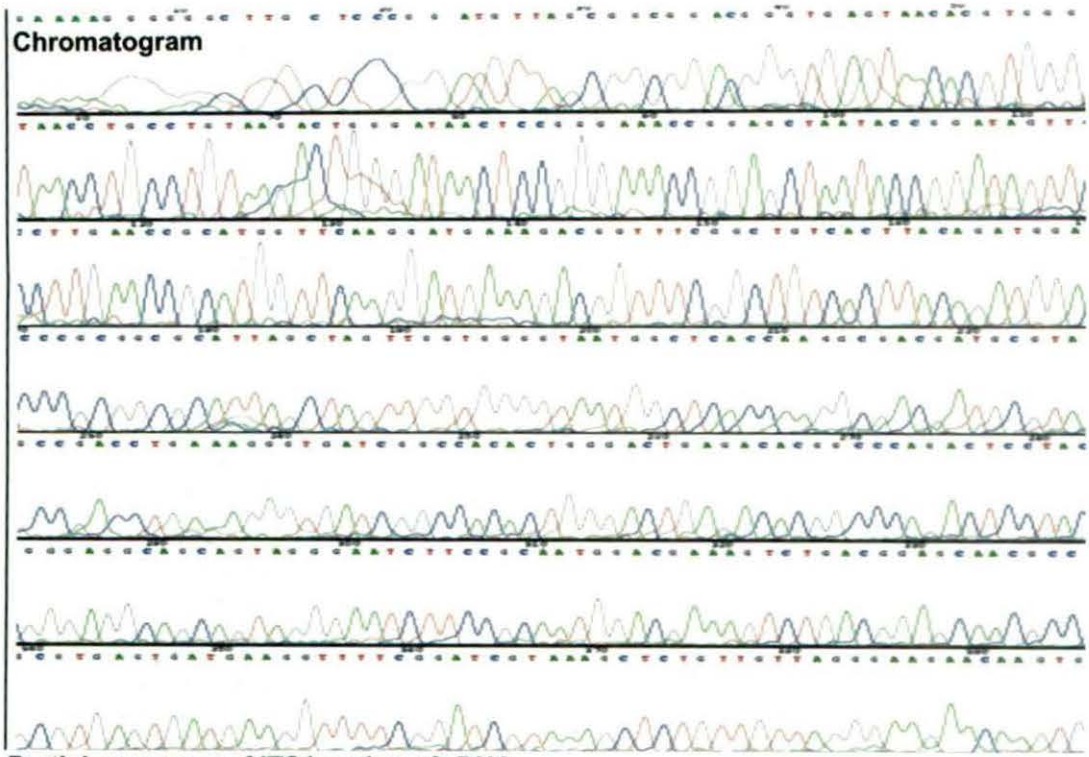

Partial sequence of ITS1 region of rDNA

GAAAAGGGGGGCTTGCTCCCGGATGTTAGCGGCGGACGGGTGAGTAACACGTGGGTAACCTGC
CTGTAAGACTGGGATAACTCCGGGAAACCGGAGCTAATACCGGATAGTTCCTTGAACCGCATG
GTTCAAGGATGAAAGACGGTTTCGGCTGTCACTTACAGATGGACCCGCGGCGCATTAGCTAGTT
GGTGGGGTAATGGCTCACCAAGGCGACGATGCGTAGCCGACCTGAGAGGGTGATCGGCCACAC
TGGGACTGAGACACGGCCCAGACTCCTACGGGAGGCAGCAGTAGGGAATCTTCCGCAATGGAC
GAAAGTCTGACGGAGCAACGCCGCGTGAGTGATGAAGGTTTTCGGATCGTAAAGCTCTGTTGTT
AGGGAAGAACAAGTGCGAGAGTAACTGCTCGCACCTTGACGGTACCTAACCAGAAAGCCACGG
CTAACTACGTGCCAGCAGCCGCGGTAATACGTAGGTGGCAAGCGTTGTCCGGAATTATTGGGCG
TAAAGGGCTCGCAGGCGGTTTCTTAAGTCTGATGTGAAAGCCCCCGGCTCTACCGGGGAGGGTC
ATTGGAAACTGGGAAACTTGAGTGCAGAAGAGGAGAGTGGAATTCCACGTGTAGCGGTGAAAT
GCGTAGAGATGTGGAGGAACACCAGTGGCGAAGGCGACTCTCTGGTCTGTAACTGACGCTGAG
GAGCGAAAGCGTGGGGAGCGAACAGGATTAGATACCCTGGTAGTCCACGCCGTAAACGATGAG
TGCTAAGTGTTAGGGGGTTTCCGCCCCTTAGTGCTGCAGCTAACGCATTAAGCACTCCGCCTGG
GGAGTACGGTCGCAAGACTGAAACTCAAAGGAATTGACGGGGGCCCGCACAAGCGGTGGAGC
ATGTGGTTTAATTCGAAGCAACGCGAAGAACCTTACCAGGTCTTGACATCCTCTGACAACCCTA
GAGATAGGGCTTTCCCTTCGGGGACAGAGTGACAGGTGGTGCATGGTTGTCGTCAGCTCGTGTC
GTGAGATGTTGGGTTAAGTCCCGCAACGAGCGCAACCCTTGATCTTAGTTGCCAGCATTTAGTT
GGGCACTCTAAGGTGACTGCCGGTGACAAACCGGAGGAAGGTGGGGATGACGTCAAATCATCA
TGCCCCTTATGACCTGGGCTACACACGTGCTACAATGGACAGAACAAAGGGCTGCGAGACCGC
AAGGTTTAGCCAATCCCATAAATCTGTTCTCATTTCGATCGCAGTCTGCAATCGACTGCGTGAA
GCTGGAACGCTAGAATCGCGAACAGCATGCCGCGGTGATTACGTTCCGGGCCTGTCCCCACGCC
GTACACCCGAAAGTTTGTACCCCGAGTCGGTAGTGACCTTTTGACTCCCCCCAAC

Sequences producing significant alignments:

Accession	Description	Max score	Total score	Query coverage	E value	Max ident
AB576891.1	Bacillus sp. CSL09-1 gene for 16S rRNA, partial sequence	2396	2396	98%	0.0	98%
EU308307.1	Bacillus sp. F1A07 16S ribosomal RNA gene, partial sequence	2396	2396	98%	0.0	98%
EU869263.1	Bacillus pumilus strain BG-B79 16S ribosomal RNA (rrs) gene, partial seque	2396	2396	98%	0.0	98%
EU379253.1	Bacillus pumilus strain 1RN-3E 16S ribosomal RNA gene, partial sequence	2396	2396	98%	0.0	98%
EU379249.1	Bacillus pumilus strain 1RN-3B 16S ribosomal RNA gene, partial sequence	2396	2396	98%	0.0	98%
CP000813.1	Bacillus pumilus SAFR-032, complete genome	2396	1.677e+04	98%	0.0	98%
AM237370.1	Bacillus pumilus partial 16S rRNA gene, isolate OS-70	2396	2396	98%	0.0	98%
AY690701.1	Bacillus sp. MH07 16S ribosomal RNA gene, partial sequence	2396	2396	98%	0.0	98%
AY690700.1	Bacillus sp. MH06 16S ribosomal RNA gene, partial sequence	2396	2396	98%	0.0	98%
AY167862.1	Bacillus pumilus strain SAFN-034 16S ribosomal RNA gene, partial sequenc	2396	2396	98%	0.0	98%
AB020208.1	Bacillus pumilus gene for 16S ribosomal RNA, strain: OM-F6	2396	2396	98%	0.0	98%
AB374310.1	Bacillus sp. RV103 gene for 16S rRNA, partial sequence	2392	2392	97%	0.0	98%
FJ237280.1	Bacillus pumilus strain XJAS-ZB-14 16S ribosomal RNA gene, partial seque	2392	2392	98%	0.0	98%
FJ237277.1	Bacillus pumilus strain XJAS-ZB-28 16S ribosomal RNA gene, partial seque	2392	2392	98%	0.0	98%
DQ180948.1	Bacillus sp. MI-23a1 16S ribosomal RNA gene, partial sequence	2392	2392	97%	0.0	98%
HQ891969.1	Bacillus sp. MM110(2011) 16S ribosomal RNA gene, partial sequence	2390	2390	98%	0.0	98%
GU968462.1	Bacillus sp. RS114(2010) 16S ribosomal RNA gene, partial sequence	2390	2390	97%	0.0	98%
HM585071.1	Bacillus pumilus strain AUEC29 16S ribosomal RNA gene, partial sequence	2390	2390	98%	0.0	98%
HM585070.1	Bacillus pumilus strain AUEM12 16S ribosomal RNA gene, partial sequence	2390	2390	98%	0.0	98%
HM585069.1	Bacillus pumilus strain AUEM104 16S ribosomal RNA gene, partial sequenc	2390	2390	98%	0.0	98%
HM585067.1	Bacillus pumilus strain AUES82 16S ribosomal RNA gene, partial sequence	2390	2390	98%	0.0	97%

Figure 9: Chromatogram and 18S rDNA sequence of *Bacillus pumilus* (B/RHS/C1) and significant alignments by BLAST analysis

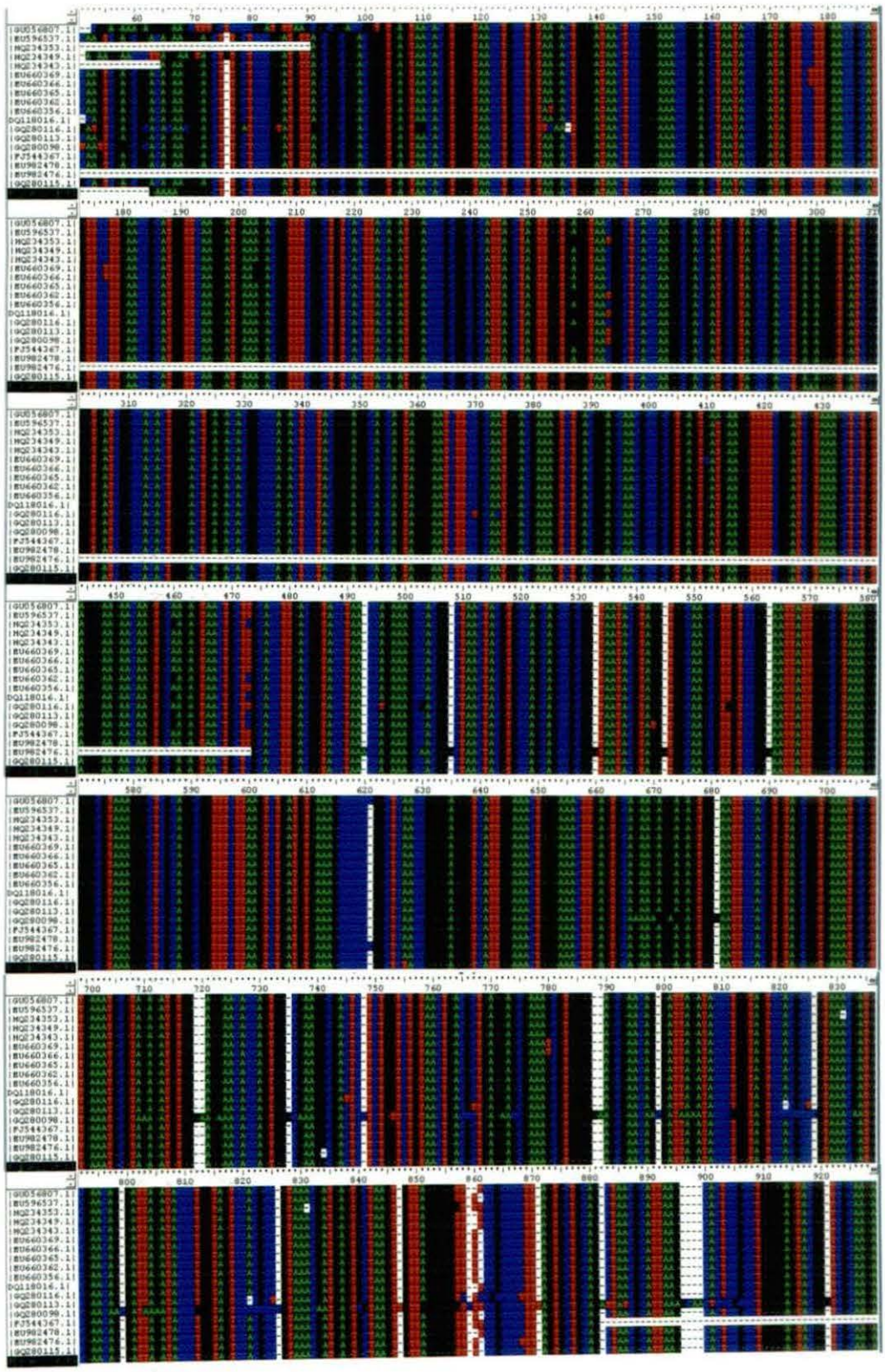

Figure 10: 18S rDNA sequence alignments of *Bacillus pumilus* (B/RHS/C1). Data for other species were gathered from NCBI. The conserved regions of the gene are demonstrated in the different colour.

Table 22: Identified *Bacillus pumilus* and comparison with referred NCBI GenBank sequences

Accession No.	Strain No	rDNA Sequence	Country	Organisms
GU056807	SRS-3	1470 bp	India	*Bacillus pumilus*
EU596537	HN005	1457 bp	China	*Bacillus pumilus*
HQ234353	AK39885	1337 bp	India	*Bacillus pumilus*
HQ234349	AK39674	1385 bp	India	*Bacillus pumilus*
HQ234343	AK39651	1385 bp	India	*Bacillus pumilus*
EU660369	CT19	1505 bp	India	*Bacillus pumilus*
EU660366	CT14	1513 bp	India	*Bacillus pumilus*
EU660365	CT13	1511 bp	India	*Bacillus pumilus*
EU660362	CT10	1512 bp	India	*Bacillus pumilus*
EU660356	CT3	1512 bp	India	*Bacillus pumilus*
DQ118016	RGR7	1369 bp	India	*Bacillus pumilus*
GQ280116	JS-46	1413 bp	India	*Bacillus pumilus*
GQ280113	JS-43	1424 bp	India	*Bacillus pumilus*
GQ280098	JS-28	1445 bp	India	*Bacillus pumilus*
FJ544367	st9	1449 bp	China	*Bacillus pumilus*
EU982478	5	814 bp	China	*Bacillus pumilus*
EU982476	4-1-14-c	994 bp	China	*Bacillus pumilus*
GQ280115	JS-45	1424 bp	India	*Bacillus pumilus*

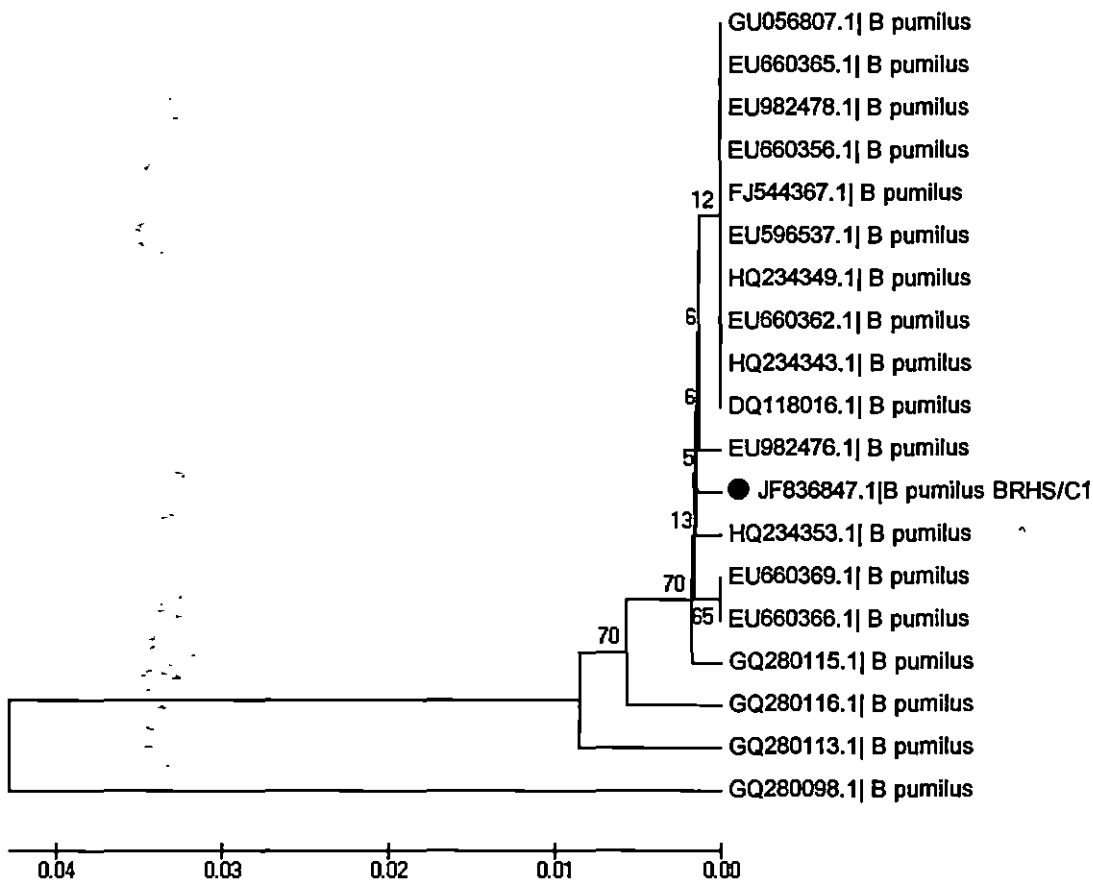

Figure 11 : Phylogenetic placement of *Bacillus pumilus* (B/RHS/C1) with extype strains from NCBI genebank

4.12. Effect of bioinoculants on suppression of charcoal rot disease of *Citrus reticulata*

Based on the screening of association of arbuscular mycorrhizal fungi (AMF) with mandarin roots in four locations of Darjeeling hills and percentage colonization behavior established by artificial inoculation of mandarin seedlings, predominant AMF *Glomus mosseae* and *Glomus fasciculatum* were selected for application in mandarin plants. Total phosphate content of soil was determined after application of *G. mosseae* and *G. fasciculatum* singly or jointly. Results revealed that soil P content had decreased due to application of AMF indicating that the plant could uptake phosphorus which had been solubilized by AMF (Table 23).

Table 23 . Soil phosphate content in rhizosphere of mandarin plants following root colonization with *G. mosseae* and *G. fasciculatum*

Treatment	Soil phosphate (µg/g tissue)
Control	48.25^{a}±1.12
G. mosseae	31.12^{b}±0.57
G.fasciculatum	35.25^{b}±2.10
G. mosseae + *G.fasciculatum*	30.75^{c}±1.23

Average of 3 replicates
±= Standard Error
Difference between values significant at P=0.01where superscript is different; not significant where superscript is same

Glomus mosseae was further selected as one of the important bioinoculants in this experiment. for mass multiplication in sorghum and maize seedlings (Plate 25, figs B&C), and root colonization was confirmed after three weeks (Plate 25, figs D&E).In order to develop pure cell line culture of *G. mosseae* experimental setup was made using sterilized pre-soaked sorghum seeds in sterile petriplate. After isolation of spores from the soil by wet sieving and decanting process, *G. mosseae* was carefully selected and placed in sorghum roots which were grown in aseptical conditions (Plate 25, fig.A). The same experiment was done in 3 months old mandarin seedlings. The seeds were germinated in aseptical conditions. *G. mosseae* was carefully selected and inoculated in the root of the mandarin plant and grown in

Plate 25 (figs. A-E): Experimental setup for raising single spore in sorghum seedlings[A]; mass multiplication of AMF spores in *Sorghum vulgare* [B] and *Zea mays* [C]; root colonization of sorghum grown in sterile soil [D] and maize [E] with AMF (*G. mosseae*).

pots having sterile sand. Establishment of the AM spore was confirmed a month after inoculation (Plate 26,figs.A-E). Application of *G.mosseae* in the rhizosphere of *Citrus* plants led to an increase in the growth of seedlings in terms of increase in height and number of leaves (Plate 27).

The present work was aimed at developing a management strategy to control root rot of mandarin plants by biological means. Antibiosis to *M. phaseolina* by biocontrol agent (*Trichoderma asperellum*) was evaluated in *vitro* and *in vivo* condition. The application of *T. asperellum* to the soil as a biocontrol agent, in glasshouse conditions, not only resulted in reduced disease severity but also enhanced plant growth (Table 24). Joint inoculation with both the microorganisms (G. *mosseae* and *T. asperellum*) gave most significant results (Plate 28, fig.A-D). Marked reduction in disease development was evident following dual inoculations of G. *mosseae* and *T. asperellum* (Table 25)

Table 24 : Effect of application of *G. mosseae* and *T. asperellum* on growth of citrus seedlings: % increase in height and leaves no. After 1 and 2 months. (* mo- month)

Treatments	% increase in height		% increase in leaves no.	
	1 mo*	2 mo*	1 mo*	2 mo*
Control	8.5	12.5	21.0	36.0
T.asperellum	16.0	22.0	40.0	47.0
G.mosseae	21.0	28.5	38.0	55.0
T.asperellum+G.mosseae	35.0	41.0	69.0	80.0

Table 25 : Effect of application of *G. mosseae* and *T. asperellum* on development of root rot of *Citrus reticulata*

Treatments	**Root Rot Index** (Days after inoculation)		
	15	30	45
M. phaseolina	2.0	3.2	5.8
M. phaseolina+T. asperellum	0.5	1.0	2.6
M. phaseolina+G. mosseae	0.9	2.1	3.0
M.phaseolina+T.asperellum+G.mosseae	0.3	0.9	1.8

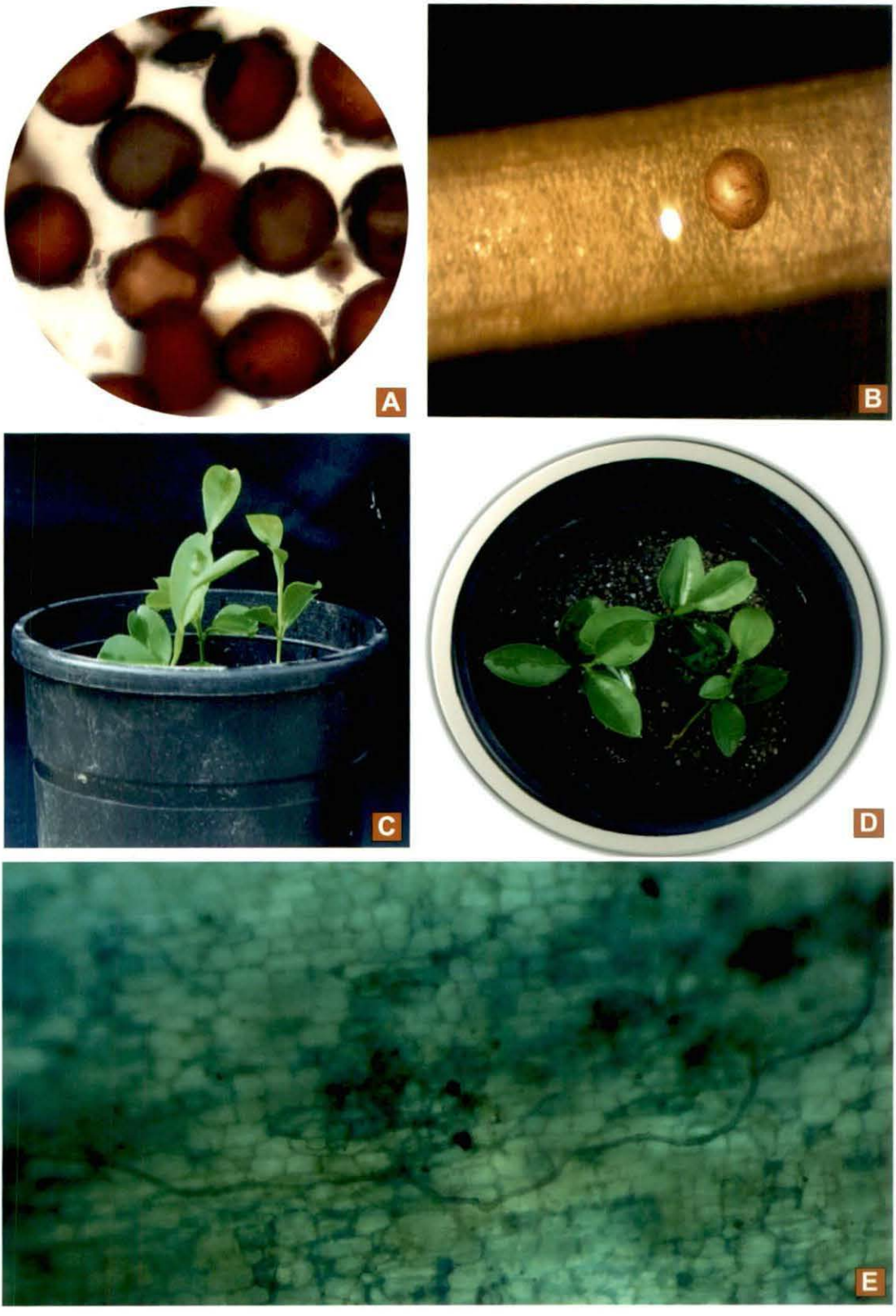

Plate 26 (figs.A-E): *Glomus mosseae* spores mass multiplied in maize roots [A]. Single spore inoculation of *G. mosseae* in mandarin root [B]. Single spore inoculated mandarin seedlings grown in sterile sand [C & D] and maintained in glass house. Mycorrhizal association observed in mandarin roots after 30 days of inoculation [E].

Plate 27 (figs. A): Joint inoculation of mandarin seedlings with AMF (*G. mosseae*) and PGPR (*B. pumilus*) and maintained in nurser .

Plate 28 (figs. A-D): Effect of *Glomus mosseae, Trichoderma asperellum* and coinoculation of *G. mosseae* and *T. asperellum* [A], *B. pumilus* alone and in combination with *T. asperellum* [B], on growth of 2 yr old potted mandarin plant and inoculated with *M. phaseolina* [C & D].

In vitro studies also confirmed PGPR activities of *Bacillus pumilus*. *B.pumilus* which produced a clear halo zone in Pikovskaya's medium indicating that it could solubilize phosphate. Similarly, production of siderophore as well as secretion of IAA into the medium were confirmed. Besides, significant inhibition of growth of root pathogens was also observed. *In vivo* application of *B.pumilus* to the rhizosphere of two year old mandarin plants grown in earthenware pots in the glass house condition resulted in an increase in growth in terms of increase in height, leaf number and number of branches (Plate 29figs.A&B) . Increase of height in seedlings was evident even one months after application. Application of *B. pumilus* and *G .mosseae* in the rhizosphere of *Citrus* plants led to an increase in the growth of seedlings in terms of increase in height and number of leaves. Joint inoculation with both the microorganisms gave most significant results (Figure 12). Total phosphate content of soil was determined after application of the microorganisms. Results revealed that soil P content had decreased due to application indicating that the plant could uptake phosphorus which had been solubilized by the microorganisms. Both acid and alkaline phosphatase activities in rhizosphere soil of mandarin plants were enhanced following application of *B. pumilus*. In rhizosphere soil of untreated plants, alkaline phosphatase activity was higher than acid phosphatase, but after treatment with *B. pumilus*, acid phosphate showed a greater increment of activity. Rhizosphere of mandarin was inoculated by *B.pumilus* and *G.mosseae* prior to challenge inoculation with *M. phaseolina*. Development of root rot was determined after 15, 30 and 45 days of inoculation. *B. pumilus* and *G. mosseae* could reduce root rot, but maximum suppression of disease was due to joint inoculation (Figure 13).

Plate 29 (figs. A-B): Control [A] and *Bacillus pumilus* treated mandarin seedlings [B].

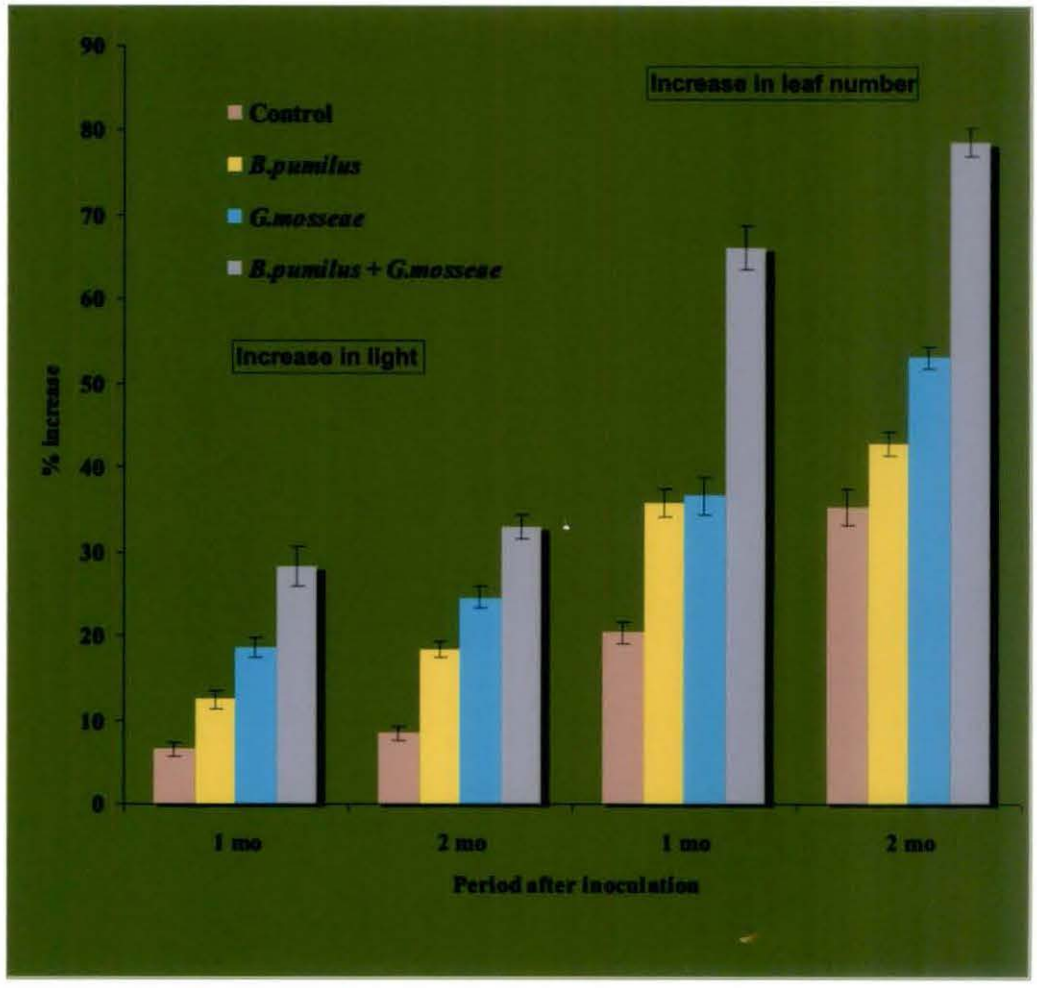

Figure 12: Effect of application of *B.pumilus* and *G.mosseae* on growth of citrus seedlings in terms of increase in height and number of leaves

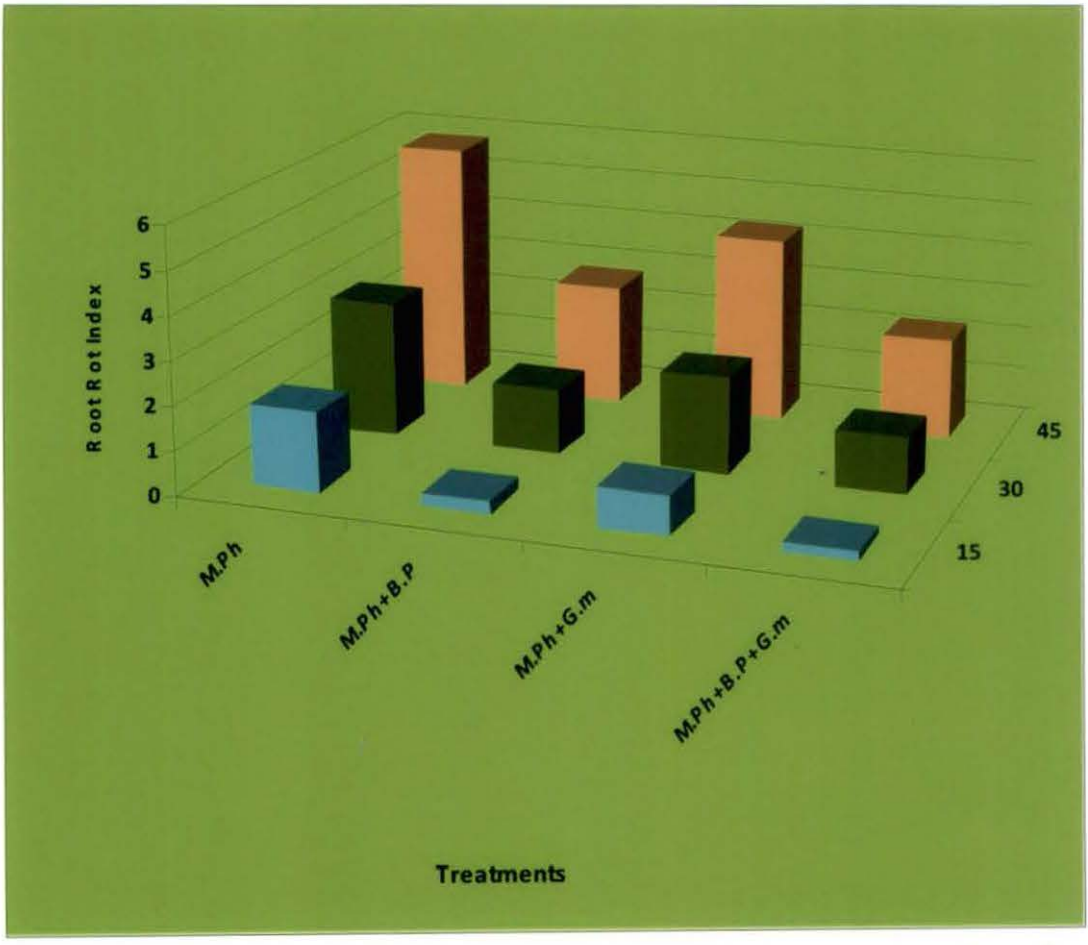

Figure 13: Influence of *B. pumilus* and *G. mosseae* on root rot caused by *M. phaseolina*

4.13. Activation of defense response of *Citrus reticulata* following application of bioinoculants against *M. phaseolina* and associated changes in defense enzymes

Defense responses of mandarin plants against root rot pathogen (*M. phaseolina*) were demonstrated during early stages of root colonization by *G. mosseae* and *T. asperellum* along with application of *B. pumilus*. Activities of 3 major defense enzymes- β 1,3 - glucanase, chitinase and peroxidase were assayed in roots and leaves and of mandarin seedlings subjected to various treatments- ie., *G. mosseae*, *B. pumilus*, *T. asperellum*, *M. phaseolina*, *B. pumilus* + *G. mosseae*, *B. pumilus* + *M. phaseolina*, *G. mosseae* +*M. phaseolina*, *T. asperellum*+ *G. mosseae*, *B. pumilus* + *G. mosseae* +*M. phaseolina*, *T. asperellum*+ *G. mosseae*+*M. phaseolina* . Activities of all 3 enzymes, in both leaves and roots, were significantly enhanced due to the various treatments (Table 26, 27, and 28; Figures 14,15 & 16). In most of the treatments, results were significantly higher than control at P=0.01 as tested by Student's't' test. Peroxidase activity was more than double in leaves compared to the roots, whereas chitinase was more or less similar.

Table 26 : Changes in chitinase activities in citrus seedlings following single as well as dual application of *T. asperellum* and *G. mosseae* following inoculation with *M. phaseolina*.

Treatments	Chitinase (µgGlc-Nac/min/gtissue)	
	Leaf	Root
Control	87	82
T.asperellum	91	85
G.mosseae	110	92
T.asperellum+*G.mosseae*	135	96
M. phaseolina	95	95
M.phaseolina+*T.asperellum*	104	100
M.phaseolina+*G.mosseae*	125	115
M.phaseolina+*T.asperellum*+*G. mosseae*	168	155

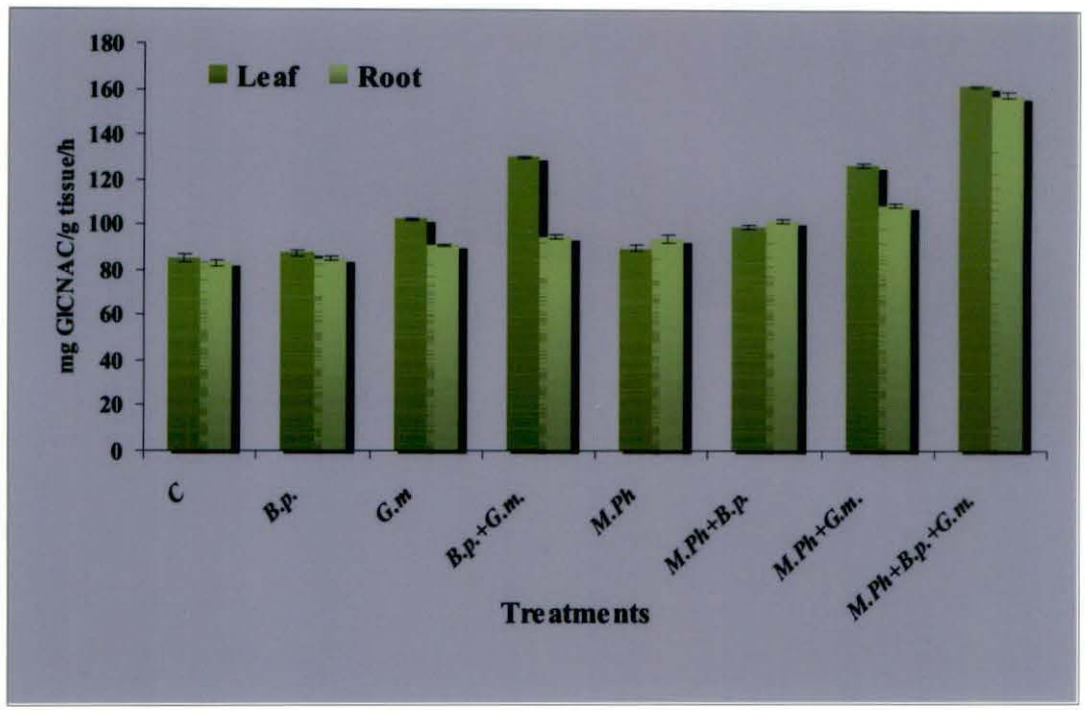

Figure 14: Activities of chitinase in roots and leaves of mandarin following application of *B. pumilus* and *G .mosseae* and inoculated with *M. phaseolina*

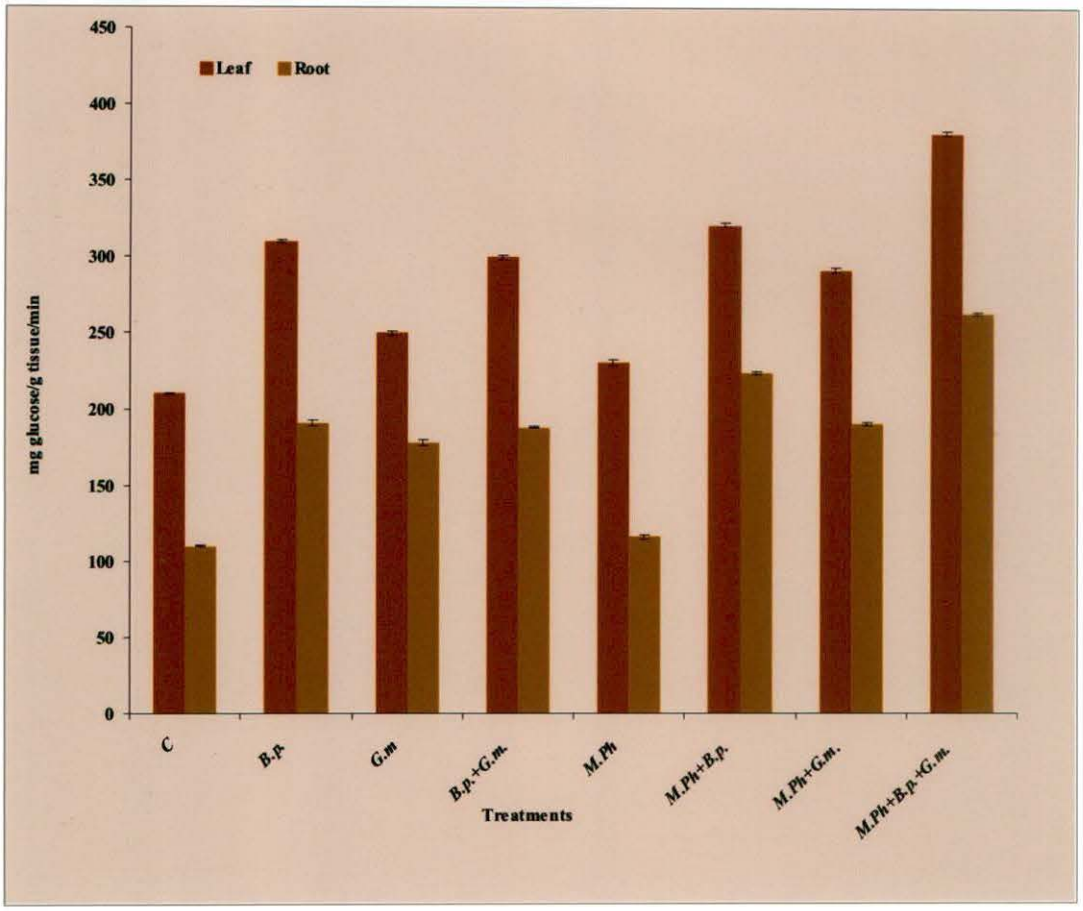

Figure 15: Activities of β1,3 glucanase in roots and leaves of mandarin following application of *B. pumilus* and *G. mosseae* and inoculated with *M. phaseolina*

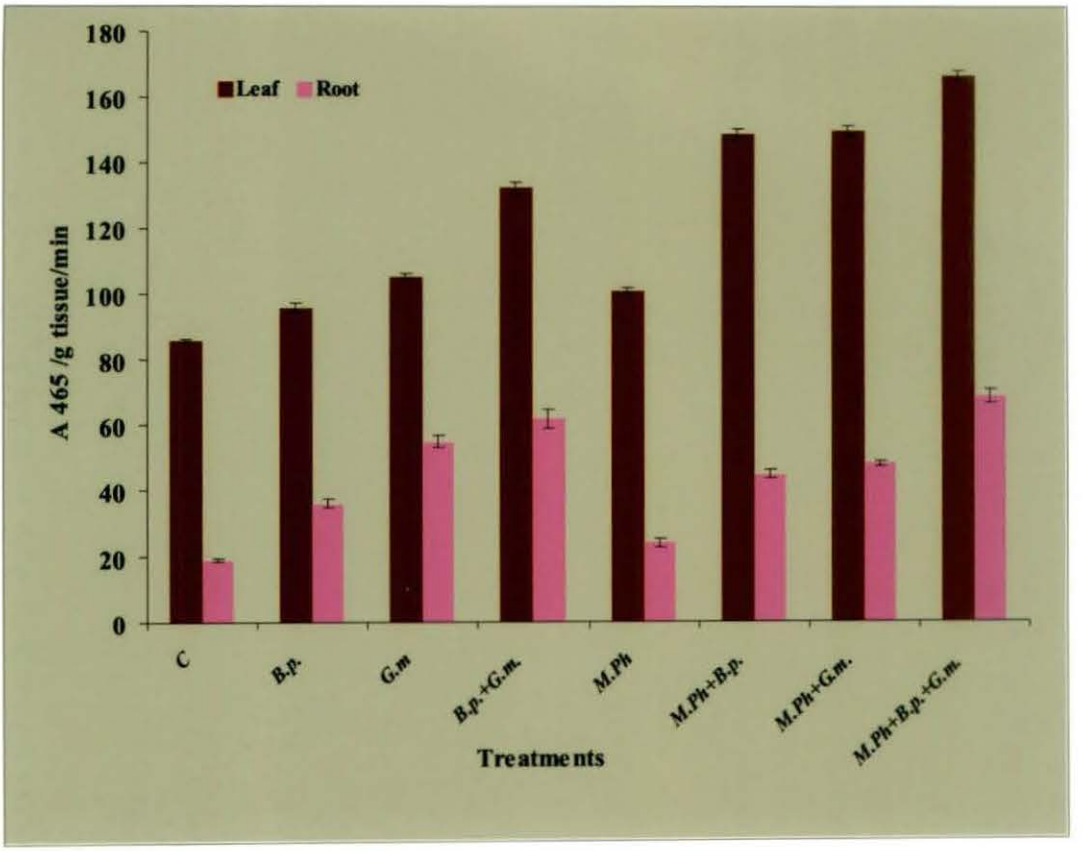

Figure 16: Activities of peroxidase in roots and leaves of mandarin following application of *B. pumilus* and *G. mosseae* and inoculated with *M. phaseolina*

Table 27: Effect on β-1,3 glucanase activities in citrus seedlings by application of *T. asperellum* and *G. mosseae* following inoculation with *M. phaseolina*

Treatments	β-1,3 glucanase (µg glucose/min/gtissue)	
	Leaf	Root
Control	211	115
T.asperellum	315	191
G.mosseae	255	181
T.asperellum+G.mosseae	303	189
M. phaseolina	230	118
M.phaseolina+T.asperellum	320	221
M.phaseolina+G.mosseae	296	193
M.phaseolina+T.asperellum+G. mosseae	387	260

Table 28: Effect of application of *T. asperellum* and *G. mosseae* on peroxidise activities of citrus seedland following inoculation with *M. phaseolina*

Treatments	Peroxidase (ΔA465/min/gtissue)	
	Leaf	Root
Control	88	27
T.asperellum	108	48
G.mosseae	114	68
T.asperellum+G.mosseae	138	72
M. phaseolina	107	39
M.phaseolina+T.asperellum	157	51
M.phaseolina+G.mosseae	159	55
M.phaseolina+T.asperellum+G. mosseae	170	72

Reduction of root rot in *Citrus reticulata* following application of bioinoculants (*G. mosseae*, *T. asperellum* and *B. pumilus*) were evident both singly or jointly. However, joint inoculation with both AMF (*G. mosseae*) and PGPR (*B. pumilus*) as well as AMF (*G. mosseae*) and BCA (*T. asperellum*) reduced disease markedly. These observed root rot reduction following separate and dual application of bioinoculants may be correlated with increased accumulation of defense enzymes such as β- 1, 3- glucanase (Fig.17A) chitinase (Fig.17B), and peroxidase (Fig.17C).

In order to confirm the induction of enhanced activities of defense enzymes due to treatment with *B.pumilus*, *G.mosseae* and *T. asperellum* or both, immunological tests were done using PAbs raised against two enzymes- chitinase and β 1,3 glucanase.

Enzyme extracts were used as antigens and PTA-ELISA and Dot immunobinding assays were carried out. Results (Table 29) revealed that ELISA values of reaction of PAbs of chitinase and β 1,3-glucanase with enzyme extracts from leaves of mandarin plants grown in treated soil were higher than the control values. Similarly, in Dot-Blot, more intense dots were observed in treated plants.

Table 29: . PTA-ELISA and Dot-Blot values of reactions between PAbs of defense enzymes and enzyme extracts from mandarin plants inoculated with *G. mosseae* and *T. asperellum* challenge inoculation with *M. phaseolina*

Antigen source*	PAb of chitinase		PAb of β 1,3-glucanase	
	A 405 ELISA	Colour intensity# Dot-Blot	A 405 ELISA	Colour intensity# Dot-Blot
Control	0.034	+	0.049	+
M.phaseolina inoculated	0.036	+	0.052	+
G.mosseae treated +*M.phaseolina* inoculated	0.520	+++	0.368	++
B.pumilus treated +*M.phaseolina* inoculated	0.426	++	0.345	++
T. asperellum treated +*M.phaseolina* inoculated	0.768	++	0.445	++
G.mosseae + *T.asperellum* treated +*M.phaseolina* inoculated	0.982	++++	0.865	+++
G.mosseae+ *B.pumilus* treated +*M.phaseolina* inoculated	0.954	++++	0.741	+++

* Enzyme extracts from leaves of plants treated as mentioned;
# Colour Intensity - += Light pink; ++ = Dark pink; +++ = Deep purplish

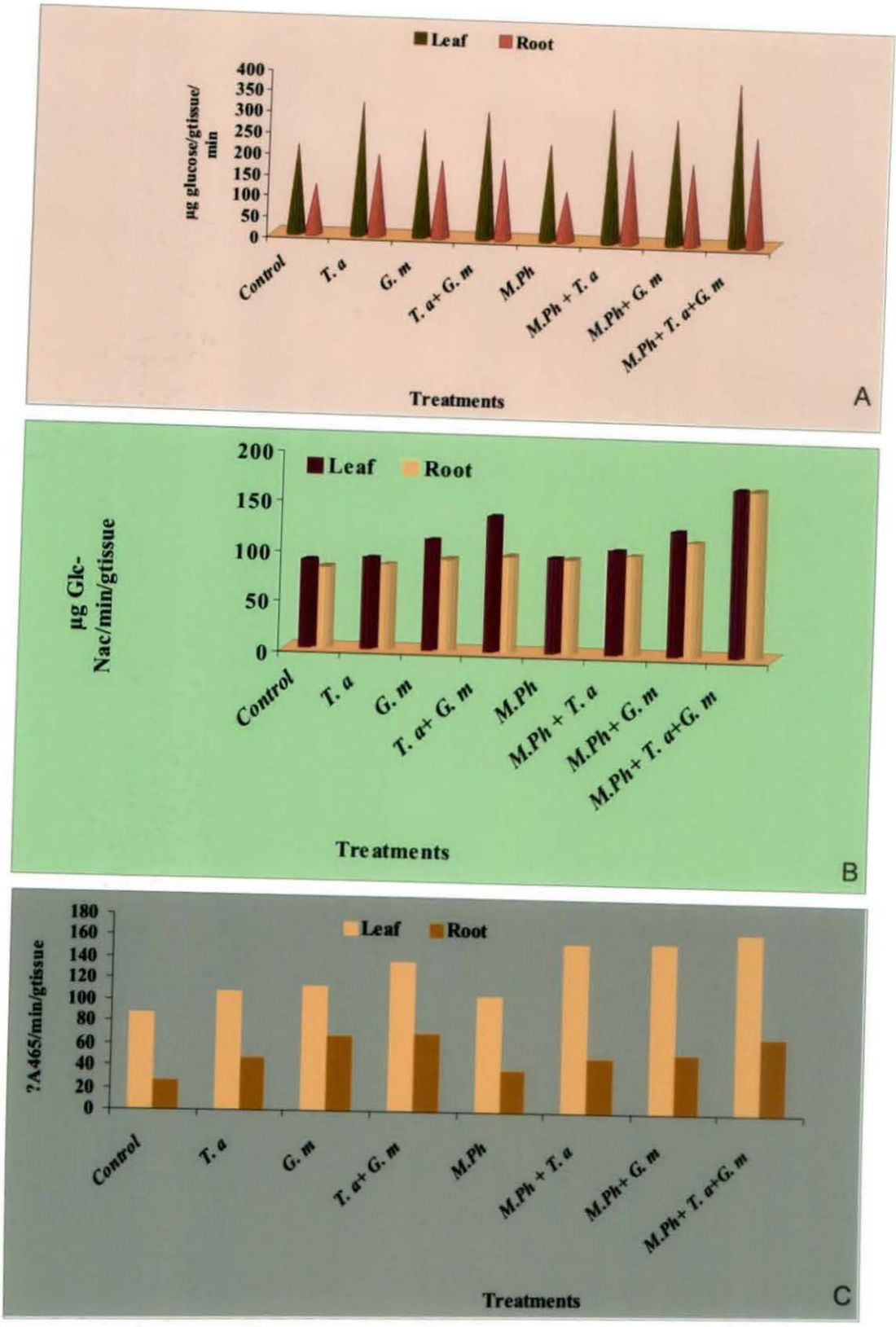

Figure 17: Changes in defense enzyme activities in citrus seedlings following single as well as dual application of *T. asperellum* and *G. mosseae* and challenged inoculation with *M. phaseolina*. (A- β-1,3 glucanase, B- chitinase, C- Peroxidase)

4.14 Cellular location of Chitinase in root and leaf tissues of *Citrus reticulata* following induction of resistance

The induction of systemic resistance was confirmed in the present study since the enhanced activities of defense enzymes were noted not only in the roots which were the sites of inoculation, but also in the leaves as evident in immunological assays. Accumulation of both the defense enzymes (β, 1.3- glucanase and chitinase) in leaf tissues were always higher than the root tissues as evident in PTA-ELISA reaction using PAbs of Chitinase and β, 1.3- Glucanase. Enhanced activities were noted in bioinoculant(s) treated (singly or jointly) mandarin plants following challenge inoculation with the pathogen (*M. phaseolina*)

Keeping this in mind root and leaf samples were collected from the bioinoculant(s) treated plants. Similarly root and leaf samples were collected from healthy plants for immunoflorescence study. Main objective was to localize chitinase (PR-3) at the cellular level in the root and leaf tissues of *Citrus reticulata* following induction of resistance.

Cross sections of the root and leaf tissues (Plate 30,fig.A&C) were treated separately with normal antiserum and PAb of Chitinase and labeled with FITC as mentioned in materials and methods. Leaf tissues exhibited a natural autoflorescence under UV- Light but was not characteristic of FITC fluorescence. Observations in the treatement with the normal antiserum was the same. When the cross sections of the untreated and treated root and leaf tissues were incubated with PAb- chitinase and labeled with FITC, fluorescence was observed in the treated root (Plate 30, fig.B) and leaf tissues (Plate 30, fig.D). Bright apple green fluorescence was evident in the epidermal and homogenously in the mesophyll tissues (Plate 30, fig.E-J). Similarly bright fluorescence was also observed in the cortical tissues of the treated root sections. So strong reaction with FITC in plant tissues gave indication of the induction of chitinase (PR-3) in *Cirtus reticulata* plants following induction of resistance with bioinoculants

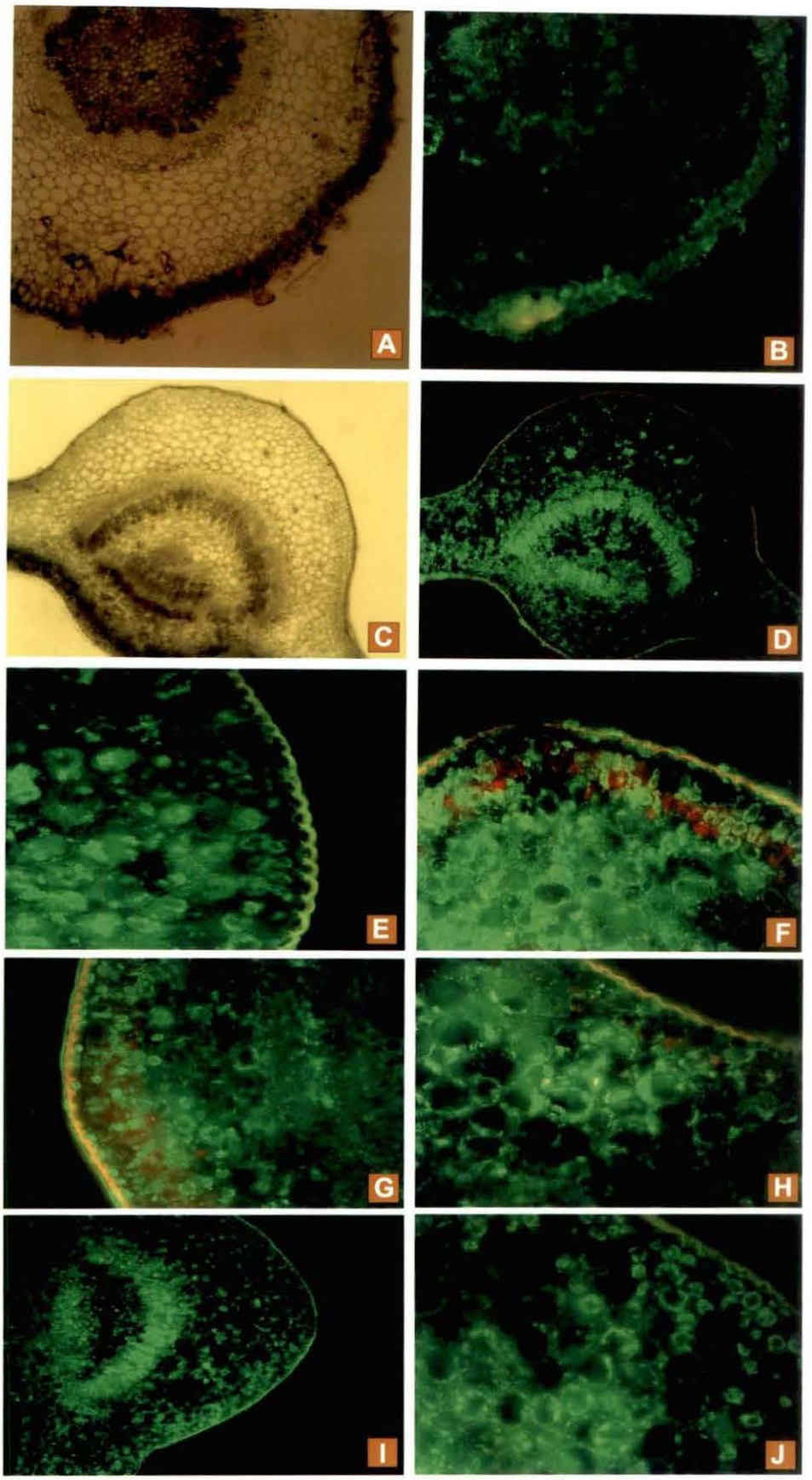

Plate 30 (figs. A-J): Cross section of mandarin root [A & B] and leaf [C-J] following inoculation with *G. mosseae*, and treated with *T. asperellum* and *B. pumilus* under bright field [A & C] and probed with PAb-chitinase and labeled with FITC conjugates.